2024

Lysophosphatidylcholine acyltransferase-2 (LPCAT-2) & protein S-acylation in macrophage innate immunity

Good, Christian Robin

COPYRIGHT STATEMENT

Copyright and Moral rights arising from original work in this thesis and (where relevant), any accompanying data, rests with the Author unless stated otherwise[1].

Re-use of the work is allowed under fair dealing exceptions outlined in the Copyright, Designs and Patents Act 1988 (amended)[2], and the terms of the copyright licence assigned to the thesis by the Author.

In practice, and unless the copyright licence assigned by the author allows for more permissive use, this means,

- that any content or accompanying data cannot be extensively quoted, reproduced or changed without the written permission of the author / rights holder; and

- that the work in whole or part may not be sold commercially in any format or medium without the written permission of the author/rights holder.

Any third-party copyright material in this thesis remains the property of the original owner. Such third party copyright work included in the thesis will be clearly marked and attributed, and the original licence under which it was released will be specified. This material is not covered by the licence or terms assigned to the wider thesis and must be used in accordance with the original licence; or separate permission must be sought from the copyright holder.

The author assigns certain rights to the University of Plymouth including the right to make the thesis accessible and discoverable via the British Library's Electronic Thesis Online Service (EThOS) and the University research repository, and to undertake activities to migrate, preserve and maintain the medium, format and integrity of the deposited file for future discovery and use.

---

[1] *E.g.* in the example of third party copyright materials reused in the thesis.

[2] In accordance with best practice principles such as, Marking/Creators/Marking third party content (2013). Available from: https://wiki.creativecommons.org/wiki/Marking/Creators/Marking_third_party_content [accessed 28th February 2022]
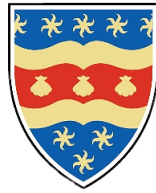
UNIVERSITY OF PLYMOUTH

Lysophosphatidylcholine acyltransferase-2 (LPCAT-2) & protein S-acylation in macrophage innate immunity

by

Christian Robin Good

A thesis submitted to the University of Plymouth

in partial fulfilment for the degree of

DOCTOR OF PHILOSOPHY

School of Biomedical Sciences

June 2024

Acknowledgements

I would like to start by expressing my deepest gratitude to Professor Simon Jackson for the guidance and financial support that enabled me to start this research. I'm extremely thankful to my PhD supervisory team Dr Gyorgy Fejer, Dr Wondwossen Abate and Professor Simon Jackson. Your continued support, guidance and feedback throughout my PhD journey have been invaluable.

I am grateful to everyone in and around the laboratory that I shared so much time working with for their help and support. I especially want to mention Dr Paul Waines, Dr Connor Wood, Justyna Lopatecka, Sean Kelly and Victory Poloamina for their technical help and advice.

Thanks of course to my family for their unwavering support. Finally, thank you to my wife Zoe for being supportive and patient.

Author Declaration

At no time during the registration for the degree of Doctor of Philosophy has the author been registered for any other University award without prior agreement of the Doctoral College Quality Sub-Committee.

Work submitted for this research degree at the University of Plymouth has not formed part of any other degree either at the University of Plymouth or at another establishment.

The following scientific seminars and conferences were attended:

Poster presentations:

Good, C. R., Abate, W., and Jackson, S., CD36/SR-B2 modulates murine macrophage cytokine production in response to E. coli lipopolysaccharide. British Society of Immunology conference 2017, Brighton, UK.

Good, C. R., Abate, W., and Jackson, S., CD36 modulates murine macrophage cytokine production in response to E. coli lipopolysaccharide. Annual Research Event 2018, Plymouth, UK.

Oral presentations:

Good, C. R., Research Progress Seminar 2017, Plymouth University. "LPCAT2 regulates the TLR4 receptor complex through acylation of accessory co-receptor proteins" (Oral presentation)

Word count of main body of thesis: 30,128

Signed:

Date: 06/08/2024

Abstract

Lysophosphatidylcholine acyltransferase-2 (LPCAT-2) & protein S-acylation in macrophage innate immunity

by Christian Robin Good

Lysophosphatidylcholine acyltransferase (LPCAT)2 is an enzyme involved in remodelling glycerophospholipids within cell membranes and the generation of platelet-activating factor. LPCAT2 also mediates lipopolysaccharide (LPS)-induced cytokine responses in both murine and human macrophages. Investigations into the mechanism behind LPCAT2 involvement into LPS-induced cytokine responses identified that LPCAT2 translocates to membrane lipid raft domains and associates with toll-like receptor (TLR)4 following activation by LPS. The mechanism behind this is not known, however LPCAT2 appears to have a role in regulating innate immune responses via lipid raft signalling complexes and understanding the molecular details of these mechanisms could help in the development of targeted anti-inflammatory therapies.

The aim of this thesis is to build on these findings to develop a detailed molecular analysis of the mechanisms by which LPCAT2 can regulate inflammatory responses in macrophages. It has been reported that LPCAT1 can catalyse the acylation of histone proteins. The addition of lipid groups to a protein can impact membrane-protein association, protein structure and protein stability ultimately affecting a proteins function. This gave rise to the main research question explored in this thesis: Does LPCAT2 play a role in the S-acylation of proteins involved in LPS signalling?

To identify if LPCAT2 plays a role in protein S-acylation in LPS stimulated macrophages, siRNAs were used to knockdown the protein expression of LPCAT2 in LPS stimulated RAW264.7 cells combined with acyl-biotin exchange chemistry, a method of purifying S-acylated proteins. The purified proteins could then be identified by tandem mass spectrometry and western blotting. Changes in the level of protein S-acylation could then be compared between cells expressing normal levels of LPCAT2 and cells expressing reduced levels of LPCAT2.

This thesis identified for the first time a link between LPCAT2 and protein S-acylation in LPS stimulated macrophages. Western blot analysis confirmed the acylation of the scavenger receptors CD36 and Lysosome membrane protein II. Further investigation established that CD36 positively regulates LPS induced cytokine responses in macrophages and that S-acylation of CD36 regulates both lipid raft association and surface expression. This highlights a mechanism in which LPCAT2 mediates the S-acylation of CD36 which is required for surface and lipid raft association where CD36 most likely influences LPS signalling. These findings are not only relevant to inflammatory conditions that are mediated by LPS and TLR4 signalling but could also have implications for various inflammatory diseases such as Atherosclerosis and Alzheimer's disease in which CD36 plays a major role in their pathology.

Contents

5 Conclusion

List of Figures

List of Tables

Chapter 1

Introduction

1.1 Innate immunity

The mammalian immune system can be broadly divided into two parts, the innate and the adaptive immune system [1]. Innate immunity is the first line of defence against a potential threat and can be characterised as being rapid and relatively non-specific. Examples of innate immune strategies include anatomical barriers, physiological barriers, phagocytic and endocytic barriers, and inflammation. There are a broad range of innate immune cells of both myeloid and lymphoid origin. These include neutrophils, mast cells, eosinophils, basophils, natural killer cells, dendritic cells, innate lymphoid cells, and macrophages [2]. A commonality amongst these cells is that they lack somatically recombined antigen-receptors and as a result they are unable to develop true immunologic memory that is a hallmark of the adaptive immune system [3]. By contrast, adaptive immunity involves antigen specific responses mediated by T- and B-lymphocytes and is highly specific, develops immunologic memory and is slower to respond to new pathogens. The development of adaptive immunity is critical when innate immunity is

1

unable to prevent or eliminate infection. However, both systems complement each other and deficiencies in either system will leave the host vulnerable [2].

1.2 Macrophages

Macrophages are a type of innate immune cell that are specialised in the detection, phagocytosis and elimination of microbes, apoptotic cells and other potentially harmful debris. Historically, macrophages were first discovered during the 1880s by Ilya Ilyich Metchnikoff a Russian born zoologist when he published a seminal paper identifying phagocytic cells in frogs [4] and he referred to these cells in Greek as "the big eaters" coining the name macrophages. He described how these cells were not only involved in host defence, but they were also key in removing dying cells during the metamorphosis of tadpoles to frogs and these observations hold true today as macrophages are known to phagocytose dying cells both in development and adult life, and to protect the host through innate immune mechanisms [5]. In 1908 Ilya Metchnikoff was awarded the Nobel Prize in Physiology or Medicine in recognition of his work on immunity.

Macrophages are a heterogeneous cell type that can be broadly divided into self-renewing tissue resident macrophages or monocytes derived macrophages [4, 5]. Tissue resident macrophages originate from the yolk sac or foetal liver during embryogenesis and differentiate into niche subsets of self-renewing tissue resident macrophages during development becoming highly specialised for the tissues they reside in. These specialised tissue resident macrophages include Microglia in the central nervous system, Kupffer cells in liver, Osteoblasts in bone, Langerhans cells in skin, and Alveolar macrophages in lung. Tissue resident macrophages carry out a range of homeostatic functions such as immune surveillance, inflammation,

and clearance of debris/dying cells and are the dominant macrophage during health [6]. In contrast, monocyte derived macrophages are short lived and develop postnatally from circulating monocytes that are recruited under inflammatory conditions allowing a rapid expansion in cell number to clear an infection or potential threat [7].

Macrophages are highly efficient phagocytic cells and are classed as professional phagocytes along with neutrophils, monocytes, and dendritic cells [8]. Phagocytosis is a process that involves the ingestion and elimination of particles greater than 0.5µm diameter and is the mechanism responsible for the clearance of bacteria, fungi, and apoptotic cells, which is a vital process to fight infection and resolve inflammation [9]. Phagocytosis is a targeted process that requires dedicated receptors to recognise a target particle. Upon binding to a receptor, the activation of signalling pathways lead to the remodelling of the cell membrane and actin cytoskeleton extending the membrane around the particle forming a phagosome [8]. The phagosome then sequentially fuses with endosomes and lysosomes to mature into phagolysosomes which are highly microbicidal compartments [10]. Within the phagolysosomes proteases such as cathepsins degrade proteins into short peptides that are loaded onto major histocompatibility complex (MHC) II molecules that are then transported to the cell surface [11]. Surface expressed MHC II molecules loaded with peptide in combination with additional co-stimulatory signals can then activate CD4$^+$ T lymphocytes, a process known as professional antigen presentation and illustrates how innate immunity bridges adaptive immunity [12].

In the setting of immune surveillance, macrophages act as sentinels detecting infiltrating microbes or tissue damage through an array of receptors known as pattern recognition receptors (PRRs). Upon detection of "Danger signals", macrophages respond by secreting signalling molecules such as cytokines,

nitric oxide, and lipid mediators, orchestrating the ensuing inflammatory response. Some examples are: the production of high levels of nitric oxide stimulate vascular smooth muscle cells to relax causing vasodilation and tissue oedema [13]. The cytokines interleukin (IL)-1β, IL-6 and tumour necrosis factor (TNF)α stimulate endothelial cells to upregulate the expression of adhesion molecules such as selectins and integrins, triggering the adhesion-recruitment cascade of neutrophils and monocytes [14]. The secretion of CXCL8 (IL-8), a chemotactic cytokine (chemokine), enhances cellular adhesion of neutrophils guiding them via a concentration gradient to the site of inflammation, a process called chemotaxis [15]. These examples illustrate how macrophages can modulate other cells to initiate inflammation.

Once an acute injury or infection is controlled, the tissue microenvironment will shift away from being pro-inflammatory towards being anti-inflammatory. The uptake of apoptotic cells at the site of injury supresses the expression of pro-inflammatory cytokines, while the expansion of regulatory T-cells within injured tissue release TGF-β and IL-10, driving an immunomodulatory macrophage phenotype that plays an important role in resolving inflammation and promoting tissue repair through the production of anti-inflammatory cytokines, growth factors, and matrix metalloproteinases [16].

Macrophages display plasticity and can adopt distinct phenotypes depending on their environment [17]. The exposure of macrophages to the Th1 cytokine interferon (IFN)γ in combination with LPS or TNFα enhances their cytotoxic activity and is called classical activation [18, 19]. In contrast, the exposure of macrophages to the Th2 cytokines IL-4 and IL-13 induce a different phenotype that exhibits reduced pro-inflammatory cytokine production, increased MHCII antigen expression and increased endocytic clearance of mannosylated ligands and is called alternative activation [18]. To mimic the

established Th1/Th2 nomenclature these states of macrophage polarisation are now more commonly referred to as M1 and M2 respectively. Other stimuli not linked with Th1 or Th2 responses also induce similar phenotypes to alternatively activated macrophages leading to further subdivisions of the M2 macrophage phenotype [20]. Under the subdivided M2 category, alternatively activated macrophages are designated as M2a. Binding of immune complexes to Fc receptors combined with activation of TLRs generates the M2b macrophage phenotype that drives Th2 responses by down-regulating IL-12 and up-regulating IL-10 production. Exposure to IL-10, a product of regulatory T-cells, leads to an immunomodulatory M2c macrophage involved in matrix deposition and tissue remodelling. Finally, there are tumour-associated macrophages that secrete high levels of IL-10, TGF-β, and VEGF and are designated as M2d [21].

The M1/M2 model of polarisation is a useful tool, however, this model often paints an overly simplistic and sometimes misleading view of macrophage biology *in vivo*. During pathological conditions, macrophages can be exposed to both M1 and M2 stimuli and can develop mixed M1/M2 phenotypes, as seen in inflammatory multiple sclerosis lesions. An intermediate macrophage activation state was shown to express both CD40 and mannose receptor which are M1 and M2 markers respectively [22]. Therefore, macrophage polarisation is best viewed as a dynamic process, the balance of activating stimuli can shift during pathology and macrophages will adapt to their environment.

This brief overview of macrophage function illustrates how macrophages are positioned throughout the immune response, from the initiation of inflammation to the resolution of inflammation, making the study of macrophages particularly interesting.

1.2.1 RAW264.7 cells

This project has used the RAW264.7 cells murine macrophage-like cell line as a model to study the role LPCAT-2 plays in protein S-acylation during inflammatory response to LPS. RAW264.7 cells were first established in 1978 from an ascites of an Abelson murine leukaemia virus-induced tumour in a male BALB/c mouse [23]. Since their discovery over 40 years ago, RAW264.7 cells have become one of the most used macrophage-like cell lines in biomedical research. These cells were initially characterised as being able to pinocytose neutral red, phagocytose zymosan and latex beads, kill antibody-coated erythrocytes and secrete lysozyme, all normal properties of macrophages. RAW264.7 cells express the typical markers expressed by murine macrophages such as F4/80, CD11b, CD11c, MHCII, TLR4 and CD14 [24].

In their basal state (M0), RAW264.7 cells posses the capacity to polarise into the proinflammatory M1 phenotype following stimulation with INFy and LPS or into an anti-inflammatory M2 phenotype following stimulation with IL-4 ad IL-13 [25, 26]. The M1 RAW264.7 phenotype showed increased expression of iNOS and MHCII while the M2 phenotype showed increase expression of CD163 and CD206. This highlights that despite originating from a BALB/c mouse, which have historically been used to predominantly study Th2 responses, RAW264.7 cells are a valid model to study Th1 proinflammatory pathologies. Moreover, RAW264.7 cells have been shown to be phenotypically and functionally stable for up to 30 passages [24].

Pioneering studies into LPCAT2 function initially used RAW264.7 cells to overexpress LPCAT2 for the first time and study its role as a catalyst of platelet-activating factor (PAF) [27]. Further mechanistic studies into LPCAT2 allosteric regulation also utilized RAW264.7 cells to investigate

phosphorylation at Ser[34] to enhance PAF production in LPS stimulated murine macrophages [28]. Tarui *et al*, [29] also utilised RAW264.7 cells to investigate the effect of selective inhibition of the PAF biosynthetic enzyme LPCAT2. This demonstrates a precedent for the use of RAW264.7 cells to study LPCAT2 in a proinflammatory setting.

1.3 Pattern recognition receptors (PRRs)

PRRs are a class of receptor that recognise molecules with distinct molecular structures that can originate from both self and non-self but share the commonality that they signal danger to the host. These molecules are collectively known as pathogen-associated molecular patterns (PAMPs) when originating from microbes or damage-associated molecular patterns (DAMPs) when originating from self resulting from tissue damage or stress. Examples of these are the PAMP LPS [30], a molecule present in the outer membrane of Gram-negative bacteria or the DAMP High-mobility group box 1 (HMBG1) that is an intracellular protein released by pyroptotic and necroptotic cell death [31].

There are five main types of PRRs in mammals and these are: TLRs, C-type lectin receptors, retinoic acid-inducible gene-I-like receptors, nucleotide oligomerization domain-like receptors (NLRs), and absent in melanoma-2-like receptors. In the simplest form PRR are comprised of three parts: a ligand binding domain, an intermediate domain, and an effector domain. Ligands are bound via the binding domain that in turn leads to the recruitment of adaptor proteins by the effector domains leading to the activation of signalling pathways and a specific response [32].

1.3.1 Toll-like receptors (TLRs)

TLRs are type I integral transmembrane glycoproteins comprised of an
N-terminal ectodomain consisting of 16-28 leucine-rich-repeats, a single
transmembrane helix domain and an intracellular C-terminal
toll–interleukin-1 receptor (TIR) homology domain that is required for the
recruitment and interaction of adaptor proteins [33]. TLRs are widely
expressed among subsets of both immune and non-immune cells such as
macrophages, monocytes, neutrophils, dendritic cells, T- and B-
lymphocytes, epithelial cells, and fibroblasts. There are ten functional TLRs
in humans (TLR1-10) and these can be divided based on their cellular
location, TLR1, 2, 4, 5, 6, and 10 are expressed on the cell surface, while
TLR3, 7, 8, and 9 are expressed intracellularly in endosomal membranes
[34]. Generally, intracellular TLRs recognize nucleic acids while surface
expressed TLRs recognize microbial cell wall and/or membrane components.
There is a diverse repertoire of ligands recognised by TLRs that can be either
of endogenous or exogenous origin and this diversity is in part due to the
ability of certain TLRs to form not only homodimers but also heterodimers
with other TLRs, some examples of TLR ligands and the dimers they form are
shown in table 1.1.

Table 1.1: Toll-like receptors and their associated ligands

Receptor	Exogenous Ligands	Endogenous Ligands
TLR1 + TLR2	Triacyl lipopeptides [35]	
TLR2		Glycosaminoglycan hyaluronan [36]
TLR2 + TLR6	Diacyl lipopeptides, Lipoteichoic acid [37]	
TLR3	Double-stranded RNA [38]	
TLR4	LPS [30]	HMBG1 [31]
TLR4 + TLR6		Oxidized LDL, β-amyloid [39]
TLR5	Flagellin [40]	
TLR7	Single-stranded RNA [41]	
TLR8	Single-stranded RNA [42]	
TLR9	Unmethylated CpG DNA [43]	
TLR10	Double-stranded RNA [44]	

1.3.2 Toll-like receptor 4 (TLR4)

TLR4 is a PRR that primarily recognises LPS and its activation requires the co-operation of several proteins. LPS is an amphipathic molecule and forms micelles in aqueous solutions, sequestering the hydrophobic lipid A moiety that is responsible for its endotoxic activity. The acute phase serum protein LPS-binding protein (LPB) is required to facilitate the transfer of LPS monomers from these micelles to the GPI-anchored glycoprotein CD14 located in cholesterol- and sphingolipid-rich microdomains of the plasma membrane termed lipid rafts [45]. Subsequently, CD14 transfers the LPS to the TLR4/MD-2 complex where a combination of charged phosphate groups and overhanging acyl chains of the lipid A moiety interact with neighbouring TLR4/MD-2 complexes facilitating dimerization of their extracellular domains [46]. In turn, the cytoplasmic Toll/interleukin-1 domains (TIRs) dimerise forming a scaffold for the recruitment of two pairs of adaptor proteins, MyD88/TIRAP and TRAM/TRIF triggering the MyD88-dependent and TRIF-dependent pathways respectively [47, 48]. Signalling cascades

originating from TIRAP/MyD88 result in the early-phase activation of NFκB
and MAP kinases that control the production of pro-inflammatory cytokines
like TNFα, IL-6 etc. Activation of TRAM/TRIF however, requires
CD14-dependent endocytosis of the activated TLR4 complex [49, 50] and
triggers a signalling cascade that activates interferon regulatory factor 3
(IRF3) leading to the expression of type I interferons (IFN), followed by the
late-phase activation of NFκB and MAP kinases (Figure 1.1). In addition to
CD14, other raft proteins like Lyn tyrosine kinase, acid sphingomyelinase,
CD44, heat shock proteins 70 and 90, and CD36 have been shown to
co-cluster with TLR4 and participate in signalling triggered by LPS or
endogenous ligands [51]. However, there is still much to learn about the
precise role these accessory proteins play in TLR4 signalling.
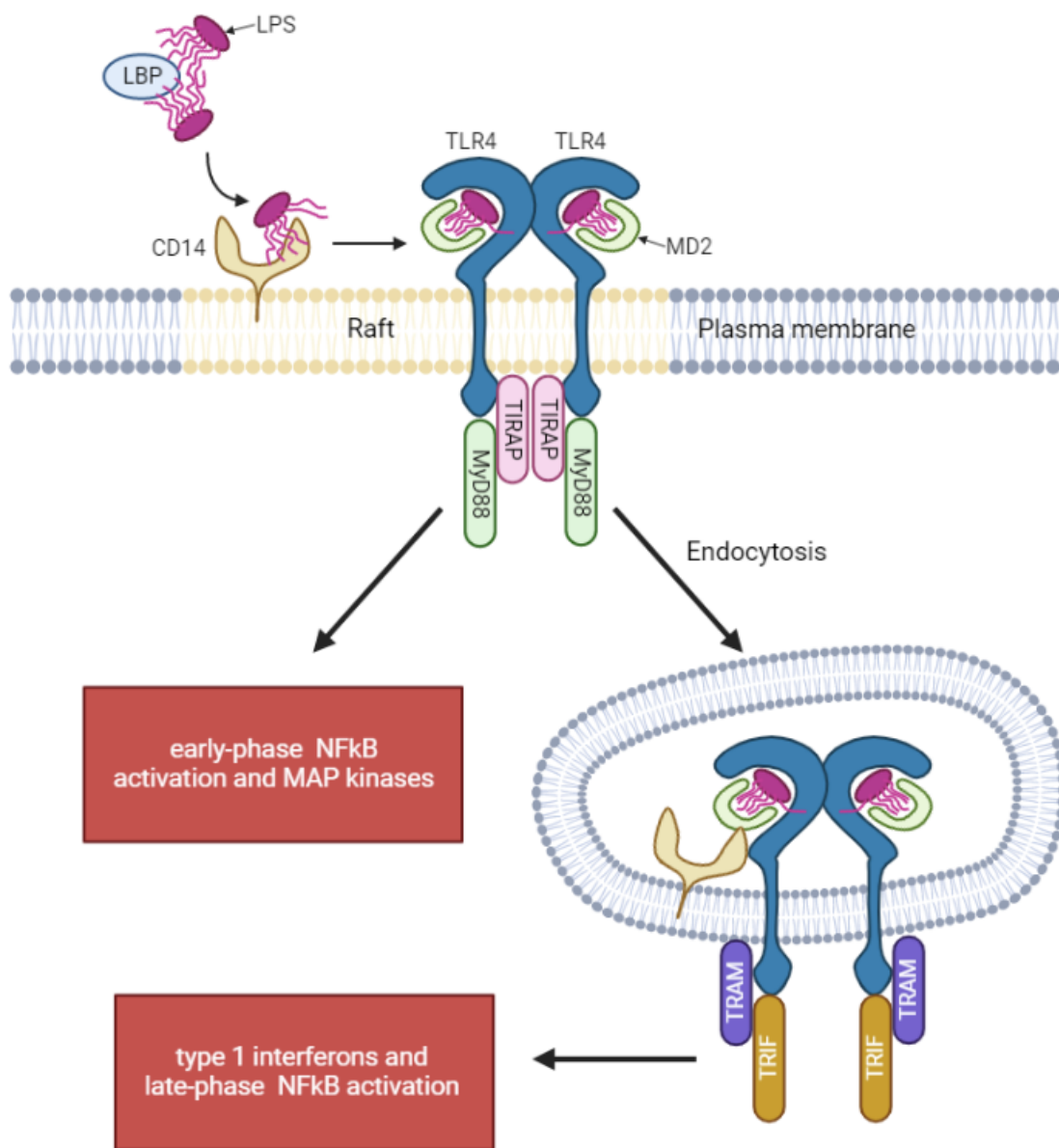
Figure 1.1: LPS activation of TLR4 through the co-operation of associated proteins. LBP and CD14 facilitate the transfer of LPS to the TLR4/MD2 complex, causing dimerisation with neighboring TLR4/MD2 complexes. This enables the assembly of the adapter proteins TIRAP/MyD88 resulting in a signaling cascade that culminates in the production proinflammatory cytokines. CD14 mediated endocytosis of the receptor complex allows the assembly of the adapter proteins TRAM/TRIF leading to the expression of type I interferons and pro-inflammatory cytokines. MD2:myeloid differentiation factor 2, MyD88:myeloid differentiation primary response gene 88,TIRAP:TIR domain-containing adaptor protein,TRAM:TRIF-related adaptor molecule, TRIF:TIR-domain-containing adapter-inducing interferon-β. Adapted from [51].

1.4   Scavenger receptors

Scavenger receptors are large superfamily of proteins that are grouped together into classes based on their ligand preferences and currently there are twelve classes of scavenger receptor (class A-L) [52]. Primarily expressed by myeloid cells, scavenger receptors function by recognising a diverse repertoire of ligands and internalising them. These ligands are usually PAMPs or DAMPs but also include other endogenous molecules such as lipoproteins, apoptotic cells, cholesterol ester and phospholipids etc. By removing these potentially harmful molecules scavenger receptors play a key role in maintaining homeostasis [53].

1.4.1   CD36

CD36 is an 88-KDa transmembrane glycoprotein [54] that functions as a scavenger receptor, recognising many ligands of endogenous and exogenous origin. First identified in human platelets it was named platelet glycoprotein IV [55], then later identified as the putative fatty acid translocase in adipose tissue and named FAT [56]. Following the standardisation of scavenger receptor nomenclature, the latest designation for CD36 is scavenger recepter-B2 (SR-B2) [53], however the cluster of differentiation (CD) nomenclature is mainly used.

Many cell types express CD36, including epithelial cells, endothelial cells, adipocytes, hepatocytes, myocytes, and the professional phagocytes: monocytes, macrophages, dendritic cells and neutrophils [57]. This ubiquitous expression reflects the many ligands and functions that have been attributed to CD36 (Table 1.2). Although the repertoire of ligands associated with CD36 are many, they generally all share the common

features of being lipid-based and/or are polyanionic.

Table 1.2: CD36 ligands and associated functions.

Ligand	Cell type/Function/Year identified
Thrombospondin-1	Endothelial cells, negative regulator of angiogenesis (1987) [58].
Phosphatidylserine	Macrophages, phagocytosis/clearance of apoptotic cells (1992) [59].
Longchain fatty acids	Adipocytes, myocytes, uptake of longchain fatty acids (1993) [60].
Oxidised low density lipoprotein	Macrophages, endocytic clearance, foam cell formation, inflammation (1993) [61].
Advanced glycation endproducts	Macrophages, endocytic clearance (2002) [62].
β-Amyloid	Microglia, endocytic clearance, induces inflammation (2003) [63].
Falciparum malaria infected erythrocytes	Macrophages, opsonin-independent pathogen phagocytosis (2003 [64].
Lipoproteins	Macrophages, co-receptor for di-acylglyceride recognition through the TLR2/6 complex (2005) [65].
LPS (*H. pylori* and *P. gingivalis*)	Endothelial cells & HEK-293 cells, co-receptor for LPS recognition through the TLR2/1 complex (2007) [66].
LPS (*E. coli* K12) & LTA (*S. aureus*)	HEK-293 and HeLa cells, cJUN N-terminal kinase (JNK) signaling independent of TLR2/4 (2008) [67].
β-Glucan	Macrophages, host defense against fungal pathogens (2009) [68].
E. coli, LPS or Chaperonin 60	HeLa cells, recognizing and mediating inflammatory signaling (2012) [69].
LPS (*E. coli* K12 or O111:B4)	Macrophages, positively regulates signaling (serum free), negatively regulates signaling (with serum) (2016) [70].
LPS (*E. coli*) or *E. coli*	Epithelial cells, TLR4-mediated phagocytosis of *E. coli*, positively regulates LPS signaling (2016) [71].
LPS (*K. pneumoniae*) or *K. pneumoniae*	Host protection against infection *in vivo*, CD36 enhances LPS responsiveness *in vitro* (2016) [72].

CD36 has a large extracellular loop with two transmembrane domains and two short cytoplasmic tails at the N-terminus and C-terminus [73]. The extracellular loop contains three distinct ligand binding sites, there are lysine clusters that binds negatively charged ligands [74], a hydrophobic cavity that forms a tunnel for hydrophobic molecules to access the outer leaflet of the membrane [75] and a negatively charged CD36, LIMPII, Emp sequence

homology (CLESH) domain that interacts with thrombospondin-1 [76]. Several post-translational modifications of CD36 have been identified, these are phosphorylation [77], glycosylation [56], ubiquitylation [78], S-acylation [79] and acetylation [80]. Glycosylation, ubiquitination and palmitoylation have regulatory effects on CD36 trafficking between plasma membranes and intracellular compartments, while phosphorylation and lysine acetylation have been shown to regulate fatty acid uptake (Figure 1.2).
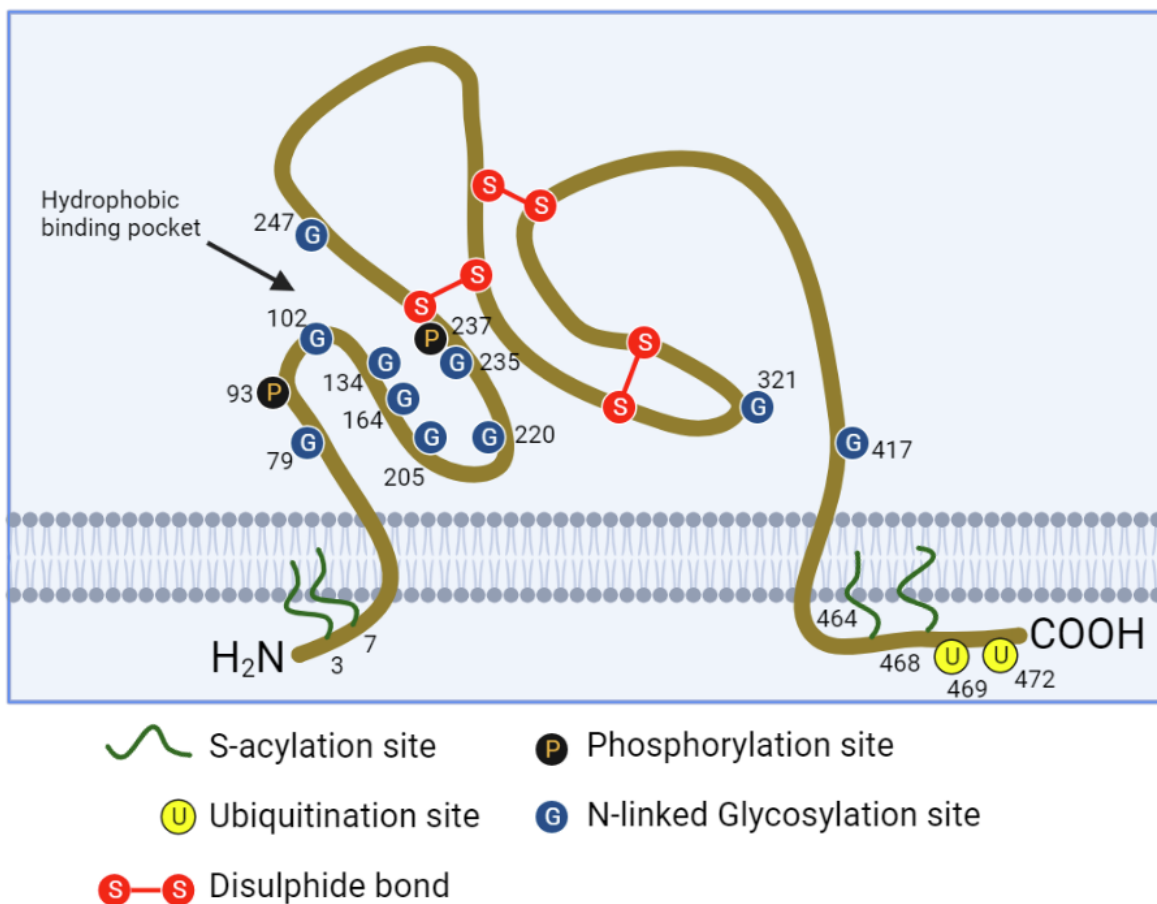
Figure 1.2: CD36 structure. Adapted from [81].

The cytoplasmic tails of CD36 are S-acylated at cysteines 3, 7, 464, and 466, anchoring them into the membrane [79]. The inhibition of S-acylation at these sites, either pharmacologically or by mutation, revealed that these modifications facilitate efficient processing at the endoplasmic reticulum and trafficking through the secretory pathway but are not required for surface expression of CD36. Additionally, the lack of S-acylation reduced the half-life

of the CD36 protein and prevented its efficient incorporation into lipid rafts [82]. In the setting of innate immunity, CD36 clearly plays a role in the detection of a variety of microbial molecular patterns (Table 1.2), yet precisely what those roles are remain somewhat unclear. One line of reasoning is that CD36 acts as a co-receptor, like CD14, delivering bacterial components to TLRs [70, 65, 66]. In response to the endogenous ligands, oxidized low-density lipoprotein (oxLDL) or β-amyloid, CD36 becomes phosphorylated on Tyr463 and associates with Lyn tyrosine kinase, TLR4 and TLR6 forming a heteromeric complex that signal via the MyD88- and TRIF-dependant pathways [39]. This highlights a mechanism in which CD36 can facilitate the dimerization of different TLRs to broaden their ligand repertoire. It has also been reported that CD36 can detect LPS or LTA independent of TLRs, inducing JNK-dependent pro-inflammatory cytokines in HEK293 and HeLa epithelial cell lines transfected with CD36 [67]. Macrophages from C3H/HeJ mice with a loss of function mutation in the TLR4 gene, however, fail to produce inflammatory cytokines in response to LPS [83], this highlights possible differences between how CD36 behaves in various cell types.

There are also conflicting reports on the effect of CD36-deffciency on macrophage responses to LPS, with some studies finding no effect [65, 84, 85], while a more recent study found it reduced LPS responsiveness [72]. Another study found the role of CD36 in LPS detection to be dependent on both LPS chemotype and the presence of serum [70]. This highlights the need to investigate the role CD36 plays in the detection of LPS and other ligands further.

1.4.2 Lysosomal integral membrane protein-II (LIMPII)

LIMPII (also known as LGP85) is a transmembrane glycoprotein belonging to the CD36 superfamily of scavenger receptors. Structurally LIMPII is similar to CD36 with both proteins having C- and N- terminal domains located in the cytoplasm, two hydrophobic membrane spanning domains and a large looped domain that is highly glycosylated. A feature distinguishing LIMPII from CD36 however is that it is located in the membranes of lysosomes and late endosomes and not on the cell surface [75].

The overexpression of LIMPII in COS1 cells resulted in the enlargement of endosomes and lysosomes revealing a role for LIMPII in their biogenesis and maintenance [86]. Further studies identified LIMPII as a binding partner for the enzyme beta-glucocerebrosidase facilitating its transport from the endoplasmic reticulum into lysosomes [87] and the deficiency of which causes Gaucher disease, a type of lysosomal storage disease [88].

LIMPII deficient mice display defective macrophage activation in response to *Listeria monocytogenes* infection, producing less of the acute phase cytokines TNFα, IL-6, and monocyte chemoattractant protein-1 (MCP-1/CCL2) leading to a 25-fold increase susceptibility to *Listeria* infection [89]. Impaired endosomal/lysosomal fusion prevented the microbicidal activity of phagosomes and the loading of peptide onto MHCII contributing to this phenotype. LIMPII has also been shown to mediate the endosomal translocation of TLR9 in plasmacytoid dendritic cells, regulating interferon alpha production in response to the synthetic TLR9 ligand CpG [90].

More recently LIMPII has been identified as a receptor for phospholipids and cholesterol in cellular uptake experiments using murine fibroblasts [91]. A cavity in the luminal loop has been shown to deliver cholesterol to the lysosomal membrane and later to lipid droplets [92].

1.5   Cytokines

Cytokines are small secreted proteins that enable cells to communicate and coordinate an effective immune response. For a cytokine to elicit an effect, a target cell is required to express a complimentary cytokine receptor and engagement of which triggers intracellular signalling cascades leading to altered gene expression. Secreted cytokines can act on distant cells (endocrine signalling), near cells (paracrine signalling), and on the same cell (autocrine signalling) [93]. Many cytokines have overlapping activities, such as IL-6, TNFα and IL-1β which all induce the acute phase response, among other functions [94].

1.5.1   Tumour necrosis factor alpha (TNFα)

First identified as a serum protein that induced cell death in tumour cells [95], TNFα is now known to be a proinflammatory cytokine produced early during inflammation primarily by monocytes and macrophages [96]. Initially TNFα is produced as a 26 KDa transmembrane protein expressed on the cell surface and can be actively cleaved by TNF alpha converting enzyme to yield a 17 KDa soluble form, both of which are biologically active [97]. There are two receptors for TNFα, TNF receptor (TNFR) 1 and 2, with the former being expressed on all tissues and the latter being primarily expressed on immune cells, neurons, and endothelial cells [98]. A major difference between TNFR 1 and 2 is the structure of their intracellular domains, TNFR1's cytoplasmic tail contains a death domain that recruits TNFR1-associated death domain (TRADD), an adaptor protein that can induce a cell death response and/or lead to the activation of nuclear factor-kappa B (NF-$\varkappa$B) [99]. TNFR2 does not contain a death domain and alternatively recruits TNFR associated factor (TRAF) 1 and 2 proteins leading to the activation of NF-$\varkappa$B [100]. Both

receptors can induce a cell survival response and cross talk between TNFR 1 and 2, and the cellular environment dictate the outcome of TNFR signalling [101, 102].

1.5.2   Interleukin-1 beta (IL-1β)

The IL1 family of cytokines consists of 11 members with a diverse range of effects of which IL-1β is a member that has potent pro-inflammatory role [103]. IL-1β is initially translated as an inactive precursor called pro-IL-1β that is transcribed following NF-$\varkappa$B activation. Following the initial priming event that produces pro-IL-1β, a second step is required to produce mature active IL1 β. The second step requires the activation of cytosolic PRRs, such as NLRs, to form large protein complexes called inflammasomes which are composed of a PRR, pro-caspase-1 and apoptosis-associated speck-like protein containing a caspase recruitment domain [104]. Activation of the inflammasome leads to the cleavage of pro-IL-1 β to the mature form by caspase-1 and the mature IL-1 β is then secreted [105].

Secreted IL-1 β only exerts an effect once recognised by cell surface receptors and there are two IL-1 receptors: IL-1 receptor type 1 (IL-1R1) and IL-1 type 2 receptor (IL-1R2). IL-1R2 is a decoy receptor that dampens IL1 responses, while IL-1R1 initiates signal transduction [106]. Upon binding IL-1 β, IL-1R1 forms a complex with IL-1R accessory protein bringing together their ectodomains that contain TIR domains initiating MyD88 signalling pathways [107]. IL-1R1 is reported to be expressed by endothelial cell, T-lymphocytes, epithelial cells, and fibroblasts while IL-1R2 is primarily expressed on haematopoietic cells [108].

1.5.3   Interleukin-6 (IL-6)

IL-6 is a predominantly pro-inflammatory cytokine that has a protective role in many infections, however chronic IL-6 signalling plays a central role in many inflammatory diseases such as Rheumatoid arthritis [109], castleman disease [110], and inflammatory bowel disease [111]. At the cellular level IL-6 has many roles such as inducing the production of acute phase serum proteins by hepatocytes [112], inducing the proliferation of T-cells [113], inducing the maturation of B-cells, and stimulating the production and release of immunoglobulins [114, 115].

IL-6 signalling requires the formation of an IL-6 and IL-6 receptor (IL-6R) complex that once formed associates with glycoprotein130 (gp130) initiating intracellular signalling via the RAS-dependent MAPK signalling cascade, and the Janus kinase (JAK) and signal transducer and activator of transcription (STAT) pathway [116]. Only hepatocytes, leukocytes and some epithelial cells express IL-6R whereas gp130 is ubiquitously expressed. Cells that express both IL-6R and gp130 respond to IL-6 by the classical pathway which relies on membrane bound receptors. Alternatively, soluble IL 6R which is produced by cleavage of membrane-bound IL 6R by a disintegrin and metalloproteinase domain-containing protein 17 can bind IL-6 and activate cells that only express gp130, known as IL-6 trans-signalling [117].

1.5.4   Interleukin-10 (IL-10)

IL-10 is an anti-inflammatory cytokine that was first discovered over 30 years ago as a factor released by Th2 cells that inhibited the production of cytokines by Th1 cells and was originally named cytokine synthesis inhibitory factor (CSIF) [118]. It is now known that cells of both the lymphoid

and myeloid lineage produce IL-10, and these include CD4^{+} and CD8^{+} T cells, B cells, monocytes/macrophages, dendritic cells, neutrophils, natural killer cells, eosinophils, and mast cells [119].

To induce a cellular response IL-10 needs to bind the IL-10 receptor (IL-10R) which is composed of two subunits, the IL-10Rα and IL-10Rβ. Engagement of the IL-10R leads to the recruitment and activation of STAT3 that is the predominant driver of the IL-10 mediated anti-inflammatory response [120]. Macrophages express the highest level of the IL-10R as compared to other cell types [121], and the activation of which supresses the transcription of cytokines [122], MHCII molecules, co-stimulatory molecules and adhesion molecules [123, 124]. Other responses to IL-10 stimulation include the inhibition of nitric oxide biosynthesis that leads to a reduced microbicidal activity [125]. IL-10 can directly modulate T-cell responses by inducing CD4^{+} T-cell anergy [126] and by promoting Foxp3 expression in regulatory T cells [127] to name some example. Due to the widespread anti-inflammatory properties of IL-10 it is no surprise that there has been a lot of interest in its therapeutic manipulation for inflammatory diseases such as rheumatoid arthritis [128], psoriasis [129], or inflammatory bowel disease [130].

1.5.5   Interferon beta (IFNβ)

IFNs have been divided into three families based on their complementary receptor, these are type I-III. The type I IFN family which consists of IFNα subtype 1-13, IFNβ, and the less well-defined cytokines IFNε, IFNτ, IFNϰ, IFNω, IFNδ and IFNζ [131]. Type 1 IFNs signal through a heterodimeric transmembrane receptor composed of the interferon alpha and beta receptor subunit (IFNAR) 1 and IFNAR2 subunits, ligation of the IFNAR activates the JAK/STAT pathways inducing around 2000 IFN-stimulated gene products

that mount a predominantly antiviral state and can be both detrimental and protective during bacterial infection [132].

1.6 Lipid rafts

Plasma membranes are composed of hundreds of different lipid subtypes with some interacting more favourably with each other than others. The interaction of saturated sphingolipids, cholesterol, and certain proteins form dynamic nanoscale assemblies and these are known as lipid rafts [133]. The formation of lipid rafts compartmentalises proteins/receptors with regulatory and/or effector molecules serving as critical platforms for signal transduction.

The concept of lipid rafts initially faced scepticism due to a lack of direct visualisation and the reliance on biochemical methods that use cold temperature detergent solubilisation to generate detergent resistant membranes that are inherently prone to developing artifacts [133]. However, the lipid raft hypothesis has now been largely accepted due to technological advances enabling extensive reporting on the detection of nanoscopic lipid domains, these techniques include: electron microscopy [134, 135], single-molecule tracking [136], super-resolution diffusion [137, 138], fluorescence quenching [139] and fluorescence resonance energy transfer [140, 141, 142, 143, 144].

Due to the high content of saturated acyl chains of sphingolipids within lipid rafts, the thickness of the lipid bilayer and packing of lipids is much greater than that of the surrounding bilayer that is composed primarily of unsaturated glycerophospholipids. This makes the insertion of proteins that are modified with saturated fatty acids into lipid rafts energetically favourable

such as proteins with a glycosylphosphatidylinositol (GPI) anchor or palmitoyl moiety. Conversely, proteins with branched or unsaturated anchors such as prenyl groups prefer non-raft regions [145].

1.7   Protein S-acylation

S-acylation is a type of posttranslational modification that involves the covalent binding of a lipid group to a protein. The addition of these lipid groups can impact membrane-protein association, protein structure and protein stability through increased protein hydrophobicity and this will ultimately affect a proteins function [146, 147]. The most common lipid attached to a protein by S-acylation is the 16-carbon saturated fatty acid palmitate, via the intracellular fatty acid donor palmitoyl CoA and therefore this modification is also described as palmitoylation or S-palmitoylation [148]. Unique among lipid modifications, the thioester bond formed by S-acylation is reversible allowing dynamic regulation of this modification in a similar way to protein phosphorylation or ubiquitination. This reversibility makes S-acylation a particularly interesting posttranslational modification to investigate in terms of cell signalling.

S-acylation of proteins has been attributed to a group of protein acyltransferases that contain a common 51 amino acid zinc finger domain containing a conserved DHHC (Asp-His-His-Cys) motif [149]. In humans there are 23 genes encoding proteins containing this DHHC motif, however not all these proteins have been confirmed as S-acyl transferases. These DHHC S-acyl transferases are integral membrane proteins that are predicted to have four to six transmembrane domains with their active site facing the cytoplasmic side of the membrane and are localised to the ER and Golgi, with a small proportion located on post-Golgi compartments [150].

There appears to be a certain degree of redundancy with the substrate specificity of DHHC enzymes. Single DHHC enzymes can have many different protein substrates such as DHHC7 which has been reported to S-acylate Fyn, Fas, Fas Ligand, TLR2 and STING to name a few [151, 152, 153, 154, 155]. Likewise, a single protein can be the substrate for multiple DHHC enzymes such as DHHC2, 3, 6, 7 and 15 have all been reported to S-acylate TLR2 [151]. However, it has also been observed that certain substrates require a specific DHHC enzyme for efficient S-acylation to occur. This was initially shown using knockout experiments targeting single DHHC enzymes in the yeast *Saccharomyces cerevisiae* [156] and has been demonstrated more recently in mammalian cells. For example, bone marrow derived macrophages generated from DHHC5 knockout mice displayed decreased NOD1/2 membrane association and activation due to impaired S-acylation demonstrating that a single DHHC enzyme is critical for this modification [157].

Numerous studies have tried to identify consensus sequences responsible for specific enzyme-substrate pairs, but they have been unable to robustly predict these interactions [158, 159, 160]. The promiscuity of DHHC enzymes and the difficulty identifying consensus sequences raises questions about how these enzymes can display substrate specificity. One hypothesis is that spatial organisation may be critical for this [161]. This can be illustrated by two functionally redundant enzymes DHHC5 and DHHC8 that are located in two distinct domains of hippocampal neurons, dendritic shafts and the synapse respectively. Glutamate receptor-interacting protein 1 (GRIP1) is a substrate for both DHHC5 and DHHC8, however GRIP1 co-localises with DHHC5 in the dendritic shafts of hippocampal neurons while DHHC8 is spatially separate within the synapse. Knockdown of DHHC8 therefore has little effect on GRIP1 S-acylation highlighting how compartmentalisation is critical to substrate specificity of DHHC enzymes [162, 163].

The availability of fatty acid donors for S-acylation can markedly affect the type of fatty acids that are incorporated onto proteins [164], with fatty acids ranging from shorter 14-carbon to longer 26-carbon acyl chains being found to be attached via S-acylation [165].

Less is known about the deacylation of S-acylated proteins, but two groups of acyl thioesterases of the serine hydrolase family have been characterised to date. There are the protein palmitoyl thioesterases that are located within lysosomes and catalyse deacylation during protein degradation [166], and the acyl protein thioesterases that are cytoplasmic enzymes implicated in dynamic deacylation of proteins [167].

The reversible nature of protein S-acylation allows cycles of palmitoylation and depalmitoylation that can dynamically alter the localisation and activity of proteins. For example, the small G proteins N-Ras and H-Ras are shuttled between membrane domains and the cytosol by cycles of palmitoylation and depalmitoylation regulating their activity [147]. Furthermore, varying length saturated and polyunsaturated fatty acids can be attached to S-acylated proteins, including myristate, palmitoleate, stearate, oleate, arachidonate and eicosapentanoate, with functional consequences [168, 146, 169]. For example, S-acylation of Src family kinases with unsaturated or polyunsaturated fatty acids reduces lipid raft localisation compared to acylation with saturated fatty acids [146]. Although S-acylation has been shown to regulate the activity of proteins, not much information is known about how this dynamic process is itself regulated.

1.8   Lysophosphatidylcholine acyltransferase 2 (LPCAT2)

Glycerophospholipids are the main component of cell membranes and are generated *de novo* by the Kennedy pathway [170]. Fatty acids attached at the sn-2 position of glycerophospholipids can be liberated by phospholipase A2s and utilised to produce lipid mediators such as eicosanoids or platelet activating factor [171]. A glycerophospholipid with a vacant sn-2 carbon is termed a lysophospholipid and can be remodelled by the activity of lysophospholipid acyltransferases (LPLATs) in an acyl-CoA dependant reaction. This remodelling pathway allows for much greater diversity in the fatty acid composition of glycerophospholipids and is known as the Lands cycle [172] (Figure 1.3). LPCAT2 is an LPLAT with a substrate preference for lysophosphatidylcholine as an acyl acceptor and arachidonyl-CoA (C20:4) as the acyl donor [27]. Other LPCAT2 acyl acceptors include: lyophosphatidic acid and lysophosphatidylserine, and other acyl donors include: oleoyl-CoA (C18:1), palmitoyl-CoA (C16:0), linoleoyl-CoA (C18:2) and heptadecanoyl-CoA (C17:0) [173].
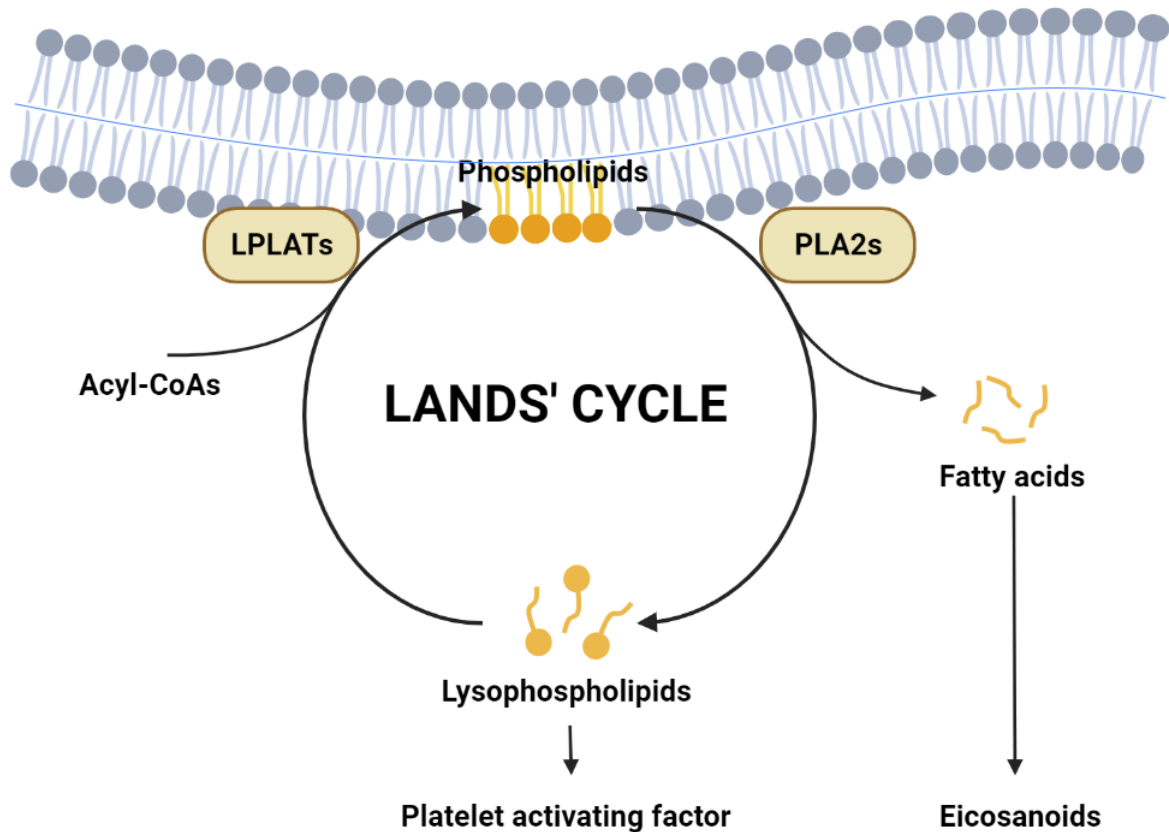
Figure 1.3: The Lands' cycle [172]. LPLATs:Lysophospholipid acyltransferases, PLA2s:Phospholipase A2s.

In addition to acyltransferase activity, LPCAT2 has been identified as having lyso-platelet-activating factor (PAF) acetyltransferase activity [27]. In macrophages, the acetyltransferase activity of LPCAT2 is enhanced by phosphorylation of serine residue 34 by protein kinase C alpha following a 1 minute stimulation with PAF or ATP [174] or following a 30 minute stimulation with LPS by MAP kinase-activated protein kinase 2 [28]. LPCAT2 contains putative EF-hand-like motifs and phosphorylation of serine residue 34 is dependent on intracellular calcium levels being elevated [174]. The expression of LPCAT2 is upregulated following 16 hour LPS stimulation at both the mRNA and protein level [27].

The highest level of LPCAT2 expression is found within immune cells such as resident macrophages, casein-induced neutrophils, and thioglycolate-induced macrophages [27]. LPCAT2 is a 60 KDa monotopic

membrane protein [175] that contains a KKXX endoplasmic reticulum retention motif at the C-terminal and is primarily located within the endoplasmic reticulum [27]. LPCAT2 also localises to the surface of lipid droplets where it synthesises phosphatidylcholine and lipid droplet growth [175, 176]. Following stimulation of macrophages with LPS, LPCAT2 has also been shown to translocate to membrane lipid raft domains and associate with TLR4 [177]. This association with TLR4 facilitates TNFα and IL-6 expression at both the mRNA and protein level via activation of p38 mitogen-activated protein kinase. Recently, the mechanism by which LPCAT2 regulates TLR4 translocation into lipid rafts was explored further and acetylated lysine residues were detected on TLR4 and the acetylation of these residues were influenced by LPCAT2 expression, however the role of these lipidations remain to be elucidated [178].

1.9 Sepsis

Sepsis is fundamentally an inflammatory disorder that is triggered by excessive activation of the host immune system by bacteria, viruses, fungi and/or tissue damage. Binding of PAMPs and DAMPs to PRRs on immune, epithelial, and endothelial cells initiate signalling pathways that generally result in the activation of transcription factors such as NF-$\varkappa$B, interferon regulatory factors, and activator protein 1 that are responsible for the early induction of pro-inflammatory cytokines and other inflammatory mediators [179]. The release of cytokines such as IL-1β, IL-6 and TNFα initiate inflammation which is vital for rapid clearance of infection, however during sepsis the magnitude of the stimulus is often far greater than regular infection leading to aberrant responses that can produce excessive inflammatory mediators which can ultimately lead to the cardiovascular

derangements and organ dysfunction that are the hallmarks of sepsis and septic shock [180, 181]. During inflammation the cytokines IL-1β, IL-6, IL-8, and TNFα stimulate endothelial cells, monocytes, and macrophages to increase the expression of tissue factor, a protein that initiates coagulation [182]. At a local level coagulation is a protective mechanism that not only prevents bleeding in the case of trauma but also helps contain infection [183], however during sepsis excessive activation of coagulation cascades can lead to the development of disseminated intravascular coagulation that is an independent predictor of organ failure and mortality [184]. The levels of the inflammatory mediators prostacyclin and nitric oxide are elevated during septic shock and are responsible for refractory hypotension [185, 186]. Both prostacyclin and nitric oxide regulate the tone of vascular smooth muscle cells and at elevated concentrations relax vascular smooth muscle causing vasodilation that results in relative hypovolemia. Reduced perfusion of vital tissues ensues leading to inadequate oxygen delivery to cells and the accumulation of metabolites that can cause cell damage or death [187].

Paradoxically, immunosuppression can occur during sepsis. Patients that survive the initial storm of cytokines during the early phase of sepsis can enter a protracted immunosuppressed state, leaving them vulnerable to secondary infection by opportunistic pathogens [188]. This immunosuppressed state is called the persistent inflammation/immunosuppression and catabolism syndrome (PICS) and is characterised by immune cell death, tolerance, and dysfunction [189]. Apoptosis during sepsis drives the depletion of dendritic cells [190], B cells, CD4^{+} T cells, and CD8^{+} T cells [191, 192] resulting in lymphopenia which is a positive predictor for sepsis mortality [193]. Uptake of apoptotic cells by macrophages supresses pro-inflammatory cytokine production and induces the release of anti-inflammatory cytokines IL-10 and TGF-β [194, 195]. Additionally, during PICS macrophages and dendritic cells fail to express the

MHCII molecule human leukocyte antigen-antigen D related (HLA-DR) skewing the T-cell phenotype towards a suppressive T helper (Th) 2 phenotype. Furthermore, FoxP3+ (forkhead box P3) regulatory T cells are not subjected to apoptosis, exacerbating the immunosuppressive state [196].

Attempts to modulate the proinflammatory response, although largely successful in animal models, have proven unsuccessful in clinical sepsis trials [197, 198, 199]. A common experimental rodent model of sepsis involves intravenous or intraperitoneal injection of LPS [200]. In these models, the serum levels of IL-6, TNFα and IL-1 are drastically elevated [201, 202], similar to patients with sepsis [180, 181]. Blockade of TNFα using anti-TNFα antibodies blunted the pulmonary neutrophilia and prevented peripheral blood changes in mice following intraperitoneal LPS injection showing promise as a potential strategy to treat sepsis in humans [201]. Based on the success of animal studies blocking TNFα, clinical trials were undertaken using a TNFR:Fc fusion protein, however this approach did not reduce mortality, and at higher doses appeared to be associated with increased mortality [203].

Experimental evidence also demonstrates the importance of TLR expression on various cell types during sepsis. Peripheral blood mononuclear cells from sepsis patients have up-regulated expression of both TLR2 and TLR4 compared to healthy individuals [204]. Experimental peritonitis induced by cecum ligation and puncture in mice demonstrated that TLR2 and TLR4 mRNA and protein expression in the lungs and liver was significantly upregulated compared to controls and that expression correlated with mortality. Blunting TLR gene and protein expression with glucan phosphate improved long-term survival of these mice [205]. Moreover, using antagonistic antibodies to block TLR2 and TLR4 in sepsis models of Gram-positive and Gram-negative bacteria was successful at decreasing

disease severity [206, 207]. Blocking TLR activation with therapeutic compounds showed much promise in animal models, however fell short again in clinical trials. TAK-242, a small-molecule inhibitor of TLR4 failed to supress IL-6 cytokine levels and improve 28-day mortality rates in patients with sepsis and shock or respiratory failure [208].

One reason given for failed clinical trials blocking specific pathways is due to inherent redundancies built into immune responses, such as the cytokines IL-1β, IL-6, IL-8, and TNFα that can all activate coagulation pathways [182]. Another explanation for the different outcomes observed between animal models and clinical trials is that patients presenting with sepsis or septic shock may have progressed past the initial proinflammatory stage of pathology and be in a state of immunosuppression at which point blocking proinflammatory mediators would be counterproductive. Animal models mimic the early proinflammatory stage of sepsis which would benefit from early anti-inflammatory intervention to limit the production of inflammatory mediators and the tissue damage that ensues, leading to favourable outcomes.

The repurposing of immune adjuvants used in cancer treatment are being trailed to reverse sepsis-induced immune suppression to prevent secondary infection [209]. One compound, nivolumab, a human programmed death-1 immune checkpoint inhibitor recently passed phase 1/2 clinical trials. Results showed that nivolumab was well tolerated, and absolute lymphocyte counts and monocyte human leukocyte antigen-DR subtype expression levels increase over time [210].

Retrospective analysis of clinical trials targeting TNFα and IL-1 receptor have shown significant benefit in specific sub-groups of patients [199], highlighting that a blanket approach to treating sepsis cannot be adopted and immunophenotyping patients will be vital to identify the particular

sepsis phenotype enabling clinicians to administer appropriate treatment. It seems evident that the shortcomings of many sepsis clinical trials are due to an oversimplification of what is a complex condition. An approach of tailored medicine through immunophenotyping patients coupled to the identification of new regulatory pathways involved in inflammation will be needed to effectively treat sepsis.

1.10   Rationale and aims

Early work by Professor Jackson's research group identified alterations to the molecular species of membrane phospholipids in activated macrophages [211] and this led to the identification of the LPCAT enzymes playing a key role in LPS-induced macrophage activation [212, 213, 214]. Four enzymes with LPCAT activity have been cloned and characterised to date, LPCAT1-4 [215] and of these LPCAT2 has been shown to be highly expressed in macrophages and to be induced by LPS treatment [27]. Recently, using RNAi knockdown, researchers in Professor Jackson's research group demonstrated that LPCAT2 is the key LPCAT to mediate LPS-induced responses in both murine and human macrophages [216] and that LPCAT2 translocates to membrane lipid raft domains and associate with TLR4 following activation by LPS [177]. As such, LPCAT2 appears to have a role in regulating innate responses via lipid raft signalling complexes and understanding the molecular details of these mechanisms will be key to the development of targeted anti-inflammatory therapies that could be used to treat inflammatory disorders like sepsis. Therefore, the aim of this thesis is to build on these findings to develop a detailed molecular analysis of the mechanisms by which LPCAT2 can regulate inflammatory responses in macrophages.

It has been reported that LPCAT1, in addition to the acylation of LPC, can catalyse histone protein O-palmitoylation to regulate mRNA synthesis [217]. Coupled with previous reports by researchers in Professor Jackson's research group that show LPCATs facilitate LPS-stimulated translocation of TLR4 into membrane lipid raft domains [212], gave rise to the main research question explored in this thesis: Does LPCAT2 play a role in the S-acylation of proteins involved in LPS signalling?

The aim of this project is to develop a detailed molecular analysis of the mechanisms by which LPCAT2 can regulate inflammatory responses in macrophages. In particular, to better understand the link between LPCAT2 and the proteins in the LPS receptor complex that induce TLR4-mediated signaling.

The main objectives of this thesis are:

1. To identify if LPCAT2 S-acylates lipid raft-associated proteins in LPS-stimulated macrophages.

2. To determine the function LPCAT2 S-acylation has on the proteins identified in objective 1.

3. To determine the role of the proteins identified in 1 in the context of TLR4 signalling.

4. To repeat key experiments using primary cells to ensure applicability of findings.

Chapter 2

Materials & methods

2.1 Materials lists

2.1.1 Suppliers

Table 2.1: Supplier information

Supplier	Location
Applied Biosystems	Waltham, USA
BD Biosciences	Fanklin Lakes, USA
Bio-Rad	Hercules, USA
Biosera	Cholet, France
Cayman Chemical	Ann Arbor, USA
Cell Signalling Technology	Danvers, USA
Gibco	Carlsbad, USA
Greiner Bio-One	Stonehouse, UK
List Biological Laboratories	Campbell, USA
Lonza	Slough, UK
New England BioLabs	Ipswich, USA
Polyplus	Graffenstaden, France
Proteintech	Manchester, UK
R&D Systems	Minneapolis, USA
Santa Cruz Biotechnology	Dallas, USA

| Sigma-Aldrich | Gillingham, UK |
| Thermo Fisher Scientific | Altrincham, UK |

2.1.2 Consumables

All disposable plasticware including pipette tips, centrifuge tubes, microcentrifuge tubes, cell culture flasks, cell culture plates, cell scrapers, serological pipettes, 96 well plates, plate sealers, reagent reservoirs, PCR tubes and PCR plates were purchased from Greiner Bio-One unless otherwise stated.

2.1.3 Reagents

Table 2.2: List of reagents and kits

Product	Product code	Supplier
1-Bromo-3-chloropropane	B9673	Sigma-Aldrich
2-Mercaptoethanol	M6250	Sigma-Aldrich
Acetic acid	A6283	Sigma-Aldrich
Amplification Grade DNase I Kit	AMP-D1	Sigma-Aldrich
Bromophenol blue	B0126	Sigma-Aldrich
Chloroform	288306	Sigma-Aldrich
DEPC-Treated Water	AM9922	Thermo Fisher Scientific
DMEM	BE12-709F	Lonza
DMSO	276855	Sigma-Aldrich
D-PBS	BE17-512F	Lonza
E. coli LPS J5 (Rc)	301	List Biological Laboratories
E. coli LPS K12, D31m4 (Re)	302	List Biological Laboratories
E. coli LPS O111:B4	L2630	Sigma-Aldrich
Ethylenediaminetetraacetic acid	E9884	Sigma-Aldrich
FBS	FB-1101	Biosera
Glycine	BP381	Thermo Fisher Scientific
Guanidine thiocyanate	G9277	Sigma-Aldrich
Halt Protease Inhibitor Cocktail	87785	Thermo Fisher Scientific
High-Capacity RNA-to-cDNA™Kit	4387406	Applied Biosystems
HPDP-biotin	PI 21341	Thermo Fisher Scientific

Hydrogen peroxide	1086001000	Sigma-Aldrich
Hydroxylamine	438227	Sigma-Aldrich
INTERFERin® transfection reagent	409-10	Polyplus
L-Glutamine 200nM	BE17-605E	Lonza
Live Cell Imaging Solution	A14291DJ	Thermo Fisher Scientific
Luminol	123072	Sigma-Aldrich
Methanol	179337	Sigma-Aldrich
Micro BCA Protein Assay Kit	23235	Thermo Fisher Scientific
Monarch® Total RNA Miniprep Kit	T2010S	New England BioLabs
NEM	PI 23030	Thermo Fisher Scientific
N-lauroylsarcosine	J60040	Thermo Fisher Scientific
Opti-MEM	31985047	Gibco
Oxidised LDL Uptake Assay Kit	601180	Cayman Chemical
PBS-EDTA	BE02-017F	Lonza
p-Coumaric acid	C9008	Sigma-Aldrich
Phenol, Saturated (pH 4.3)	4367659	Thermo Fisher Scientific
pHrodo™ Green E. coli BioParticles™ Conjugate	P35366	Thermo Fisher Scientific
Power SYBR Green Master Mix	4367659	Applied Biosystems
Silencer® Select siRNA CD36	s63620	Thermo Fisher Scientific
Silencer® Select siRNA LPCAT2	s114511	Thermo Fisher Scientific
Silencer® Select siRNA Negative control	4390843	Thermo Fisher Scientific
Silver Stain Plus™	161-0449	Bio-Rad
Sodium acetate	BP333	Thermo Fisher Scientific
Sodium chloride	BP358-1	Thermo Fisher Scientific
Sodium citrate	BP327	Thermo Fisher Scientific
Sodium dodecyl sulfate (SDS)	75746	Sigma-Aldrich
Sodium orthovanadate	S6508	Sigma-Aldrich
Streptavidin-agarose	PI 20349	Thermo Fisher Scientific
Sucrose	A15583	Thermo Fisher Scientific
Super AquaBlue ELISA Substrate	00-4203-56	Thermo Fisher Scientific
SureCast™ Acrylamide (40% w/v)	HC2040	Thermo Fisher Scientific
SureCast™ Ammonium Persulfate	HC2005	Thermo Fisher Scientific
SureCast™ Resolving Buffer	HC2215	Thermo Fisher Scientific
SureCast™ Stacking Buffer	HC2115	Thermo Fisher Scientific
SureCast™ TEMED	HC2006	Thermo Fisher Scientific
Tris-base	10376743	Thermo Fisher Scientific
Triton X-100	T8787	Sigma-Aldrich
Trypan Blue Solution, 0.4% (w/v)	15250061	Gibco

Trypsin EDTA	CC-5012	Lonza
Tween-20	T/4206/60	Thermo Fisher Scientific

2.1.4   Antibodies and proteins

Table 2.3: List of antibodies and proteins

Product	Product code	Supplier
Anti-biotin HRP-linked	7075	Cell Signalling Technology
Anti-Calnexin antibody	2433	Cell Signalling Technology
Anti-CD36 antibody	AF2519	R&D Systems
Anti-CD36 biotinylated antibody	BAF2519	R&D Systems
Anti-GAPDH antibody	sc-32233	Santa Cruz Biotechnology
Anti-Goat IgG HRP-linked antibody	HAF109	R&D Systems
Anti-LIMPII antibody	AF1888	R&D Systems
Anti-LPCAT2 antibody	15082-1-AP	Proteintech
Anti-rabbit IgG, HRP-linked antibody	7074	Cell Signalling Technology
Anti-TLR4 antibody	sc-293072	Santa Cruz Biotechnology
APC Mouse Anti-Mouse CD36	562744	BD Biosciences
APC Mouse IgA$\varkappa$ Isotype Control	562140	BD Biosciences
Biotinylated Protein Ladder	81851	Cell Signalling Technology
Cholera Toxin Subunit B HRP-linked	C34780	Thermo Fisher Scientific
HRP-conjugated streptavidin	18-4200-93	Thermo Fisher Scientific
IL-6 Capture Antibody	14-7061-81	Thermo Fisher Scientific
IL-6 Detection Antibody	13-7062-81	Thermo Fisher Scientific
Mouse BD Fc Block™	553141	BD Biosciences
Mouse IL-6 Recombinant Protein	29-8061-65	Thermo Fisher Scientific
Mouse TNF-α Recombinant Protein	29-8321-65	Thermo Fisher Scientific
Normal Goat IgG Control	AB-108-C	R&D Systems
SeeBlue Pre-stained Protein Standard	LC5625	Thermo Fisher Scientific
TNFα Capture Antibody	14-7423-81	Thermo Fisher Scientific
TNFα Detection Antibody	13-7326-81	Thermo Fisher Scientific
Mouse IgG$\varkappa$ binding protein HRP-linked	sc-516102	Santa Cruz Biotechnology

2.1.5   Buffers and solutions

Table 2.4: List of buffers and solutions

+HA buffer

50mM Tris-Cl (pH7.4), 0.7M hydroxylamine, 1mM HPDP-biotin, 0.2% (v/v) Triton X-100,

1X Halt Protease Inhibitor Cocktail

2% (w/v) SDS buffer

50mM Tris-Cl (pH7.4), 2% (w/v) SDS, 5mM EDTA

4% (w/v) SDS buffer

50mM Tris-Cl (pH7.4), 4% (w/v) SDS, 5mM EDTA

ABE Lysis buffer

50mM Tris-Cl (pH7.4), 150mM NaCl, 5mM EDTA, 1X Halt Protease Inhibitor Cocktail

---

Denaturing solution

25mM sodium citrate (pH 7), 4M guanidinium thiocyanate, 0.5% (w/v) N-lauroylsarcosine,

0.1M 2-mercaptoethanol

ECL detection reagent

100mM Tris-Cl (pH 8.6), 1.25mM Luminol, 200nM p-Coumaric acid,

0.01% (v/v) H_2O_2(made according to Murk and Cheng 2011)

ELISA blocking buffer

PBS (pH7.4), 2% (w/v) BSA

ELISA wash buffer

PBS (pH7.4), 0.05% (v/v) Tween-20

Flow cytometry staining solution

D-PBS (pH7.4), 1% w/v BSA (0.45µm filtered)

-HA buffer

50mM Tris-Cl (pH7.4), 1mM HPDP-biotin, 0.2% (v/v) Triton X-100,

1X Halt Protease Inhibitor Cocktail

Low HPDP-biotin buffer

50mM Tris-CL (pH7.4), 150mM NaCl, 5mM EDTA, 0.2mM HPDP-biotin, 0.2% (v/v) Triton X-100,

1X Halt Protease Inhibitor Cocktail

Lysis buffer

50mM Tris-Cl (pH8), 150mM NaCl, 2mM EDTA, 1% v/v Triton X-100,

1X Halt Protease Inhibitor Cocktail

Plutznik medium

DMEM, 20% v/v FBS, 20% v/v L929 cell conditioned medium, 1mM sodium pyruvate,

2mM L-glutamine, 100U/ml Penicillin, and 100U/ml Streptomycin

---

SDS sample buffer (4X)

200mM Tris-Cl (pH 6.8), 8% (w/v) SDS, 0.016% (w/v) Bromophenol blue, 40% (v/v) glycerol,

20% (v/v) β-Mercaptoethanol (added fresh before use)

TNEV buffer

10mM Tris–Cl (pH 7.5), 150mM NaCl, 5mM EDTA, 1mM Sodium orthovanadate	

Tris-Buffered Saline (TBS)

50mM Tris-Cl (pH7.5), 150mM NaCl

Tris-Buffered Saline with Tween-20 (TBS-T)

50mM Tris-Cl (pH7.5), 150mM NaCl, 0.1% (v/v) Tween-20

Tris-glycine SDS running buffer (10X)

250mM Tris base, 1.92M glycine, 1% (w/v) SDS

Tris-glycine transfer buffer (25X)

120mM Tris base, 0.96M glycine

Western blot blocking Buffer

50mM Tris-Cl (pH7.5), 150mM NaCl, 5% (w/v) non-fat dry milk

2.2   Cell culture methods

2.2.1   RAW264.7 cells

RAW264.7 cells are a murine macrophage-like cell line derived from an Abelson murine leukaemia virus-induced tumour in a male BALB/c mouse. These cells were maintained in $75cm^2$ tissue culture flasks in 10mL DMEM supplemented with 10% FBS, 2mM L-glutamine, 25mM Hepes and 4.5g/L glucose (herein referred to as complete DMEM) in a humidified incubator at 37°C with 5% CO_2 unless otherwise stated. Cells were sub-cultured at a 1/6 ratio every Monday and Friday with the medium being changed every Wednesday giving a confluencey of 50-70% when split. This was done by carefully detaching the cells with a cell scraper, then transferring them to a 50mL centrifuge tube and pelleting the cells by centrifugation at 160xg for 5min. The supernatant was then discarded, and the cells were resuspended in 6mL fresh complete DMEM and 1mL of the cell suspension was added to a fresh $75cm^2$ tissue culture flask and the volume was made up to 10mL with complete DMEM. The flask was then agitated back and forth, and then side

to side to distribute the cells evenly before being returned to the incubator. The cells were grown for no longer than 20 passages.

2.2.2   Cryopreservation and resuscitation of RAW264.7 cells

To resuscitate frozen cells, a vial of RAW264.7 cells was removed from the liquid nitrogen vapour phase and thawed for immediate use. The thawed cells were transferred into a centrifuge tube containing 10mL complete DMEM and carefully mixed. The cells were then pelleted by centrifugation at 160xg for 5 minutes and the supernatant was discarded to remove the DMSO. The cells were then resuspended in 4mL complete DMEM and transferred into a $25cm^2$ tissue culture flask and grown to 70% confluency. The cells were then maintained as normal. To cryopreserve a stock of RAW264.7 cells for the project, cells at passage 7 were grown to 70% confluency in a $75cm^2$ tissue culture flask. The cells were then scraped, collected in a centrifuge tube, pelleted by centrifugation at 160xg for 5 minutes and the supernatant was discarded. The cells were then resuspended in 10mL complete DMEM, counted, the viability determined, and resuspended at a concentration of $6\text{-}8x10^6$ cells/mL in fresh complete DMEM. An equal volume of complete DMEM supplemented with 20% (v/v) DMSO was added drop wise while gently swirling to give a final concentration of 10% (v/v) DMSO. From this, aliquots of 1mL were transferred into cryopreservation-vials and immediately placed into a Mr. Frosty™ freezing container (Thermo Fisher Scientific) and incubated at -80°C overnight before transferring the vials to a storage box in the vapour phase of liquid nitrogen for long-term storage. Ample cells were cryopreserved at the start of the project for all experiments.

2.2.3   Cell counting and viability determination

Cells were counted using a haemocytometer (Hirschmann, Eberstadt, Germany) as follows: First, the glass haemocytometer (Hirschmann) and coverslip were cleaned using alcohol before use and allowed to dry. The cover slip was then moistened and gently pressed onto the haemocytometer and the presence of Newton's refraction rings indicated that the coverslip had properly affixed. Collected cells were then carefully mixed to ensure a single cell suspension by pipetting up and down, then 20µL of the cell suspension was added to an equal volume of culture medium in a 1.5mL microcentrifuge tube and mixed. Then 40µL of 0.4% Trypan blue was added to the tube and mixed. The cells were incubated at room temperature for 1 minute to allow the stain to be taken up by non-viable cells before 10µL was carefully loaded onto the edge of the affixed coverslip allowing capillary action to draw the cell suspension into the chamber evenly. Using an inverted light microscope with 100x magnification, the unstained (viable) and stained (non-viable) cells in each set of 16 corner squares of the grid were counted. To calculate the number of viable cells/mL, the average number of viable cells in each set of 16 corner squares was then multiplied by 10,000 and then by multiplying by 4 to correct for the 1/4 dilution, giving the number of viable cells/mL. To calculate the cell viability, the non-viable and viable cells were added together to give the total cell count. The viable cell count was then divided by the total cell count and multiplied by 100 to give the percentage viability. A cell viability of greater than 90% was used for all experiments.

2.2.4   Bone marrow derived macrophages (BMDMs)

Surplus BMDMs were kindly donated by Dr Connor Wood. These were obtained from the femur and tibia of 6- to 8-week-old female and male

C57/Black6/J mice that were killed in accordance with schedule 1 methods. The epiphyses of the femurs and tibias were removed, and the bone marrow was collected by inserting a 19G needle into one end and gently flushing D-PBD through the bones. The pooled bone marrow was then pelleted at 160xg for 5 minutes and the supernatant was discarded. The bone marrow cells were counted and seeded in $75cm^2$ tissue culture flasks at $1x10^6$ cells/ml using Plutznik medium. The cells were grown for 10 days in a humidified incubator at 37°C with 5% CO^2, with the medium changed on day 7 to remove non-adherent cells. After 10 days the cells were ready for experiments [218].

2.3 Experiments

2.3.1 Acyl-biotin exchange experiments

Cell culture

A total of six $25cm^2$ tissue culture flasks were each seeded with $5x10^5$ RAW264.7 cells in 3mL complete DMEM and cultured for 24 hours before siRNA transfection. The medium was exchanged for 3.9mL Opti-MEM and the flasks were divided into three equal groups. One group of flasks only had the medium changed while the other 2 groups were either transfected with 5nM negative siRNA or LPCAT2 siRNA. The siRNAs were delivered into the cells using INTERFERin® transfection reagent as per the manufacturer's instructions using 20µL transfection reagent per flask. The cells were then cultured for 72 hours before having the medium exchanged for complete DMEM. The transfected cells were then stimulated with 1µg/mL *E. coli* O111:B4 LPS for 45 minutes before cell lysis and sample processing.

Cell lysis and preparation of protein extracts

Working on ice with ice cold buffers, the cells were washed twice with 3mL D-PBS, then detached using a scraper and flasks of identically treated cells were pooled in 15mL centrifuge tubes. The cells were pelleted by centrifugation at 160xg for 5 min, the supernatant discarded, and the cells were then resuspended in 500 µL of ABE lysis buffer supplemented with 1% Triton X-100, 0.1% SDS and 10 mM N-Ethylmaleimide (NEM). The cells were then transferred into a 2mL microcentrifuge tube and incubated for 60 minutes at 4°C on a rotary mixer. The lysates were then sonicated using a Microson XL2000 Ultrasonic Cell Disruptor (Misonix) at 20% amplitude for 4 x 10s bursts at 30s intervals at 4°C. Cell debris were then removed by centrifuging at 200xg for 5 minutes at 4°C and keeping the supernatants. The proteins were then precipitated from the cell lysate with chloroform-methanol (see method section 2.3.1) and dissolved in 150µL 4% SDS buffer supplemented with 10mM NEM by heating to 37°C with occasional agitation. Once the protein pellets had fully dissolved, 450µL lysis buffer containing 0.2% Triton X-100 and 1mM NEM was added, and the samples were incubated overnight at 4°C on a rotary mixer.

Chloroform-methanol precipitation of proteins

The method developed by Wessel and Flugge [219] to precipitate proteins with a defined methanol-chloroform-water mixture was used with minor modifications. Using 2mL microcentrifuge tubes, protein extracts were diluted to a volume of 600µL in ABE lysis buffer. To this 400µL of methanol was added, then 700µL of chloroform mixing between each step by inverting the tubes. Samples were then centrifuged at 20,000xg for 10 minutes at 4°C. This caused the phases to separate and the protein precipitate to settle at the

interface. The upper aqueous phase was discarded and then 1mL of methanol was added and mixed by inverting the tube several times carefully. The protein precipitate then sank to the bottom of the tube and the samples were centrifuged at 20,000xg for 5 minutes at 4°C. The supernatant was then discarded, and the protein pellet allowed to air dry for 5 min.

Acyl-biotin exchange reactions

To remove all traces of NEM the samples were precipitated with chloroform-methanol (see method section 2.3.1), then dissolved in 150 µL 4% SDS buffer by heating to 37°C with occasional agitation and then diluted with 450µL ABE lysis buffer supplemented with 0.2% Triton X-100. This step was repeated 3 times to ensure all traces of NEM were removed. The protein concentration of each sample was determined using BCA protein assay. The three samples were then divided into 2 portions each containing 1mg of protein. These were then precipitated with chloroform-methanol (see method section 2.3.1) and dissolved in 150µL 4% SDS buffer. Like samples were then incubated with 600µL of either +HA (Hydroxylamine) or -HA buffer at room temperature for 1 h on a rotary mixer. The samples were then precipitated with chloroform-methanol (see method) to remove the HA, dissolved in 150µL 4% SDS buffer and diluted with 600µL Low HPDP-biotin buffer and incubated at room temperature for 1 h on a rotary mixer. The samples were then precipitated with chloroform-methanol (see method) three times to remove residual HPDP-biotin and HA with the protein being dissolved in 75µL 4% SDS buffer on the final precipitation.

Affinity purification of biotinylated proteins

To reduce the concentration of SDS to 0.1% the samples were diluted 20-fold in ABE lysis buffer containing 0.2% Triton X-100 and incubated at room temperature for 30 minutes on a rotary mixer. Debris were then removed by centrifuging at 15,000xg for 1 minute and transferring the supernatants to fresh tubes containing 15μL pre-equilibrated streptavidin-agarose. The samples were then incubated at room temperature for 90 minutes on a rotary mixer. Unbound protein was then removed by 3 sequential washes of 1mL ABE lysis buffer containing 0.1% SDS and 0.2% Triton X-100 and pelleting the agarose by centrifugation at 1000xg for 1 min. Following the final wash, the resin was resuspended in 150μL ABE lysis buffer containing 0.1% SDS, 0.2% Triton X-100 and 1% 2-mercaptoethanol and incubated at 37°C for 15 minutes with occasional agitation. Finally, the proteins were concentrated by trichloroacetic acid precipitation, dissolved in 30μL 2% SDS buffer and diluted with 150 μL ABE lysis buffer. The samples were stored at -80°C prior to analysis.

2.3.2   Isolation of lipid rafts through discontinuous sucrose gradient centrifugation

A total of four 25cm^2 tissue culture flasks were each seeded with $5x10^5$ RAW264.7 cells in 3mL complete DMEM and cultured for 24 hours before siRNA transfection. The medium was exchanged for 3.9mL Opti-MEM and the flasks were divided into two equal groups that were either transfected with 5nM negative siRNA or LPCAT2 siRNA. The siRNAs were delivered into the cells using INTERFERin® transfection reagent as per the manufacturer's instructions using 20μL transfection reagent per flask. The cells were then

cultured for 72 hours before being processed.

Cells were washed twice in 5mL ice cold D-PBS, detached with a cell scraper, and collected in a 15mL centrifuge tube. Cells were then pelleted at 200xg for 5 min, the supernatant discarded, and then the cell pellet was resuspended in 450µL TNEV buffer with 1% Triton X-100 and 1X Halt Protease Inhibitor Cocktail and incubated at 4°C for 30 min. The cells were then passed through a ball bearing homogeniser pre-cooled to 4°C with a 4µm gap (bore:8.020mm, ball bearing: 8.012mm) ten times. The cell lysate was transferred to a 1.5mL microcentrifuge tube, centrifuged at 200xg for 8 minutes at 4°C, and then the supernatant was transferred to a fresh tube. The protein concentration of the cell lysate was determined by BCA assay and 1.5mg of protein was added to a 5mL ultracentrifuge tube (Beckman Coulter) and the volume was adjusted to 425µL in TNEV buffer. An equal volume of 85% w/v sucrose in TNEV was added and mixed carefully to avoid foaming, then 2.55mL 35% w/v sucrose in TNEV was carefully overlayed followed by 1.5mL 5% w/v sucrose in TNEV and on inspection sharp interfaces between the three layers were visible. The tubes were balanced by adding 5% w/v sucrose in TNEV if required, then added to a pre-cooled SW 55 Ti Swinging-Bucket Rotor and centrifuged at 257,000xg for 18 hours at 4°C in an ultracentrifuge (Beckman Coulter). From the top of the gradient, ten 490 µL fractions were collected in 1.5mL microcentrifuge tubes and stored at -20°C prior to SDS-PAGE or dot-blotting.

2.3.3   Flow cytometry

Cell culture setup

RAW264.7 cells were seeded in 6 well tissue culture plates at $2x10^5$ cells/well in 2mL complete DMEM and cultured for 24 hours. The medium was exchanged for 2mL Opti-MEM and the cells were transfected with either 5nM LPCAT2 siRNA or negative siRNA for 48 hours using 12µL of INTERFERin™ transfection reagent per well following the manufacturer's instructions. The medium was exchanged for 2mL complete DMEM and the cells were stimulated with 1µg/mL O111:B4 LPS for 45 minutes before processing.

CD36 surface staining

Cells were washed twice in 2mL ice cold D-PBS-EDTA, detached with a cell scraper, and collected in a 15mL centrifuge tube. The cells were pelleted at 160xg for 5 min, resuspended in 500µL staining solution, counted and the cell density adjusted to $4x10^6$ cells/mL with staining solution. Aliquots of 100µL were added to 1.5mL microcentrifuge tubes and 2µL Mouse BD Fc Block™ was added to each tube, mixed, and incubated for 5 minutes at 4°C to prevent FcγR-mediated non-specific binding of antibodies. The cells were then either stained with APC anti-mouse CD36 antibody or APC isotype control antibody at a dilution of 1/100 for 30 min, at 4°C in the dark. The cells were washed twice in 500µL staining solution by pelleting the cells at 160xg for 5 minutes at 4°C and carefully discarding the supernatant. The cells were finally resuspended in 400 µL staining solution, transferred into 5mL FACS tubes and stored on ice in the dark ready for immediate analysis. Samples were resuspended by pipette and briefly vortexed directly before being analysed using a BD FACSAria II (BD Biosciences) flow cytometer

loaded with a 70µm nozzle. A total of 10,000 events were acquired and data were exported using the FACSDiva software as .fcs files for later analysis using FlowJo™ v10.

CD36 Intracellular staining

Cells were washed twice in 2mL ice cold D-PBS-EDTA, detached with a cell scraper, and collected in a 15mL centrifuge tube. The cells were pelleted at 160xg for 5 min, resuspended in 500µL D-PBS, counted and the cell density adjusted to $4x10^6$ cells/mL with D-PBS. The cells were then fixed in 2% formaldehyde for 15 minutes at 4°C, then washed three times in D-PBS 0.2% Tween-20 and then permeabilised with D-PBS 0.1% triton X-100 at 4°C for 15 min. The cells were washed a further three times in D-PBS 0.2% Tween-20, then 100µL aliquots containing $4x10^5$ cell were added to 1.5mL microcentrifuge tubes and 2µL Mouse BD Fc Block™ was added to each tube, mixed, and incubated for 5 minutes at 4°C to prevent FcγR-mediated non-specific binding of antibodies. The cells were then either stained with APC anti-mouse CD36 antibody or APC isotype control antibody at a dilution of 1/100 for 30 min, at 4°C in the dark. The cells were washed twice in 500µL staining solution by pelleting the cells at 160xg for 5 minutes at 4°C and carefully discarding the supernatant. The cells were finally resuspended in 400 µL staining solution, transferred into 5mL FACS tubes and stored on ice in the dark ready for immediate analysis. Samples were resuspended by pipette and briefly vortexed directly before being analysed using a BD FACSAria II (BD Biosciences) flow cytometer loaded with a 70µm nozzle. A total of 10,000 events were acquired and data were exported using the FACSDiva software as .fcs files for later analysis using FlowJo™ v10.

2.3.4 Cell sorting: CD36 high and low populations

Two 25cm^2 tissue culture flasks were each seeded with 2x10^6 RAW264.7 cells in 3mL complete DMEM and cultured for 24 hours. The culture medium was then refreshed, and one flask was stimulated with 100ng/mL sLPS for 6 hours. The cells were then washed three times in ice cold D-PBS, detached using a cell scraper and collected in a 15mL centrifuge tube. The cells were then counted and 1x10^6 cells were transferred to a 1.5mL microcentrifuge tube, pelleted at 160xg for 5min and the supernatant discarded. The cells were then resuspended in 250μL staining solution and 5μL Mouse BD Fc Block™ was added to each tube, mixed, and incubated for 5 minutes at 4°C to prevent FcγR-mediated non-specific binding of antibodies. The cells were then stained with APC anti-mouse CD36 antibody at a dilution of 1/100 for 30 min, at 4°C in the dark. The cells were washed twice in 500μL staining solution by pelleting the cells at 160xg for 5 minutes at 4°C and carefully discarding the supernatant. The cells were finally resuspended in 300 μL staining solution, transferred into 5mL FACS tubes and stored on ice in the dark ready for immediate cell sorting.

Samples were resuspended by pipette and briefly vortexed directly before being sorted using a BD FACSAria II (BD Biosciences) flow cytometer loaded with a 100 μm nozzle and a two-tube collection device. A total of 469,952 events were acquired and data were exported using the FACSDiva software as .fcs files for later analysis using FlowJo™ v10. RNA from the collected cells was isolated using a Monarch® Total RNA Miniprep Kit following the manufacturer's instructions and the RNA was stored at -80°C ready for analysis by RT-qPCR.

2.3.5 Phagocytosis assay

RAW264.7 cells were seeded in 6 well tissue culture plate at 2×10^5 cells/well in 2mL complete DMEM and cultured for 24 hours. The medium was exchanged for 2mL Opti-MEM and the cells were transfected with either 5nM CD36 siRNA, LPCAT2 siRNA or negative siRNA for 48 hours using 12µL of INTERFERin™ transfection reagent per well following the manufacturer's instructions. Following the 48 hour transfection the medium was discarded and the cells were washed twice with 2mL DPBS, then carefully detached with a cell scraper and collected in a 15mL centrifuge tube. The cells were then counted and resuspended at 5×10^5 cells/mL in complete DMEM and then each treatment was plated in triplicate into a 96 well plate so that each well contained 1×10^5 cells. The cells were then incubated for 1 hour to allow the cells to adhere ready for the phagocytosis assay.

pHrodo™ Green E. coli BioParticles™ Conjugate were prepared according to the manufacturer's instructions. Briefly, this involved resuspending each tube of pHrodo™ Green E. coli BioParticles in 2mL Live Cell Imaging Solution and placing them in a bath sonicator for 10 minutes to generate a 1mg/mL suspension.

The culture medium was then removed from the adhered cells and 100µL of the pHrodo™ Green E. coli BioParticle suspension was added to each well and then the plate was incubated for 2 hours at 37°C without elevated CO_2. The fluorescence intensity of each well was then measured using a FLUOstar Omega Plate reader (BMG Labtech) using the following filter set: 485BP12 & Em 520 and the following settings: use orbital averaging, read bottom of the plate, 0.5s time delay and 10 flashes.

2.3.6 Oxidised LDL Uptake Assay

RAW264.7 cells were seeded in 6 well tissue culture plate at $2x10^5$ cells/well in 2mL complete DMEM and cultured for 24 hours. The medium was exchanged for 2mL Opti-MEM and the cells were transfected with either 5nM CD36 siRNA, LPCAT2 siRNA or negative siRNA for 48 hours using 12µL of INTERFERin™ transfection reagent per well following the manufacturer's instructions. The culture medium was then replaced with 1mL complete DMEM before 20µL oxLDL-DyLight™ was added to each treatment well and incubated for 4 hours at 37°C, as per the manufacturer's instructions.

The supernatant was removed and the cells were washed twice in 1mL D-PBS, then 1mL DPBS-EDTA was added and the cells were incubated for 15 minutes at 37°C to help detach the cells. The plate was gently tapped to dislodge the cells and any cells still attached were detached using a cell scraper. The cells were collected in a 15mL centrifuge tube, counted and then $5x10^5$ cells were added to a 1.5mL microcentrifuge tube. The cells were pelleted at 250xg for 5min, the supernatant removed and then resuspended in 100µL staining solution. Then 2µL Mouse BD Fc Block™ was added to each tube, mixed, and incubated for 5 minutes at 4°C to prevent FcγR-mediated non-specific binding of antibodies. The cells were then stained with APC anti-mouse CD36 antibody at a dilution of 1/100 for 30 min, at 4°C in the dark. The cells were washed twice in 500µL staining solution by pelleting the cells at 160xg for 5 minutes at 4°C and carefully discarding the supernatant. The cells were finally resuspended in 400 µL staining solution, transferred into 5mL FACS tubes and stored on ice in the dark ready for analysis. The provided 7-AAD solution was diluted 1in10 in DPBS and then 5 minutes before analysing the samples, 3uL of the diluted 7-AAD solution was added to each tube and vortex briefly. Samples were resuspended by pipette and briefly vortexed directly before being analysed

using a BD Accuri™ C6 (BD Biosciences) flow cytometer. A total of 10,000 events were acquired and data were exported using the FACSDiva software as .fcs files for later analysis using FlowJo™ v10.

2.3.7 Cytokine induction experiments (RAW264.7 cells)

RAW264.7 cells were seeded in 12 well tissue culture plates at $1x10^5$ cells/well in 1mL complete DMEM and cultured for 24 hours. The medium was exchanged for 1mL Opti-MEM and the cells were transfected with either 5nM CD36 siRNA or negative siRNA for 48 hours using 6µL of INTERFERin™ transfection reagent per well following the manufacturer's instructions. The medium was exchanged for 1mL complete DMEM (for experiments with serum) or 1mL DMEM supplemented with 2mM L-Glutamine (for serum free experiments). The cells were then stimulated with 100ng/mL *E. coli* O111:B4 LPS, *E. coli* J5 LPS or *E. coli* K12 LPS for 6 hours for RT-qPCR or 24 hours for ELISA.

2.3.8 Cytokine induction experiments (BMDMs)

Flasks of BMDMs were washed 3 times in 10 mL prewarmed PBS saving the washes in a centrifuge tube. Then 6mL prewarmed trypsin-EDTA was added, and the flask incubated at 37°C for 10 min. The cells were persuaded to detach by tapping the side of the flask. To inactivate the trypsin an equal volume of complete DMEM was added to the flask and the cells were transferred to the centrifuge tube containing the wash. The cells were pelleted at 160xg for 5 min, the supernatant discarded, and the cells resuspended in 10mL complete DMEM. The cells were then counted, and the viability determined. BMDMs were seeded at $5x10^5$ cells/well in 6 well plates

and cultured for 24 hours. The medium was changed for 2mL complete DMEM and the cells were either transfected with 20nM CD36 siRNA or negative siRNA for 48 hours using 16µL of INTERFERin™ transfection reagent per well following the manufacturer's instructions. The medium was then changed for 2mL complete DMEM and the cells were stimulated with 1µg/mL O111:B4 LPS for 6 hours before harvesting.

2.3.9   Immunoprecipitation

A total of four $25cm^2$ tissue culture flasks were each seeded with $3x10^6$ RAW264.7 cells in 3mL complete DMEM and cultured for 24 hours. The flasks were then divided into two equal groups and one groups was stimulated with 100ng/mL *E. coli* O111:B4 LPS LPS for 45min and the other not. The flasks were then put on ice immediately before harvesting.

All reagents/buffers were pre-cooled to 4°C and work was performed on ice. The medium was removed and the cells were washed twice with 3mL D-PBS and the wash discarded. The cells were then detached in 500µL D-PBS using a cell scraper and cells from the same treatment group were pooled in 1.5mL microcentrifuge tubes. The cells were pelleted at 200xg for 5min at 4°C and the supernatant discarded. The cells were then resuspend in 500µL lysis buffer and incubated for 30 minutes on a rotary mixer at 4°C. The lysate was then centrifuged at 12,000xg for 20 minutes to remove debris and the supernatant was transferred to a fresh tube. The protein concentration of the cell lysate was then determined by BCA assay. The lysate was then then divided into two groups each containing 500µg of protein in fresh 1.5mL microcentrifuge tubes and the volume was adjusted to 1mL in TBS.

The lysates were then precleared by adding 1µg of Normal Goat IgG Control and 20µL of protein A/G agarose, and then incubating for 1 hour on a rotary

mixer at 4°C. The lysate was the centrifuged at 1000xg for 30s at 4°C and the supernatant was transferred to a fresh 1.5mL microcentrifuge tube. To the pre-cleared lysate, 3μg of anti-CD36 antibody or Normal Goat IgG Control was added and incubated for 1 hour on a rotary mixer at 4°C. Then 30μL of protein A/G agarose was added and the tubes were incubated overnight on a rotary mixer at 4°C. The tubes were then centrifuged at 1000xg for 30s at 4°C and the supernatant was removed and stored for analysis (flow through). The agarose resin was then washed three times with 500μL PBS, gently resuspending the resin between washes and centrifuging at 1000xg for 30s at 4°C. The beads were finally resuspended in 40μL 1X SDS sample buffer ready for SDS-PAGE and western blot. Membranes were blotted using a biotinylated anti-CD36 antibody to avoid detecting the anti-CD36 capture antibody.

2.4   Analytical techniques

2.4.1   Bicinchonic acid protein assay (BCA)

Protein concentration was estimated with a Micro BCA Protein Assay Kit using the 96-well microplate format following the manufacturer's instructions. Samples were diluted 1/25 in PBS and BSA standards were prepared at the following concentrations in PBS: 200μg/ml, 100μg/ml, 50μg/ml, 25μg/ml 12.5μg/ml 6.25μg/ml, 3.125μg/ml and a blank. 50μL of sample or standard was mixed with 50μL BCA reagent and incubated at 37°C for 30 min. The optical density was then determined at 562nm using a FLUOstar Omega Plate reader (BMG Labtech). Sample protein concentration could then be determined from the standard curve generated by the MARS data analysis software.

2.4.2   Enzyme Linked Immunosorbent Assay (ELISA)

Each well of a Nunc MaxiSorp 96-well plate was coated with 50µL of capture antibody diluted in PBS at 2µg/mL for IL-6 and 3µg/mL for TNFα. The plates were sealed and incubated overnight at 4°C. The wells were emptied, washed three times in ELISA wash buffer (all wash steps were performed like this), and blocked with 100µL of ELISA blocking buffer for 1 hour at room temperature. The wells were emptied, washed and 50µL of samples and standards were added in duplicate to designated wells and incubated for 2 hours at room temperature. The standards were prepared by making a 2-fold serial dilution of recombinant IL-6 or TNFα ranging from 2000 to 31.25pg/mL in DMEM. The wells were emptied, washed and 50µL of detection antibody diluted in PBS at 2µg/mL was added to the well. The plates were incubated for 1 hour at room temperature. The wells were emptied, washed and 50µL of HRP-conjugated streptavidin diluted 1:500 in PBS was added to each well. The plates were incubated for 30 minutes at room temperature. The wells were emptied, washed and 50µL of Super AquaBlue ELISA Substrate was added to each well and incubated for 15 to 30 minutes at room temperature. The optical density was then determined at 405nm using a FLUOstar Omega Plate reader (BMG Labtech). Sample protein concentration could then be determined from the standard curve generated by the MARS data analysis software.

2.4.3   SDS-Polyacrylamide gel electrophoresis (SDS-PAGE)

Polyacrylamide gels were cast using Invitrogen's SureCast™ Handcast system (Thermo Fisher Scientific). The glass plates were assembled according to the manufacturer's instructions using a 1.0mm spacer and gel solutions were prepared immediately before use according to table 2.5.

Table 2.5: Polyacrylamide gel solution recipes

Solution	10% resolving gel solution	4% stacking gel solution
SureCast™ Acrylamide (40%)	2.0mL	0.30mL
SureCast™ Resolving Buffer	2.0mL	-
SureCast™ Stacking Buffer	-	0.75mL
Distilled water	3.9mL	1.92mL
10% SureCast™ APS	80μL	30μL
SureCast™ TEMED	8μL	3μL

The 10% resolving gel solution was added to the glass plate assembly until the fill line was reached. The resolving gel solution was then carefully overlaid with butanol to level the interface and the gel was allowed to polymerise for 10 min. The overlay was then poured off, the surface of the gel rinsed with water and any excess water wicked off with filter paper. The 4% resolving gel solution was then added till the plate was full and a 15-well comb was carefully inserted. After 10 minutes the gel was ready to be used or stored a 4°C wrapped in a damp tissue for up to a week.

The protein concentration of each sample was determined by BCA assay and the protein concentration of each sample was adjusted be the equal. The samples were then mixed with 4X SDS sample buffer yielding 1X concentration and the samples were then heated to 95°C for 5 min. Casted gels were placed into the XCell SureLock Mini-Cell tank (Thermo Fisher Scientific) and the upper and lower chambers filled with 1X Tris-glycine SDS running buffer. A pre-stained protein ladder and a biotinylated protein ladder was loaded into the first wells. A volume of 15μL of sample containing 10μg (unless otherwise stated) of protein was then added to each well. Gels were run at 125V for 2 hours at room temperature using a ZOOM™ Dual Power Supply (Thermo Fisher Scientific).

2.4.4 Western blotting

Transfer

Polyvinylidene difluoride (PVDF) membranes were activated in methanol for
30s, then rinsed twice in distilled water and soaked along with blotting pads
and filter paper in 1X transfer buffer containing 20% methanol for 30 min.
After gel electrophoresis, wet transfer was carried out using the XCell II Blot
Module (Thermo Fisher Scientific) assembling the "sandwich" in the following
order: (Cathode) blotting pad x2 - filter paper - gel-membrane - filter paper -
blotting pad x2 - (anode). A roller was used to remove any trapped bubbles
between layers during assembly. The blot module was then filled with the 1X
transfer buffer containing 20% methanol and placed inside the tank. The
outer tank was filled with the leftover 1X transfer buffer and transfer was
carried out at 25V for 2 hours at room temperature using a ZOOM™ Dual
Power Supply (Thermo Fisher Scientific).

Dot blotting

A row of ten $1cm^2$ boxes were drawn on a piece of nitrocellulose membrane in
pencil. To the centre of each box, 2μL of each sample was carefully pipetted
and allowed to air dry. The membranes were then processed the same as
western blot immunodetection.

Immunodetection

Membranes were removed from the blot module and placed in 20mL blocking
buffer for 1 hour with gently agitation at room temperature. The membranes
were then incubated with the primary antibody diluted in 5mL blocking

buffer overnight at 4°C on a tube roller. The membrane was washed for 5 minutes in TBST 3 times then incubated with HRP-linked secondary antibody and HRP-linked anti-biotin antibody diluted in 5mL TBST for 1 hour at room temperature on a tube roller. The membrane was washed again 3 times and then rinsed in deionised water. Membranes were drained, then covered in ECL detection reagent and imaged using the PXi 4 Gel Imager (SynGene). The exposure times were automatically calculated by the imager software. Antibodies and binding proteins were used at the dilutions listed in table 2.6.

Table 2.6: Antibody dilutions

Primary Antibodies	
Anti-LPCAT2 antibody	1/800
Anti-CD36 antibody	1/2000
Anti-LIMPII antibody	1/500
Anti-CD36 biotinylated antibody	1/2000
Anti-TLR4 antibody	1/200
Anti-Calnexin antibody	1/1000
Anti-GAPDH antibody	1/2000
Secondary Antibodies	
Anti-Goat IgG HRP-linked antibody	1/1000
Anti-rabbit IgG, HRP-linked antibody	1/2000
Anti-biotin HRP-linked	1/1000
Binding proteins	
Cholera Toxin Subunit B HRP-linked	1/500
Mouse IgGκ binding protein HRP-linked	1/1000

2.4.5 Silver staining

Silver staining of polyacrylamide gels was performed using the Silver Stain Plus ™ kit according to the manufacturer's instructions. Gels were developed until the desired staining was achieved (approximately 15 min) and the reaction was stopped by adding 5% v/v acetic acid solution. Gels were washed for 5 minutes in TBS-T twice and then imaged using an iPhone 6 camera (Apple Inc., USA).

2.4.6 Liquid Chromatography Tandem Mass Spectrometry (LC-MS/MS)

MS was carried out by the Proteomics Core Facility at the University of Plymouth using an Ultimate 3000 UPLC system (Thermo Fisher Scientific) connected to an Orbitrap Velos Promass spectrometer (Thermo Fisher Scientific).

2.4.7 Total RNA isolation

The method for RNA isolation used was a modified acid guanidinium thiocyanate-phenol-chloroform extraction originally developed by Chomczynski et al [220]. The use of chloroform had been substituted for 1-bromo-3-chloropropane, a far less toxic phase separation reagent that yields the same quantity and quality as chloroform [221]. Following experiments, the culture medium was aspirated and 500μL of denaturing solution was added directly to the cells and left to stand for 1 min. To facilitate cell lysis, the lysate was triturated by pipette before being transferred to RNase/DNase free 1.5 mL microcentrifuge tubes. Samples were then left to stand for 5 minutes before either being stored at -20°C or placed on ice for immediate processing. Working on ice, the following was added sequentially to the samples; 50 μL 2M sodium acetate (pH 4), 500 μL water-saturated phenol (pH 4.3) and 100 μL 1-Bromo-3-chloropropane. The samples were mixed by inverting the tubes between each step and finally shook vigorously by hand for 10 sec before incubating on ice for 15 min. The samples were then centrifuged at 15,000xg for 15 minutes at 4°C, causing phase separation. The upper aqueous phase containing the RNA was transferred to a new RNase/DNase free 1.5 mL microcentrifuge tube and

then an equal volume of 2-propanol was added to precipitate the RNA. The samples were mixed by inversion and stored at -20°C for a minimum of 1 h. At this point the samples could be stored for up to a week at -20°C. The samples were then centrifuged at 15,000xg for 20 minutes at 4°C and the supernatant was discarded. To remove residual proteins, the pellet was dissolved in 300μL of denaturing solution and the RNA precipitated by the addition of an equal volume of 2-propanol and incubation at -20°C for 30 min. The samples were then centrifuged at 15,000xg for 10 minutes at 4°C and the supernatant was discarded. Residual salts were then removed from the RNA pellet with a 75% ethanol wash, this was done by adding 500μL of 75% ethanol to the pellet, vortexing for 10s and then incubating at room temperature for 15 min. Samples were then treated with an Amplification Grade DNase I kit from Sigma-Aldrich to digest any residual DNA. This was done by centrifuging the samples at 15,000xg for 10 minutes at 4°C and carefully discarding the supernatant. The RNA pellets were then air dried at room temperature for 5 minutes before being dissolved in 16μL DEPC-treated water. To this, 2 μL of Reaction Buffer and 2 μL Amplification Grade DNase I was added. The samples were then mixed and briefly centrifuged before being incubated for 15 minutes at room temperature. To inactivate the DNase I enzymes, 2μL of Stop Solution was then added and the samples were incubated at 70°C for 10 min. RNA quantity and quality was determined using a NanoDrop 2000 spectrophotometer (Thermo Fisher Scientific). All measurements were taken in duplicate and samples were considered acceptable with 260/280 values of 1.8-2.1 and 260/230 values >1.0.

2.4.8   Reverse Transcription PCR (RT-PCR)

Reverse transcription was carried out using the High-Capacity RNA-to-cDNA kit. This was done by adding 1μg of RNA to a 0.2mL PCR tube and making

the volume up to 9μL with DEPC-treated water and then incubating at 70°C for 5 min, then cooled to 4°C to denature any RNA hairpins that may have formed. To this 1μL of RT Enzyme Mix 20x and 10μL RT Buffer Mix 2x was added and the tubes were incubated at 37°C for 60 min, then 95°C for 5 minutes and then held at 4°C in a Veriti 96-Well Thermal Cycler (Thermo Fisher Scientific). The cDNA was then either used immediately or stored at -20°C.

2.4.9   Quantitative PCR (qPCR)

SYBR® Green chemistry utilising the comparative quantification method was used to calculate relative gene expression for all experiments. Each reaction contained 0.5μL cDNA, 6μL Power SYBR® Green PCR Master Mix 2X, 5.5μL DEPC-treated water, 400nM forward primers and 400nM reverse primers. All reactions were loaded in duplicate into 96-well plates, sealed and briefly centrifuged before being loaded into the StepOnePlus Real-Time PCR System (Thermo Fisher Scientific). The following cycling conditions were used for qPCR: 50°C for 2 min, 95°C for 10 min, then 40 cycles of 95°C for 15 s then 60°C for 1 minute followed by a melt curve analysis. Data were acquired on the StepOne software v2.3. Primer sequences are listed in table 2.7 and were designed from reference gene sequences from the National Centre for Biotechnology Institute database using Primer3 and BLAST. The following search parameters were used: A Tm of 60°C ±3°C, a primer length of 18-24 bases, an amplicon length of 50-200 bp, a GC content of 20-80% and ideally the amplicon should span one intron. Primer sequences were screened using OligoAnalyzer 3.1 software (Integrated DNA Technologies) to check for hairpins, and dimer formation. Lyophilized primers were then sourced from Eurofins Genomics, re-suspended at 100μM in DEPC-treated water and stored at -20°C.

Table 2.7: RT-qPCR primer sequences

Target gene	Primer sequence (5' - 3')
Mouse ATP5B forward	AGG GTG GGA AAA TCG GAC TC
Mouse ATP5B reverse	AAA TCA TTG CCC TCA CGG GT
Mouse CD36 forward	ACC TGG GAG TTG GCG AGA A
Mouse CD36 reverse	TGT CTC CGA CTG GCA TGA GA
Mouse IFNb forward	AAG GGG ACA TTA GGC AGC AC
Mouse IFNb reverse	ATG AAA GAC CTC AGT GCG GG
Mouse IL-6 forward	AGA AGG AGT GGC TAA GGA CCA A
Mouse IL-6 reverse	ACG CAC TAG GTT TGC CGA GTA
Mouse IL-10 forward	CTT GCA CTA CCA AAG CCA CAA G
Mouse IL-10 reverse	GGA AGT GGG TGC AGT TAT TGT CT
Mouse TNFα forward	AGG ACC CAG TGT GGG AAG CT
Mouse TNFα reverse	AAA GAG GAG GCA ACA AGG TAG AGA
Mouse IL-1β forward	AAG GGG ACA TTA GGC AGC AC
Mouse IL-1β reverse	ATG AAA GAC CTC AGT GCG GG
Mouse Fasn forward	CTA ACT ACG GCT TCG CCA AC
Mouse Fasn reverse	CCA TCG CTT CCA GGA CAA TG
Mouse Slc25a1 forward	TCG AGT TCC TCA GCA ACC AC
Mouse Slc25a1 reverse	ACT ACC ACT GCT TCT GCC AC
Mouse Hif1α forward	GCC TTA ACC TGT CTG CCA CT
Mouse Hif1α reverse	GCT GCT TGA AAA GGG AGC C

2.5   Statistical analysis

All statistical analyses were performed using GraphPad Prism version 6.01 for Windows (GraphPad Software, La Jolla California USA). The variance between experimental groups were calculated using an F test for unequal variance. If each population had equal variance, the standard unpaired t test was used to compare the means between two experimental groups. If the variance was unequal, the unpaired t test with Welch's correction was used.

Chapter 3

Results: LPCAT2 knockdown reduces protein S-acylation in macrophages.

3.1   Introduction

LPCAT2 is an enzyme primarily involved in the remodelling of glycerophospholipids within cell membranes and the generation of platelet-activating factor [27]. More recently, researchers in Professor Jackson's group demonstrated that LPCAT2 can also mediate LPS-induced cytokine responses in both murine and human macrophages [216] and that LPCAT2 translocates to membrane lipid raft domains and associates with TLR4 following activation by LPS [177]. Therefore, LPCAT2 appears to have a role in regulating innate responses via lipid raft signalling complexes, however, the mechanisms behind this are not known.

S-acylation is a type of posttranslational modification that involves the covalent binding of a lipid group to a protein. The addition of these lipid groups can impact membrane-protein association, protein structure and protein stability through increased protein hydrophobicity and this will ultimately affect a proteins function [146, 147]. Unique among lipid

63

modifications, the thioester bond formed by S-acylation is reversible allowing dynamic regulation of this modification in a similar way to protein phosphorylation or ubiquitination. This reversibility makes S-acylation a particularly interesting posttranslational modification to investigate in terms of cell signalling.

It has been reported that LPCAT1, in addition to the acylation of LPC, can catalyse histone protein O-palmitoylation to regulate mRNA synthesis [217]. Coupled with previous reports by researchers in Professor Jackson's research group that show LPCATs facilitate LPS-stimulated translocation of TLR4 into membrane lipid raft domains [212], gave rise to the main research question explored in this thesis: Does LPCAT2 play a role in the S-acylation of proteins involved in LPS signalling?

This chapter explores this research question by addressing the following objectives:

1. Identifing if LPCAT2 S-acylates lipid raft-associated proteins in LPS-stimulated macrophages.

2. Determining the function LPCAT2 S-acylation has on the proteins identified in objective 1.

3.2 Results

3.2.1 Identification of LPCAT2 mediated protein S-acylation in LPS stimulated macrophages

To identify if LPCAT2 plays a role in protein S-acylation in LPS stimulated macrophages, siRNAs were used to knockdown the protein expression of LPCAT2 in LPS stimulated RAW264.7 cells, combined with a method of purifying and identifying S-acylated proteins adapted from a protocol by Wan *et al* [222]. Changes in the level of protein S-acylation could then be compared between cells expressing normal levels of LPCAT2 and cells expressing reduced levels of LPCAT2, as described in method section 2.3.1.

In brief, RAW264.7 cells were treated with 5nM LPCAT2 siRNA for 72 hours to knockdown LPCAT2 protein expression. As a negative control, cells were treated for the same duration and with the same concentration using a scrambled siRNA that has no matches on the murine genome (negative siRNA). The cells were then stimulated with 1μg/mL sLPS for 45 min. A third group of cells were left untreated as a cell only control. Protein extracts from these cells were then divided into equal portions and acylated cysteine residues were tagged with biotin (acyl-biotin exchange reactions) and the resulting biotinylated proteins were affinity purified using streptavidin agarose beads. These proteins were then identified and quantified by tandem mass spectrometry and western blotting. Changes in the level of protein S-acylation could then be compared between cells expressing normal levels of LPCAT2 and cells expressing reduced levels of LPCAT2.

A knockdown efficiency of 86% (P<0.001) at the protein level was observed for LPCAT2 relative to the negative siRNA control group as assessed by

SDS-PAGE and western blotting of the protein extracts prior to acyl-biotin exchange reactions (Figure 3.1). Crucially there was no significant change in LPCAT2 expression between the cell only control and the negative siRNA control demonstrating that the siRNA transfection method does not adversely affect the cells and that the LPCAT2 siRNA is specific.
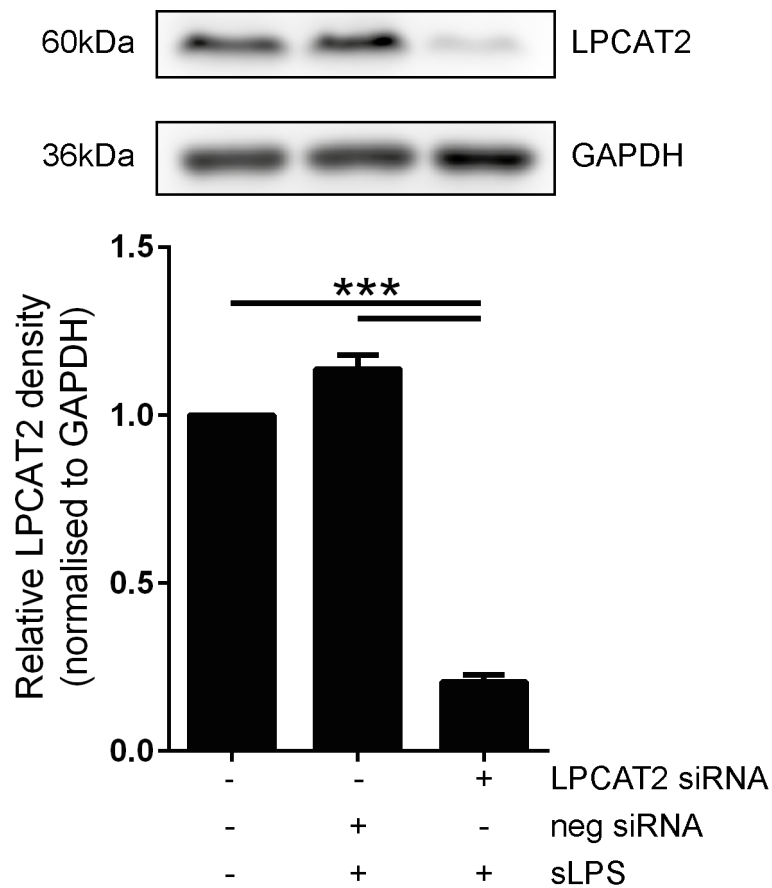
Figure 3.1: Western blot demonstrating LPCAT2 knockdown in siRNA treated RAW264 cells. The relative densities for each band were calculated using ImageJ and values were normalised to GAPDH. Each bar represents the mean +SEM of three independent experiments each performed with two technical replicates. ***P<0.001 as calculated using an unpaired t-test.

An important control to include in this analysis is to process equal portions of each sample in a parallel acyl-biotin exchange reaction without the addition of hydroxylamine. The role of hydroxylamine in this process is to cleave thioester bound acyl moieties to expose cysteine residues for biotinylation, therefore omitting this step makes it possible to identify and exclude proteins that are non-specifically purified by streptavidin agarose

[222]. This is clearly visualised by SDS-PAGE and silver staining of the purified S-acylated proteins (Figure 3.2). The lane without the addition of hydroxylamine (HA-) has multiple bands annotated by dashes and these are non-specifically purified proteins. When the same bands are also present in the lane where hydroxylamine was added to the sample (HA+) the proteins are false positives. However, there are also multiple bands that are only present or to a much higher intensity in the hydroxylamine positive lane marked by arrows and these are presumed to be S-acylated proteins.
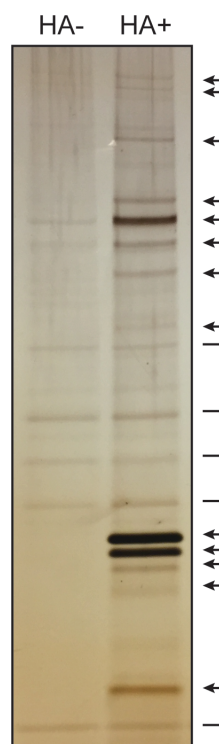
Figure 3.2: SDS-PAGE of purified proteins from RAW264.7 cells processed with or without hydroxylamine (HA). Protein extract from RAW264.7 cells was split into equal portions containing 1 mg of protein and then processed through acyl-biotinyl exchange chemistry either with or without HA. Following purification, 5% of each sample was compared by SDS-PAGE and silver staining. Proteins visualised in both the -HA and +HA lanes are annotated by a dash. While proteins that appear only in the +HA sample (or at a higher intensity) are annotated by arrows. Only the negative control is shown.

To detect global changes in the S-acylated proteome following LPCAT2 knockdown, the purified S-acylated protein samples were sent to the Proteomics Core Facility at the University of Plymouth for liquid chromatography tandem mass spectrometry. The strategy used to identify

candidate S-acylated proteins from the mass spectrometry data was to generate a ratio of $\frac{+HA}{-HA}$ for each sample to correct for signals generated by non-specific purification of proteins. When a protein was not present in the -HA sample it was given a value of 1. The fold change between the samples were then calculated based on these ratios and the top scoring proteins as determined by the greatest reduction in S-acylation following LPCAT2 knockdown. The top scoring proteins identified by the mass-spectrometry included the scavenger receptors CD36 and LIMPII, the chaperone proteins Malectin, Heat shock protein HSP 90-alpha, Heat shock cognate 71 KDa protein and Lysosome-associated membrane glycoprotein 2, the structural proteins Golgi apparatus protein 1, Ahnak and Neuroplastin, the signaling protein RasGAP-activating-like protein 1 and the enzymes E3 ubiquitin-protein ligase, Ubiquitin carboxyl-terminal hydrolase 27 and Protein disulfide-isomerase (Table 3.1).

Of the 14 proteins identified, Lysosome-associated membrane glycoprotein 2, E3 ubiquitin-protein ligase and Ubiquitin carboxyl-terminal hydrolase 27 had not been detected by previous proteomic studies [223] and are candidate novel S-acylated proteins. Further analysis using the predictive software CSS-Palm 4.0 identified potential cysteine residues for S-acylation on all the identified proteins. Only CD36, Malectin and Heat shock protein HSP 90-alpha had previously been validated by showing direct evidence of S-acylation by independent studies [224, 225, 79, 226]. From the candidate proteins identified by mass spectrometry, the scavenger receptor class B members CD36 and LIMPII were chosen for further investigation based on the criteria that they had reduced S-acylation following LPCAT2 knockdown in LPS stimulated macrophages and that there are reports that they play a role in innate immune responses in macrophages with potential links to TLR signalling [89, 90, 51].

Table 3.1: Candidate S-acylated proteins identified by LC-MS/MS that are down regulated >2-fold by LPCAT2 knockdown in LPS treated RAW264.7 cells. Proteins that have been identified in other proteomic studies are indicated according to the species used; human (H), mouse (M) or rat (R). Validated: Proteins that have been independently confirmed by direct evidence of S-acylation. Predicted sites indicate a protein contains cysteine residues that are predicted sites of S-acylation as calculated by CSS-Palm 4.0 [227]. DHHC: indicates DHHC enzymes. All data was acquired from SwissPalm: Protein Palmitoylation database [223].

Protein Name	Gene	Previously identified	Validated	Predicted	DHHC
Receptors					
CD36	Cd36	H,M,R	Yes	Yes	4,5
Lysosome membrane protein 2	Scarb2	H,M,R		Yes	
Chaperones					
Malectin	Mlec	H,M,R	Yes	Yes	
Heat shock protein HSP 90-alpha	Hsp90aa1	H,M	Yes	Yes	
Heat shock cognate 71 KDa protein	Hsc70	H,M,R		Yes	
Lysosome-associated membrane glycoprotein 2	Lamp2-c			Yes	
Signalling					
Golgi apparatus protein 1 (E-selectin ligand-1)	Glg1	H,M,R		Yes	
RasGAP-activating-like protein 1	Rasl1	H,M		Yes	
Neuroplastin	Nptn	R		Yes	
Structural					
Protein Ahnak	Ahnak	H		Yes	
Enzymes					
E3 ubiquitin-protein ligase	Rnf19b			Yes	
Ubiquitin carboxyl-terminal hydrolase 27	Usp27			Yes	
Protein disulfide-isomerase	P4hb	H,M		Yes	

To validate the mass spectrometry data, 10% of each of the remaining purified S-acylated protein samples were analysed by SDS-PAGE and western blotting for the presence of CD36 and LIMPII. CD36 was detected in the +HA samples and not in the -HA samples confirming the mass spectrometry data that CD36 is S-acylated. Stimulation with LPS for 45 minutes did not alter the acylation state of CD36 when compared to the untreated control, however knockdown of LPCAT2 reduced the level of S-acylated CD36 by 65% in the LPS treated cells compared to cell treated with negative siRNA with LPS stimulation (Figure 3.3.A).
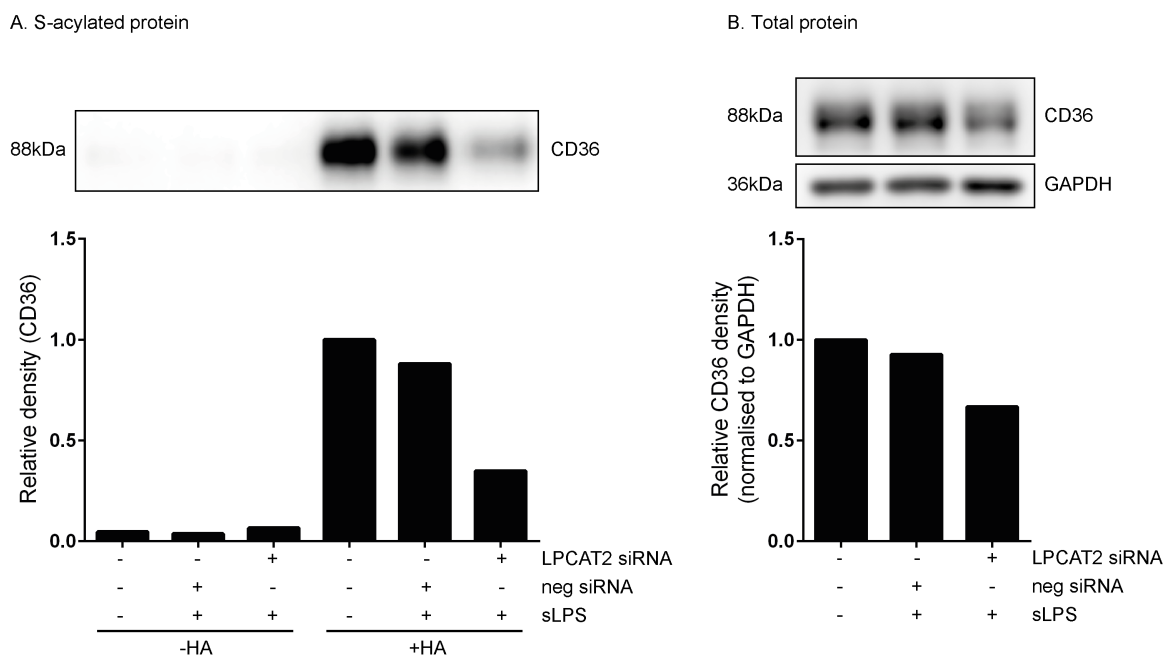
Figure 3.3: LPCAT2 expression is required for efficient S-acylation of CD36. The expression of S-acylated CD36 as determined by ABE chemistry and western blotting are shown in panel A. The expression of total CD36 is shown in panel B. The relative densities of the bands were calculated using ImageJ and for panel B values were normalised to GAPDH. The blots are representative of three independent experiments each performed with two technical replicates.

To ensure that the reduction in S-acylated CD36 observed following LPCAT2 knockdown was not due to a reduction in total CD36 protein, 10 µg of the samples prior to ABE reactions were analysed by SDS-PAGE and western blotting. This showed that total CD36 comprising of both acylated and non-acylated forms was reduced 28% by LPCAT2 knockdown in LPS treated cells compared to cell treated with negative siRNA with LPS stimulation (Figure 3.3.B). The reduction in S-acylated CD36 (Figure 3.3.A) is greater than the reduction in total CD36 (Figure 3.3.B) meaning there is a net reduction in the S-acylated form of CD36 following LPCAT2 knockdown in LPS stimulated cells.

LIMPII was also shown to be present in the +HA samples to a much greater intensity than the -HA samples confirming the mass spectrometry data that it is S-acylated. Stimulation with LPS for 45 minutes did not alter the acylation state of LIMPII when compared to the untreated control, however knockdown of LPCAT2 reduced the level of S-acylated LIMPII by 40% in the LPS treated cells compared to cell treated with negative siRNA with LPS stimulation (Figure 3.4.A). To ensure that the reduction in S-acylated LIMPII observed following LPCAT2 knockdown was not due to a reduction in total LIMPII protein, 10 μg of the samples prior to ABE reactions were analysed by SDS-PAGE and western blotting. This showed that total LIMPII comprising of both acylated and non-acylated forms remained stable following LPCAT2 knockdown (Figure 3.4.B).
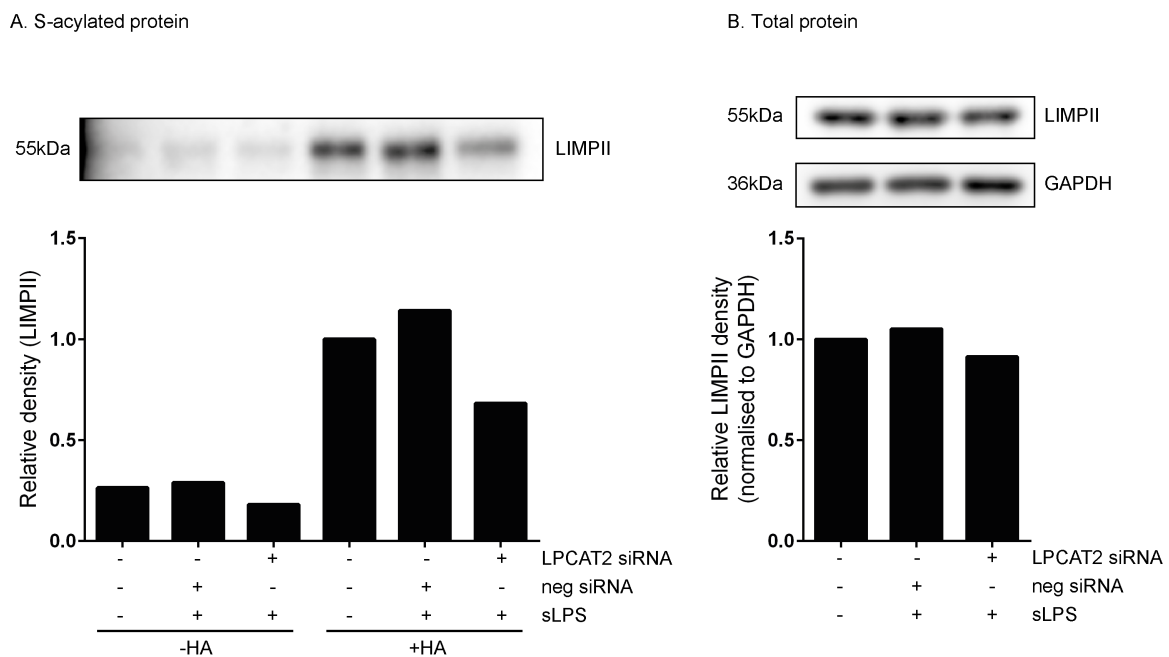
Figure 3.4: LPCAT2 expression is required for efficient S-acylation of LIMPII. The expression of S-acylated LIMPII as determined by ABE chemistry and western blotting are shown in panel A. The expression of total LIMPII is shown in panel B. The relative densities of the bands were calculated using ImageJ and for panel B values were normalised to GAPDH. The blots are representative of three independent experiments each performed with two technical replicates.

It is important to demonstrate that this purification method is specific, therefore TLR4 was used as a negative control for S-acylation based on its absence in the initial mass spectrometry data and that there are no reports of TLR4 being S-acylated in the literature. No TLR4 was detected by western blotting in the either the -HA or +HA samples but it was detected in the total protein (data not shown) reinforcing that the method is specific for purifying S-acylated proteins. As a positive control, the abundant S-acylated protein GAPDH was chosen [228]. GAPDH was present in the +HA samples to a much greater intensity than the -HA samples confirming that the method detects known S-acylated proteins and critically the expression of S-acylated GAPDH remained constant across all treatment groups demonstrating that the changes in S-acylation mediated by LPCAT2 knockdown are not global (Figure 3.5).
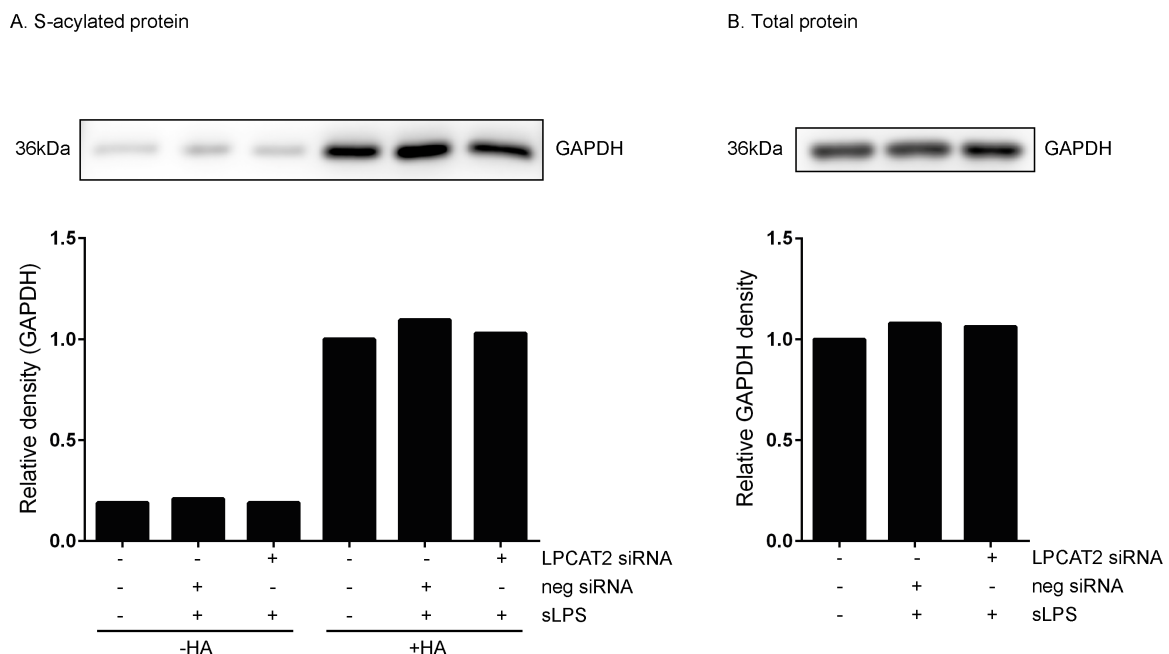

Figure 3.5: GAPDH is S-acylated and its expression is stable following LPCAT2 knockdown. The S-acylation of GAPDH remained constant (A) as did the overall expression of GAPDH (B) following knockdown of LPCAT2. The relative densities of the bands were calculated using ImageJ. The blots are representative of three independent experiments each performed with two technical replicates.

3.2.2 Reduced S-acylation of CD36 alters its distribution on the cell surface.

CD36 is a transmembrane glycoprotein that is expressed on the cell surface primarily within lipid rafts [229]. Lipid rafts are tightly packed regions of membranes that are rich in cholesterol, sphingolipids and phospholipids containing saturated fatty acids [230]. CD36 has been shown to be S-acylated with the saturated fatty acid palmitate [79] which is known to facilitate association with lipid rafts [145]. As previously shown (Figure 3.3), knockdown of LPCAT2 reduces S-acylation of CD36, therefore the membrane localisation of CD36 following LPCAT2 KD was investigated to see if the observed reduction in S-acylation directly impacts the distribution of CD36 between lipid raft and non-raft membrane domains. This was achieved through use of a discontinuous sucrose density gradient with ultracentrifugation to separate raft and non-raft membrane fractions isolated from RAW264.7 cells that had been treated with 5nM negative siRNA or LPCAT2 siRNA for 72 hours. A total of 10 fractions were collected from the sucrose gradient and these were analysed by SDS-PAGE and western blotting or dot blotting as described in methods section 2.3.2.

The majority of CD36 was detected in fractions 3 and 4, or 8, 9 and 10 which correspond to raft and non-raft fractions respectively. In cells treated with negative siRNA, the highest intensity band for CD36 was observed in fraction 3, while the highest intensity band for cells treated with LPCAT2 siRNA was in fraction 10. This demonstrates a shift of CD36 from the raft fraction to the non-raft fraction following LPCAT2 knockdown (Figure 3.6.A). Fraction 3 in the negative siRNA treated cells contained 35.5% of all the CD36, this was reduced to 21% following LPCAT2 knockdown, a reduction of 14.5%. The amount of CD36 in fractions 8, 9 and 10 in the LPCAT2 siRNA treated cells

was increased by 2%, 3% and 9% respectively, totalling a 14% increase in the collective non-raft fractions when compared to the negative siRNA treated cells (Figure 3.6.B). GM1 gangliosides are enriched in lipid rafts and are commonly used as a marker to identify these domains [231]. Here GM1 was used as a control for lipid rafts and was detected with the highest intensity in fractions 3, 4 and 5. Calnexin is commonly used as a marker for the endoplasmic reticulum and for non-raft fractions [232]. Again, Calnexin was used here as a control for non-raft fractions and was detected in fractions 9 and 10.
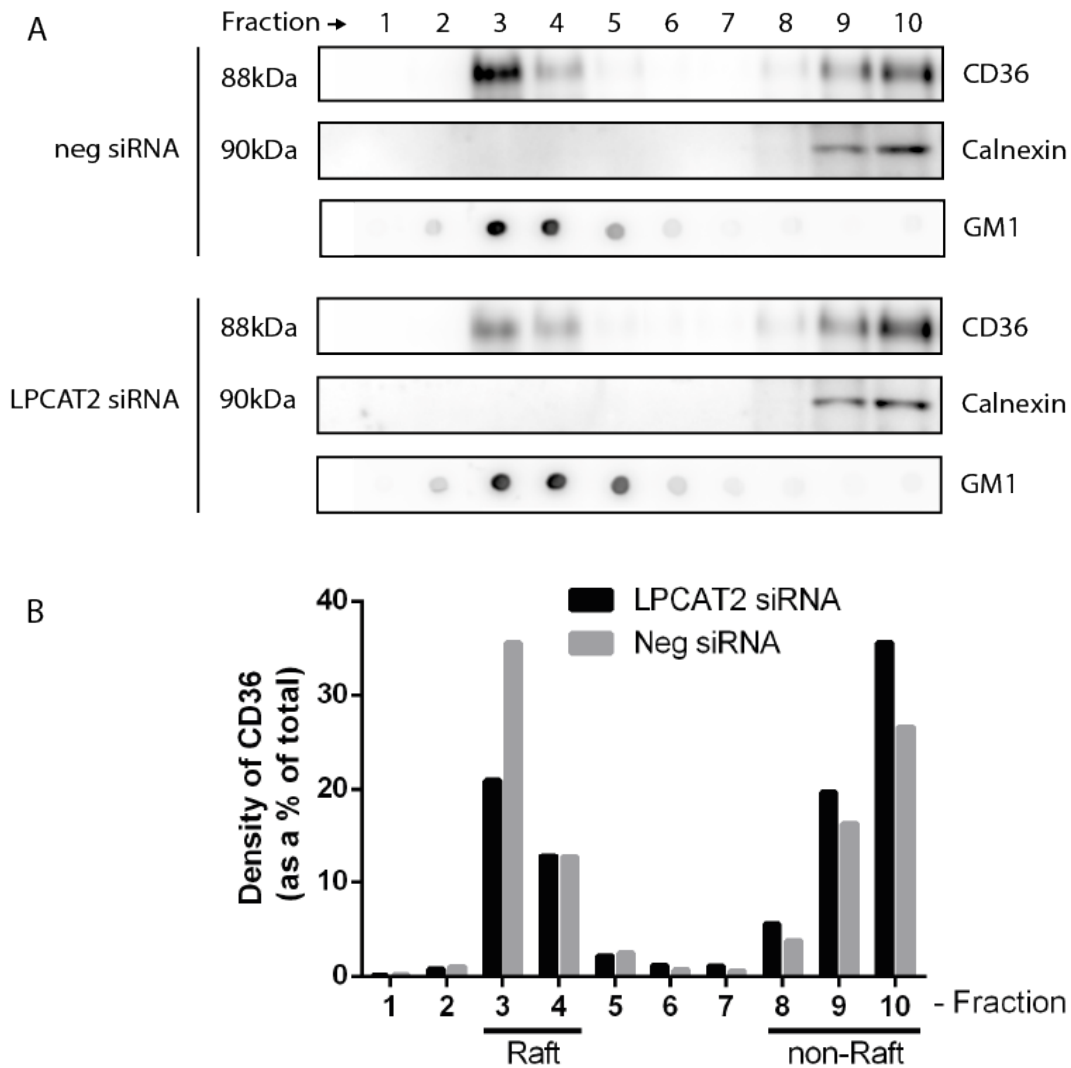
Figure 3.6: LPCAT2 knockdown reduces the amount of CD36 present in the lipid raft fraction of RAW264.7 cells. Following a 72 h Knockdown of LPCAT2 1 mg of protein was fractionated using a sucrose density gradient. 5% of each fraction was then analysed by SDS-PAGE and western blotting/dot-blotting for CD36, Calnexin and GM1 (A). The relative densities of the bands for CD36 were calculated using ImageJ and plotted (B). The blots are representative of three independent experiments each performed without technical replicates.

As LPCAT2 knockdown has been shown to reduce S-acylation of CD36 and reduce its expression within lipid-rafts it made sense to investigate if this also had an impact on CD36 surface expression. To do this, RAW264.7 cells were treated with 5nM LPCAT2 siRNA or negative siRNA for 72 hours to knockdown LPCAT2 before being stimulated with 1μg/mL sLPS for 45 min. Cells were then collected, blocked, and stained with anti-CD36-APC antibody prior to being analysed by flow cytometry, as described in section 2.3.3 of the methods.

The cells were gated to exclude debris using a forward and side scatter plot, and then clumps of cells (doublets) were identified by plotting forward scatter-hight over forward scatter-area. As the signal produced by doublets will have a greater width and therefore area than single cells while the height remains roughly the same, it is possible to gate and exclude doublets from the analysis based on this disproportion (Figure 3.7). The single cells were then analysed by plotting histograms for APC. The APC-isotype control gave a negligible shift in fluorescence intensity when compared to unstained cells indicating Fc receptors were adequately blocked and there was no non-specific binding of the antibody. Staining cells with anti-CD36-APC gave two distinct populations that were gated and labelled CD36 low or CD36 high. Knockdown of LPCAT2 caused 26% of the cells to shift from the CD36 high population to the low population without LPS stimulation and 12% of the cells to shift from the CD36 high population to the low population with LPS stimulation (Figure 3.8). Further analysis plotting the geometric mean fluorescence intensity of CD36 staining showed that following LPCAT2 knockdown, the MFI reduced by 56% ($p<0.01$) and following LPCAT2 knockdown with LPS stimulation the MFI reduced by 48% ($p<0.05$) (Figure 3.9). The reduction in MFI indicates that CD36 surface expression is reduced significantly following LPCAT2 knockdown.

Figure 3.7: Gating strategy for surface stained RAW264.7 cells. (A) The main population of cells were initially gated to exclude debris and were labelled RAW264. (B) These cells were then gated to exclude doublets and were labelled Single Cells.
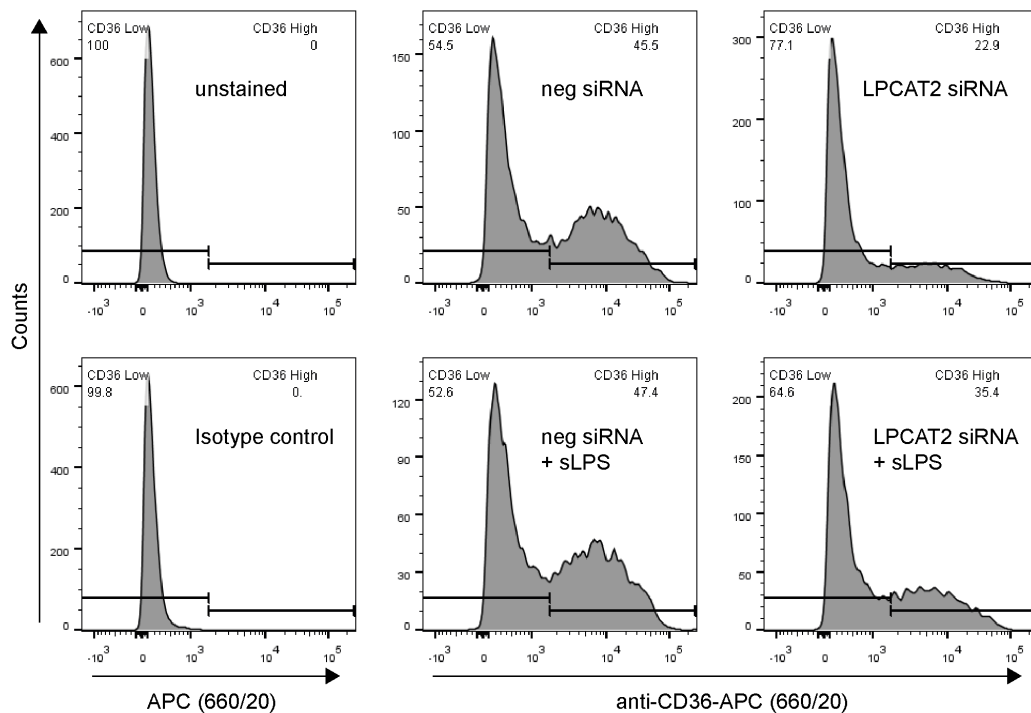
Figure 3.8: LPCAT2 knockdown reduces the surface expression of CD36 on RAW264.7 cells. Following a 72 hour knockdown of LPCAT2 cells were stimulated with or without 1μg/mL sLPS for 45 minutes prior to staining with anti-CD36-APC antibody. Histograms are representative of three independent experiments each performed without technical replicates.

Figure 3.9: CD36 surface expression is reduced following LPCAT2 knockdown in RAW264.7 cells. The mean fluorescence intensity is plotted as a percentage of untreated cells stained with anti-CD36-APC. Each bar represents the mean +SEM of three independent experiments each performed without technical replicates. *P<0.05 and **P<0.01 as calculated using an unpaired t-test.

To confirm that the reduction in surface CD36 was not due to a reduction in total CD36 expression, the same flow cytometry experiment was repeated with the modification that the cells were permeabilised prior to staining to allow intracellular CD36 to also be stained, as described in section 2.3.3 of the methods. The same gating strategy was implemented to exclude debris and doublets (Figure 3.10).

There was a minor shift in fluorescence when the permeabilised cells were stained with the isotype controls compared to the unstained cells (Figure 3.11), however staining with anti-CD36-APC caused a major shift in fluorescence (Figure 3.12). There was no shift in fluorescence intensity following LPCAT2 knockdown with or without LPS stimulation when compared to untreated cells or neg siRNA treated cells indicating that CD36 expression remained unaltered by these treatments (Figure 3.13).
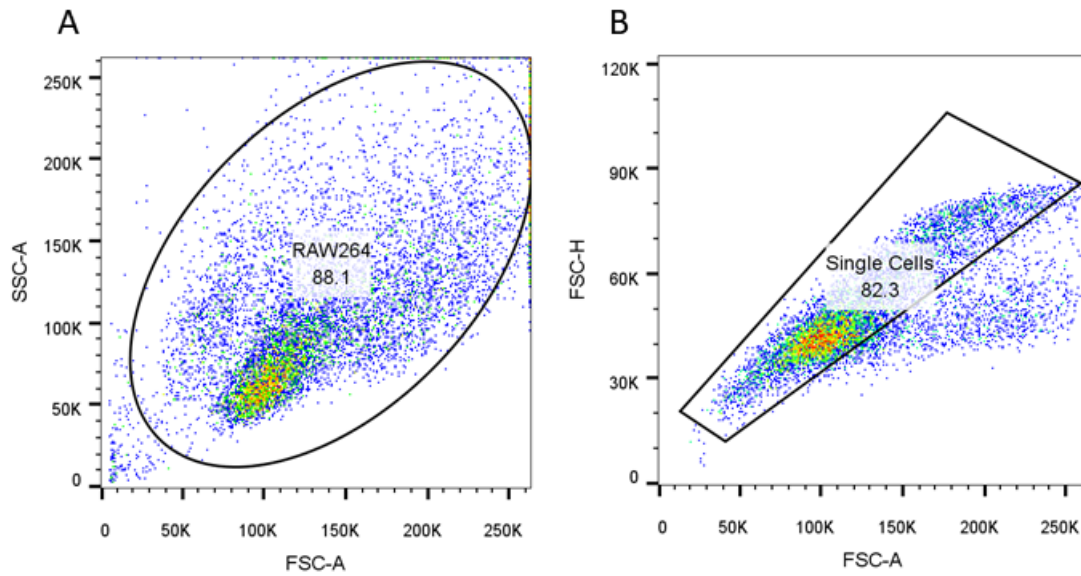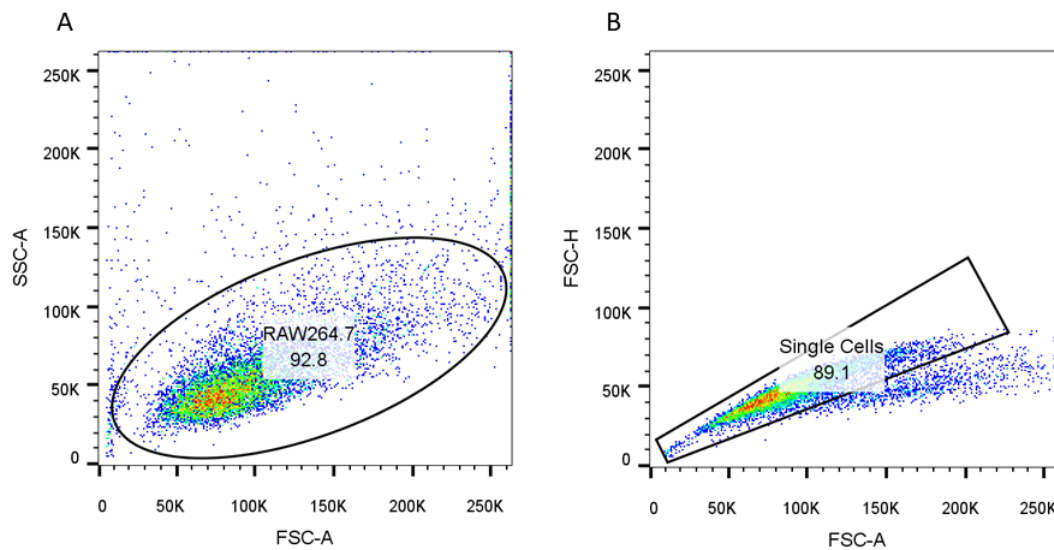
Figure 3.10: Gating strategy for permeabilised RAW264.7 cells. (A) The main population of cells were initially gated to exclude debris and were labelled RAW264.7. (B) These cells were then gated to exclude doublets and were labelled Single Cells.
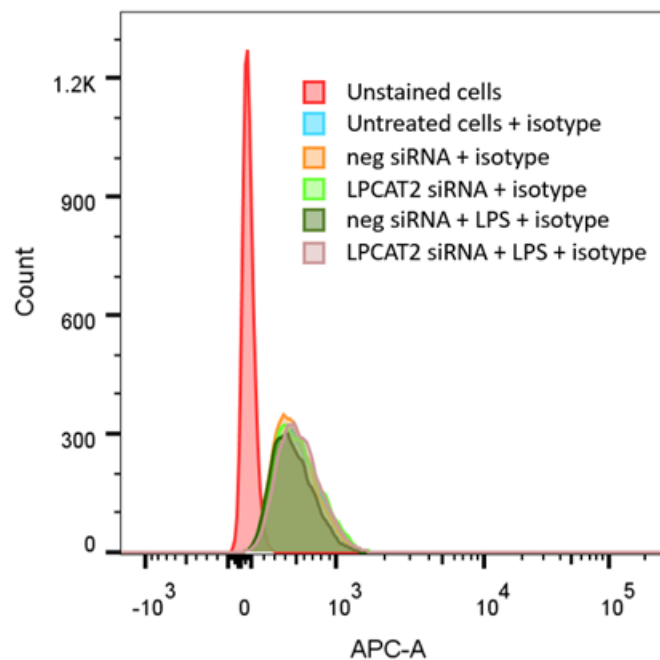
Figure 3.11: Permeabilized RAW264.7 cells stained with APC-isotype control. Histograms are representative of three independent experiments each performed without technical replicates.
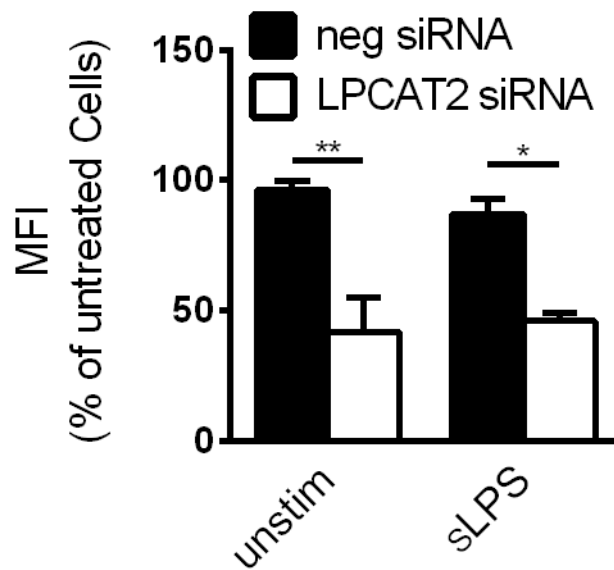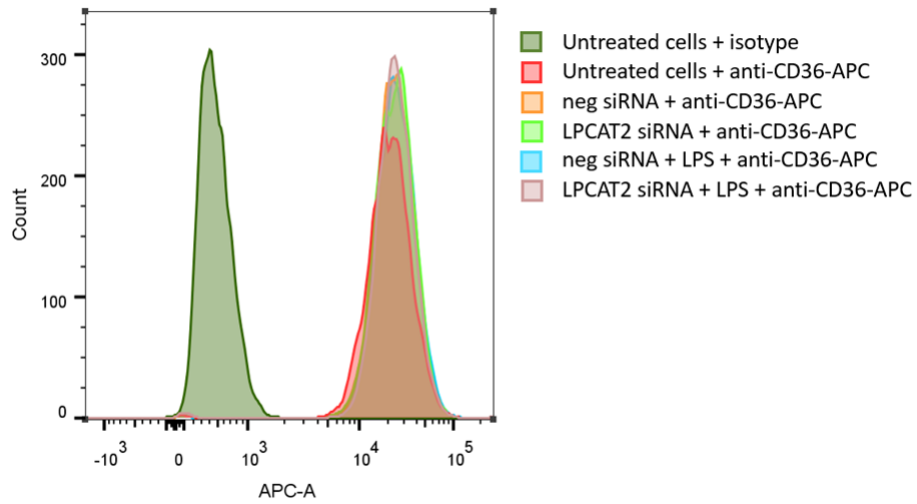
Figure 3.12: LPCAT2 knockdown does not affect total CD36 expression in RAW264.7 cells. Histograms are representative of three independent experiments each performed without technical replicates.
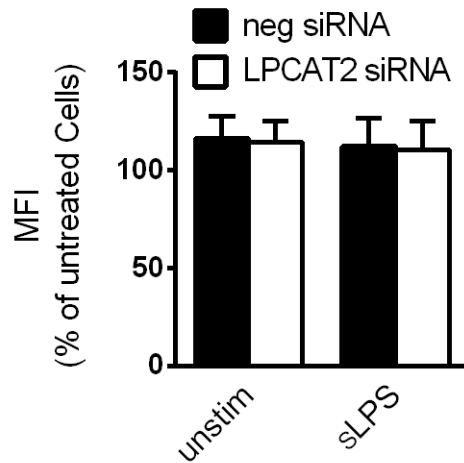
Figure 3.13: LPCAT2 knockdown does not affect total CD36 expression in RAW264.7 cells. The mean fluorescence intensity is plotted as a percentage of untreated cells stained with anti-CD36-APC. Each bar represents the mean +SEM of three independent experiments each performed without technical replicates.

To check that the two populations of RAW264.7 cells observed when staining surface CD36 (Figure 3.8) were not a staining artefact, the two populations of cells were investigated further by fluorescence-activated cell sorting. RAW264.7 cells were stimulated with or without 100 ng/mL sLPS for 6 hours before being collected, stained with anti-CD36-APC and subjected to fluorescence-activated cell sorting as described in section 2.3.4 in the methods. The same gating strategies were applied to exclude debris and doublets (Figure 3.14.A,B). The cells were then gated into CD36 high and CD36 low populations and sorted according to these gates (Figure 3.14.C). A total of 158,203 events were collected in the CD36 low population and 254,991 events were collected in the CD36 high population. The collected cells were then analysed by RT-qPCR for CD36, IL-6 and IL-10 mRNA expression. The CD36 high population expressed 15-fold more CD36 mRNA relative to the low population without LPS stimulation indicating that these are two distinct populations of cells. Stimulation with sLPS increased CD36 mRNA expression 1.8-fold in the CD36 low population and 1.3-fold in the CD36 high population (Figure 3.14.D). The CD36 high population produced

69% less IL-6 mRNA and 48% less IL-10 mRNA than the CD36 low population (Figure 3.14.E,F) following sLPS stimulation indicating that the CD36 high and low populations have different responses to sLPS.
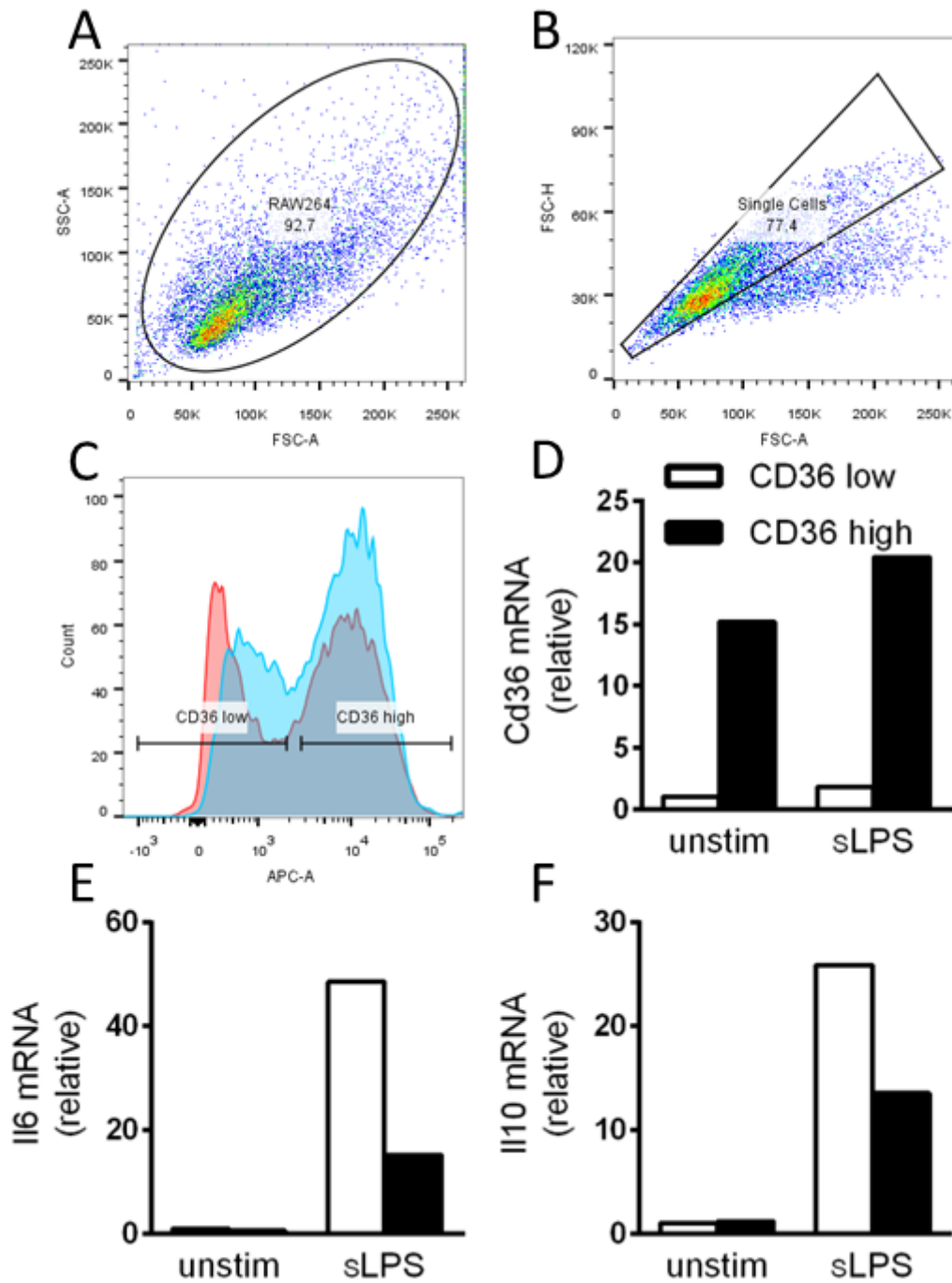
Figure 3.14: RAW264.7 cells consist of two populations that express different amounts of CD36 protein and mRNA that differently respond to LPS stimulation. Cells were stimulated with or without 100ng/mL sLPS for 6 hours prior to collection and staining with anti-CD36-APC antibody. Cells were then gated to exclude debris (A) and doublets (B). The single cells were then sorted into CD36 low and high populations (C) and the collected cells were then subjected to RT-qPCR to measure the mRNA expression of Cd36, IL-6 and Il10 relative to ATP5B. The data represents a single experiment.

CD36 has been shown to mediate the uptake of *E. coli* in HEK293 cells transfected with murine CD36 [233] and in goat mammary gland epithelial cells [71]. To check if reduced CD36 S-acylation, lipid raft association and surface expression observed following LPCAT2 knockdown has functional consequences on CD36, the uptake of pHrodo Green labelled *E. coli* bioparticles was assessed following LPCAT2 and CD36 knockdown. RAW264.7 cells were treated with 5nM siRNA for 48 hours to knockdown LPCAT2 or CD36 expression and then these cells were seeded in 96-well plates and allowed to adhere for 1 hour. The medium was then exchanged with live cell imaging solution (a physiological solution buffered with HEPES at pH 7.4) containing labelled *E. coli* bioparticles and the cells were incubated at 37°C for 2 hours without elevated CO_2 before being analysed by a plate reader as described in section 2.3.5 of the methods.

The fluorescence of pHrodo™ dyes increase as the pH decreases, as *E. coli* bioparticles are internalized via phagocytosis the pH within the vesicles decreases as they mature leading to an increase in fluorescence. The fluorescence of each treatment group was blanked against wells containing pHrodo Green labelled *E. coli* bioparticles without cells present and therefore any increase in fluorescence is due to a drop in pH. There was an increase in fluorescence for all treatment groups containing *E. coli* bioparticles indicating that the pH had dropped and due to the absence of elevated CO_2 and the presence of HEPES buffer it is likely due to endocytosis or phagocytosis of the bioparticles. The knockdown of either LPCAT2 or CD36 did not cause a significant shift in fluorescence when compared to the untreated cells or negative siRNA control cells indicating there was no effect on the uptake of *E. coli* bioparticles (Figure 3.15).
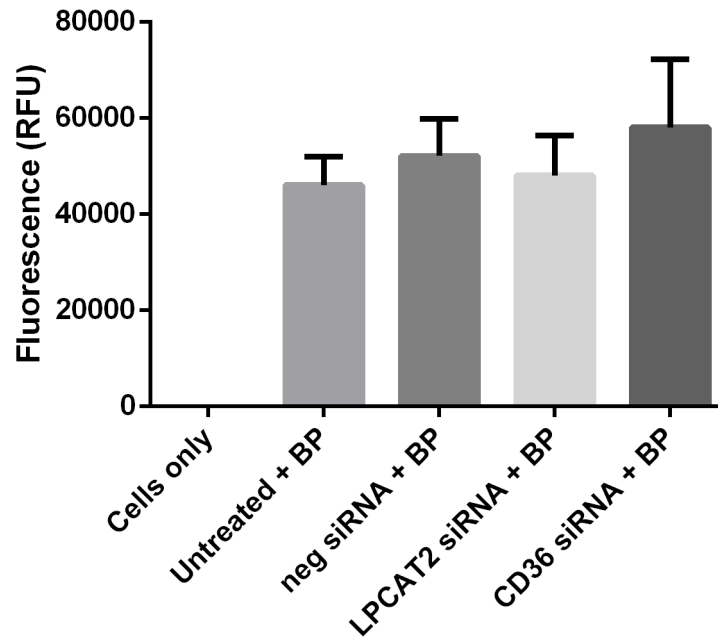
Figure 3.15: The uptake of pHrodo™ Green E. coli BioParticles is not affected by either LPCAT2 or CD36 knockdown in RAW264.7 cells. All values are blanked against pHrodo™ Green E. coli BioParticles without cells present. Each bar represents the mean +SEM of three independent experiments each performed with three technical replicates. BP: pHrodo™ Green E. coli BioParticles

As the knockdown of CD36 did not affect the uptake of *E. coli* bioparticles, a different function of CD36 needed to be investigated to demonstrate a functional consequence of reduced CD36 S-acylation. CD36 has been shown to play a role scavenging oxidized low density lipoprotein in macrophages [61], therefore the uptake of fluorescently labelled oxidized low density lipoprotein was investigated using flow cytometry.

RAW264.7 cells were treated with negative, CD36 or LPCAT2 siRNA for 48 hours prior to incubation with oxLDL-DyLight 488 for 4 hours. The cells were then collected, blocked, and stained with 7-AAD and anti-CD36-APC antibody as described in section 2.3.6 of the methods. Cells were gated to exclude debris, 7-AAD positive cells and doublets (Figure 3.16). Half of all the events collected were debris, however this does not reflect the sample quality as this was a known issue with the BD Accuri™ C6 Flow Cytometer being used. The same debris were also present following a deep clean of the

instrument and running just filtered staining solution (data not shown). To compensate for this, 10000 events were collected from the live cell population and not total events. A cell viability of 88.5% was observed across the treatment groups as determined by 7-AAD staining and this was in line with the 90% cell viability determined by trypan blue exclusion assay used to setup the initial experiment. The geometric mean fluorescence intensity of CD36 staining reduced by 98% following CD36 knockdown and 40% following LPCAT2 knockdown when compared to the negative siRNA treated cells (Figure 3.17). The uptake of oxLDL-DyLight was unchanged by all treatment groups (Figure 3.18).
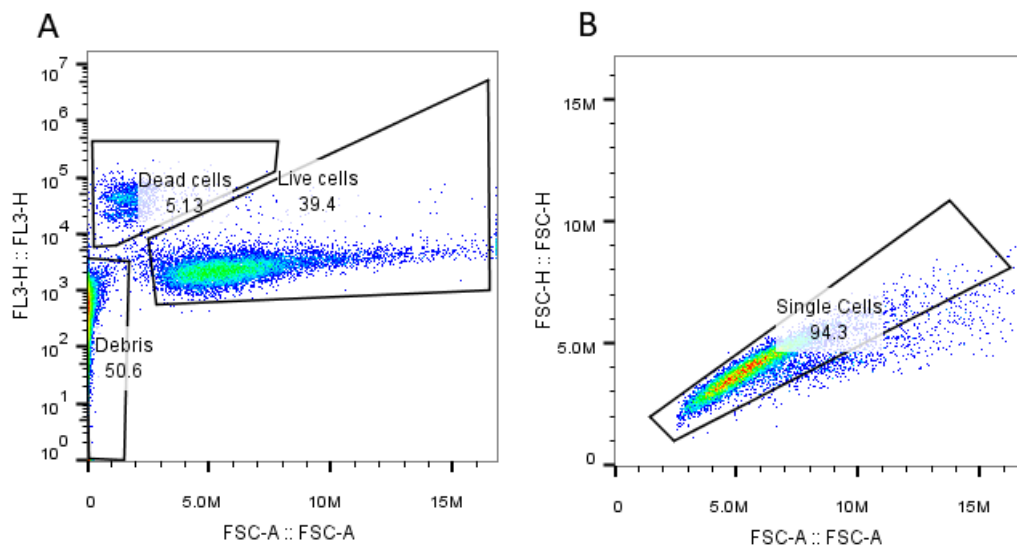
Figure 3.16: Gating strategy for RAW264.7 cells. (A) 7-AAD negative cells were gated and labelled live cells. (B) These cells were then gated to exclude doublets and were labelled Single Cells.
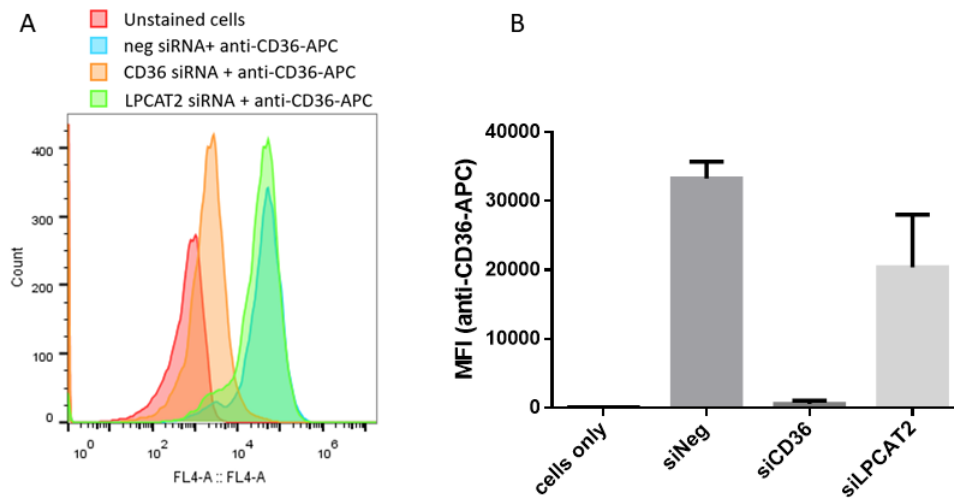
Figure 3.17: Anti-CD36-APC staining of RAW264.7 cells with or without LPCAT2 or CD36 knockdown. (A) Histograms showing the intensity of anti-CD36-APC staining. (B) Geometric mean fluorescent intensity of anti-CD36-APC staining. Each bar represents the mean +SEM of 3 independent experiments each performed without technical replicates.
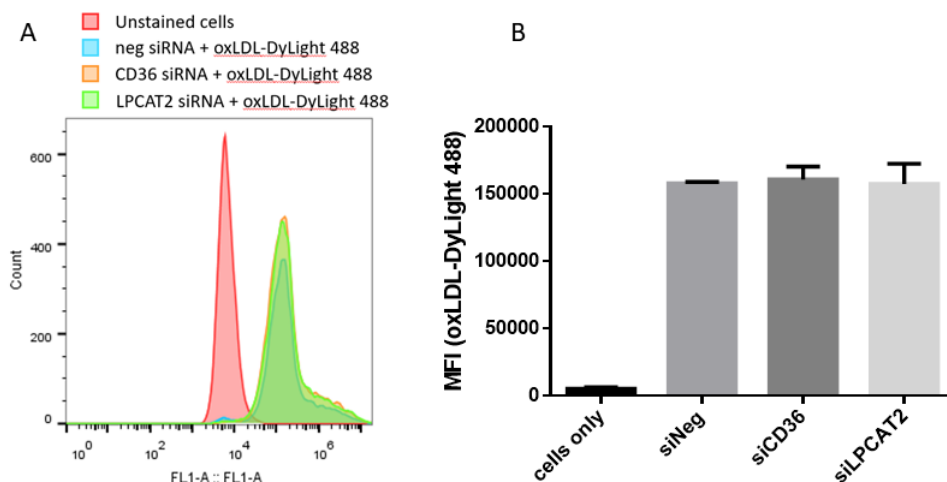
Figure 3.18: Uptake of oxLDL-DyLight 488 by RAW264.7 cells with or without LP-CAT2 or CD36 knockdown. (A) Histograms showing the intensity of oxLDL-DyLight 488. (B) Geometric mean fluorescent intensity of oxLDL-DyLight 488. Each bar represents the mean +SEM of 3 independent experiments each performed without technical replicates.

A summary of the results from chapter 3 can be found in table 3.2.

Table 3.2: Chapter 3 results summary.

Result	Section
Tandem mass spectrometry identified 14 proteins with a >2-fold reduction in S-acylation following LPCAT2 knockdown.	3.2.1
Western blot analysis confirmed the reduction in S-acylation following LPCAT2 knockdown detected by mass spectrometry for CD36 and LIMPII.	3.2.1
LPCAT2 knockdown reduces the amount of CD36 present in the lipid raft fraction of RAW264.7 cells.	3.2.2
LPCAT2 knockdown reduces the surface expression of CD36 on RAW264.7 cells.	3.2.2
LPCAT2 knockdown does not affect total CD36 expression in RAW264.7 cells.	3.2.2
CD36 and LPCAT2 knockdown does not affect the phagocytosis of *E. coli* particles by RAW264.7 cells	3.2.2
CD36 and LPCAT2 knockdown does not affect the uptake of oxLDL	3.2.2

3.3   Discussion

3.3.1   Overview

Previous research has shown that LPCAT2 is required for macrophage cytokine gene expression and release following TLR2 and TLR4 activation but not for TLR-independent stimuli [177]. Furthermore, LPCAT2 has been shown to rapidly associate with TLR4 and translocate to membrane lipid raft domains following LPS stimulation. However, the precise mechanisms as to how LPCAT2 translocates to membrane lipid rafts and regulates TLR2 and TLR4 cytokine responses remained to be investigated. Protein S-acylation is a tightly regulated and reversible post-translational modification that can regulate the association of proteins with lipid raft domains, this combined with the acyltransferase activity of LPCAT2 led to the main research questions posed in this thesis; "Does LPCAT2 play a role in the S-acylation of proteins involved in TLR signalling and is that the mechanism that enables LPCAT2 to regulate TLR2 and TLR4 cytokine responses?"

Using LPCAT2 sequence data and RNAi technology, the role LPCAT2 plays in protein S-acylation could be investigated. This was achieved through acyl-biotin exchange chemistry coupled to tandem mass spectrometry to screen for changes in the global S-acylated proteome and later confirmed by targeted analysis by SDS-PAGE and western blotting as described in method section 2.3.1. The data from these experiments demonstrate for the first time a link between LPCAT2 and the S-acylation of proteins, in particular the scavenger receptors CD36 and LIMPII that are both associated with TLR signalling [234, 65, 66, 235]. Further investigation demonstrated that the reduction in CD36 S-acylation had a direct effect on its cellular location, causing a shift in CD36 expression from lipid raft to non-raft domains and

90

further reducing the surface expression of CD36.

3.3.2 S-acylation of CD36

LPCAT2 has been shown to play a key role in TLR signalling [177, 216], however the mechanism for this is currently unknown. The data presented in this chapter shed light on a possible mechanism by which LPCAT2 can regulate TLR signalling through modulating the S-acylation of the TLR accessory protein CD36. In the context of LPS/TLR4 signalling, it has been theorised that CD36 acts as a co-receptor, like CD14, delivering LPS to the TLR4 complex [70]. The TLR4 complex has been shown to localise within lipid rafts following LPS stimulation [177] where S-acylated CD36 also resides (Figure 3.6) [82]. In the current research, knockdown of LPCAT2 reduced CD36 S-acylation by 65% leading to a reduction in surface and membrane lipid raft expressed CD36 protein. Therefore, reduced S-acylation of CD36 could potentially attenuate TLR4 signal induction by preventing CD36-LPS complexes forming within lipid rafts and presenting LPS monomers to the TLR4 receptor complex.

The scavenger receptor CD36 has also been identified as a co-receptor for various other TLRs, namely the TLR2/6 complex for the detection of di-acylglyceride [65], the TLR2/1 complex for the detection of LPS from *Helicobacter pylori* and *Porphyromonas gingivalis* [66] and the TLR4/6 complex to detect atherogenic lipids and amyloid-β [235]. The formation of these heteromeric complexes take place at the cell surface within lipid raft domains, therefore preventing CD36 from localising into lipid rafts through reduced S-acylation will potentially prevent the formation of the TLR receptor complexes. If the TLRs do not dimerise, there will be no adaptor proteins recruited and no signaling cascade [51]. This demonstrates a mechanism by

which LPCAT2 can potentially regulate TLR mediated cytokine responses by modulating the formation of these heteromeric complexes via CD36 S-acylation.

Through mutational studies, the cytoplasmic tails of CD36 have been shown to be S-acylated at cysteines 3, 7, 464, and 466, anchoring them into the plasma membrane [79]. Inhibition of S-acylation at these sites, either pharmacologically or by mutation lead to a reduction in CD36 surface expression, revealing that these modifications facilitate efficient processing at the endoplasmic reticulum and trafficking through the secretory pathway [82]. The authors concluded that these modifications were not required for surface expression of CD36 but instead for efficient trafficking to the cell surface. Additionally, the lack of S-acylation reduced the half-life of the CD36 protein and prevented its efficient incorporation into lipid rafts. These findings support the observations from the current data, as reduced S-acylation led to a reduction in membrane lipid raft expressed CD36 (Figure 3.6) and there was also reduction in surface expressed CD36 (Figure 3.9). The reduced half-life of non S-acylated CD36 protein observed [82] could also explain why there was a small reduction in total CD36 protein following LPCAT2 knockdown (Figure 3.3.B). Other research investigating the uptake of fatty acids by adipocytes demonstrated that S-acylation of CD36 is required for targeting of CD36 to the plasma membrane [236], these findings also support the observations from the current data. Further work by the same group showed that dynamic S-acylation of CD36 regulates CD36 endocytosis and recycling back to the plasma membrane [237]. The findings from these studies combined with the current data demonstrates that S-acylation of CD36 is critical for the location and therefore function of CD36.

Based on the findings by Wang *et al* CD36 is S-acylated by DHHC4 and DHHC5 that are located in the Golgi apparatus and plasma membrane

respectively [236]. They propose that newly synthesised CD36 is transported into the Golgi apparatus from the endoplasmic reticulum where it is S-acylated by DHHC4, acting as a sorting signal that enables anterograde transport to the cell surface and once at the cell surface CD36 is maintained in an S-acylated state by DHHC5. Inactivation of DHHC5 enables de-acylation of CD36 by the acyl-protein thioesterases APT1 that results in caveolar endocytosis of CD36, however, re-acylation of endocytosed CD36 will recycle it back to the plasma membrane [237]. Depending on which stage in the lifecycle of CD36 that LPCAT2 regulates it's S-acylation will determine where the missing surface CD36 (Figure 3.8) will accumulate within the cell. LPCAT2 has been identified in the endoplasmic reticulum, Golgi apparatus, plasma membrane, lipid droplets and the nucleus [177, 238, 239], therefore it is not possible to determine this based on the location of LPCAT2. If LPCAT2 knockdown prevents S-acylation of CD36 within the trans-Golgi network, then CD36 will become trapped in the Golgi apparatus and likewise if this happens at the plasma membrane then CD36 will become trapped within endosomes. It would be interesting to explore this further by using inhibitors of endocytosis to prevent internalisation of CD36 at the surface, if indeed this is where LPCAT2 acts, to help identify where LPCAT2 regulates CD36 S-acylation.

To demonstrate that reduced S-acylation of CD36 resulting from LPCAT2 knockdown would lead to a loss of CD36 function, the phagocytosis of *E. coli* particles was investigated. CD36 has been shown to mediate the uptake of *E. coli* in HEK293 cells transfected with murine CD36 [233] and in goat mammary gland epithelial cells [71]. The current data showed that knockdown of CD36 or LPCAT2 did not reduce the uptake of *E. coli*. There are a few possible explanations for this, firstly the knockdown of CD36 will not lead to complete ablation of CD36 expression and the remaining protein could be sufficient to facilitate the uptake of *E. coli*. The typical reduction

observed by CD36 knockdown in RAW264.7 cells in the current work is 89% at the mRNA level (Figure 4.2) and 98% at the protein level as assessed by surface staining and flowcytometry (Figure 3.18). If CD36 played a major role in the phagocytosis of *E. coli* then it would be expected to see a reduction in phagocytosis of *E. coli* based on the high knockdown efficiency demonstrated. The second explanation is that there is redundancy among proteins involved in phagocytosis of *E. coli*, meaning other proteins will fill the role when CD36 knocked down. The final explanation is that CD36 is not required for the uptake of *E. coli* by macrophages. This is the more likely explanation based on the high knockdown efficiency observed and it is also in line with another study that used macrophages to investigate the role CD36 plays in the phagocytosis of Gram-positive and Gram-negative bacteria. Stuart *et al* [240] found CD36-deficient macrophages showed impaired phagocytosis of Staphylococcus aureus but not *E. coli*. This indicates that the role CD36 plays in the phagocytosis of *E. coli* is likely dependent on the cell type.

As the uptake of *E. coli* by macrophages is CD36 independent, a different CD36 function needed to be explored to demonstrate a loss of CD36 function resulting from reduced S-acylation. CD36 has been shown to play a role scavenging oxidized low-density lipoprotein in macrophages [61], therefore the uptake of fluorescently labelled oxidized low-density lipoprotein was investigated using flow cytometry. The current data showed that knockdown of CD36 or LPCAT2 did not reduce the uptake of oxidized low-density lipoprotein by RAW264.7 cells. CD36 has been shown to be the predominant receptor accounting for 40% of the uptake of oxidized low-density lipoprotein in human monocyte derived macrophages [241]. However, the majority of scavenger receptors bind oxidized low-density lipoprotein [242], with the class A scavenger receptor (SR-A) and Lectin-like oxidized low density lipoprotein receptor 1 (LOX-1) playing the next most significant role after CD36 [243, 244]. This redundancy is likely the reason why CD36 knockdown

in RAW264.7 cells did not show a reduction in oxidized low-density lipoprotein uptake in these experiments.

When analyzing surface CD36 expression in RAW264.7 cells by flow cytometry, two populations of cells expressing different amounts of CD36 were clearly visible (Figure 2.3.4). These two populations of cells were indistinguishable from one another morphologically when backgated on forward and side scatter plots (data not shown) and upon further investigation these two populations of cells not only expressed different levels of CD36 mRNA but also demonstrated differing sensitivity to sLPS. These populations could be a characteristic of different types of macrophage or be unique to RAW264.7 cells and requires further investigation.

3.3.3   S-acylation of LIMPII

LIMPII has significant structural similarities with CD36 and is identified as a member of the CD36 superfamily of scavenger receptors. These similarities include sharing putative transmembrane domains yielding short cytoplasmic tails, a large extracellular/intraluminal loop that shares 37% homology, an un-cleaved N-terminal signal peptide and C-terminal stop transfer signal [245]. A major difference distinguishing LIMPII from CD36 is that it is primarily located within endosomes and lysosomes as opposed to the cell surface, where it plays a key role in their formation and reorganisation. It's here that LIMPII has been shown to regulate IFN-I production in plasmacytoid dendritic cells by acting as a chaperone for TLR9 and facilitates its translocation into endosomes from the endoplasmic reticulum [234].

Various proteomic studies investigating global S-acylation have identified LIMPII as being S-acylated [246], however there have been no studies investigating LIMPII S-acylation specifically. The findings from the current

research also identified LIMPII as being S-acylated and this supports the findings from the literature. Additionally, the current research showed that the knockdown of LPCAT2 caused a 40% reduction in LIMPII S-acylation. As the effect of this was not investigated further and there have been no studies examining LIMPII S-acylation specifically, the role of this post-translational modification can only be speculated. It is reasonable to hypothesise, based on the structural similarities between LIMPII and CD36 that reduced S-acylation of LIMPII would prevent its incorporation into lipid rafts. It has been proposed that lipid raft regions in the trans-Golgi network are focal sites where vesicle budding occurs during anterograde and retrograde trafficking to and from endosomes [247], if S-acylation of LIMPII is required for its incorporation into lipid rafts then this highlights a potential regulatory mechanism for the translocation of TLR9 into endosomes that pivots around S-acylation of LIMPII and LPCAT2. It would be interesting to investigate this further by analysing TLR9 stimulation in LPCAT2 knockdown cells.

3.3.4   Could LPCAT2 have S-acyltransferase activity?

There are currently two enzymatic activities attributed to LPCAT2, the first being lyso-platelet-activating factor acetyltransferase activity and the second being LPCAT activity. The findings in this chapter show that LPCAT2 knockdown reduced the S-acylation of several proteins, and this can be explained by one of two scenarios. Either LPCAT2 is directly S-acylating proteins and therefore possess protein S-acyltransferase activity or LPCAT2 indirectly influences the S-acylation of proteins.

With the current data it is not possible to determine if LPCAT2 directly S-acylates proteins. To make this claim further data would be required such as demonstrating a direct interaction between LPCAT2 and the candidate

substrate proteins, this could be achieved through use of fluorescence-based microscopy utilising the phenomenon of Förster resonance energy transfer that can determine molecular proximity down to 1-10 nm [248]. Or through demonstrating direct S-acylation of proteins by LPCAT2 in a reaction tube. A report by Zou *et al* demonstrated that LPCAT1 catalysed histone protein O-palmitoylation *in vitro* by combining recombinant LPCAT1 and histone H4 with [^{14}C]-labelled palmitoyl-CoA in a reaction tube at 37 °C followed by SDS-PAGE and autoradiography to detect O-palmitoylation [217]. A similar approach could be used to demonstrate that LPCAT2 directly S-acylates CD36 or LIMPII.

To date, all identified S-acyl transferases contain a common 51 amino acid zinc finger domain containing a conserved D-H-H-C motif and this is not present in LPCAT2. While it cannot be ruled out that LPCAT2 has S-acyl transferase activity based on this, it seems more likely that the role LPCAT2 plays in S-acylation is mediated via an indirect mechanism. One possible mechanism pivots around the concept of an enzyme being blocked or out-competed by similar molecules or excess substrate [249]. Both LPCAT2 and DHHC enzymes utilise fatty acyl-CoAs as a substrate, LPCAT2 has a substrate preference for arachidonoyl-CoA (20:4) [250] while DHHC enzymes tend to favour shorter fatty acyl-CoAs such as palmitoyl-CoA (C16:0), stearoyl-CoA (C18:0) and oleoyl-CoA (C18:1) [251]. In this scenario, the knockdown of LPCAT2 would lead to the accumulation of arachidonoyl-CoA that would out compete or block the preferred shorter fatty acyl-CoA substrates of the DHHC enzymes leading to a reduction in protein S-acylation. This mechanism alone would not explain why specific proteins as opposed to global proteins had reduced S-acylation following LPCAT2 knockdown. However, when taking into account that DHHC enzyme protein substrate specificity is largely dictated by spatial organisation [161], it would make sense that only DHHC enzymes that share a subcellular domain with

LPCAT2 would be affected by this mechanism.

3.3.5 Limitations

Acyl biotin exchange chemistry as a method is only semi-quantitative, this due to the method being unable to differentiate between a protein with multiple S-acylation sites and a single S-acylation site [252]. Therefore, when using this method to detect changes in S-acylation, a protein that has multiple S-acylated sites could potentially be missed if a single cysteine residue were regulated by a site-specific S-acyl transferase as the remaining S-acylated cysteines would still be available for biotin labelling and pull-down. It is possible therefore that changes in the S-acylation state of proteins were missed in this study and therefore LPCAT2 could play a larger role than observed. This could be addressed by using a complimentary method called acyl-PEG exchange that is like ABE with the difference that biotin is substituted with maleimide-functionalized polyethylene glycol of defined mass. Following labelling by acyl-PEG exchange, proteins are analysed by western blotting with appropriate antibodies and it is then possible to quantify the number of acylation sites a protein has by the cumulative shift in the observed mass of the protein allowing changes to a single site to be quantified [253]. Using acyl-PEG exchange to compliment the current data would be useful as this would support the findings and could potentially identify more proteins that are regulated by LPCAT2.

Both acyl-biotin exchange and acyl-PEG exchange methods are "cysteine centric" assays which rely on the selective cleavage of thioester bonds using hydroxylamine at a neutral pH to expose new thiol groups that can be tagged for downstream analysis [222, 253]. Due to the reliance on this mechanism, acyl-group exchange-based assays are prone to the detection of false

positives from two main sources. The first source being the incomplete blockade of free thiols, which was controlled for by including a parallel hydroxylamine negative sample. The second source of false positives are detected based on the protein in questions, biochemical use of thioester linkages and these include enzymes such as ubiquitin ligases/conjugases, pyruvate dehydrogenase, fatty acid synthase and various other enzymes utilising acyl-CoA substrates or phosphopantetheine prostheses [254, 255]. Taking this into account it is likely that the candidate protein E3 ubiquitin-protein ligase from table 3.1 is a false positive.

Due to the inherent limitations with cysteine centric labelling assays, it is recommended to combine this approach with a metabolic labelling assay, also known as a "lipid centric" approach [251]. The most widely used lipid centric labelling method to date relies on the metabolic incorporation of radiolabelled fatty acids to proteins. However, due to the health hazards associated with radioactive materials, this tool has largely been superseded by the much safer and more versatile technique that relies on click chemistry. Briefly, this is a coupling reaction (Huisgen cycloaddition) between an azide and alkyne group, which forms a very stable triazole ring as a linker. As azide and alkyne groups do not occur normally in nature they are very stable, furthermore, these groups are relatively small meaning they don't prevent the uptake of labelled molecules by cells and as such can be used for metabolic labelling experiments. For example, introducing an azido fatty acid probe into a cell will lead to its incorporation onto S-acylated proteins. These proteins can then be tagged downstream with much larger molecules to facilitate their detection, for-instance using alkyne biotin or alkyne containing fluorescent dyes.

3.3.6 Conclusion

The data presented in this chapter demonstrate for the first time a link between LPCAT2 and the S-acylation of proteins, in particular the scavenger receptors CD36 and LIMPII. This highlights a possible mechanism by which LPCAT2 can regulate TLR signalling through modulating the S-acylation and therefor function of these TLR accessory proteins. However, it remains to be determined whether LPCAT2 directly or indirectly S-acylates these proteins. Likewise, it was not possible to determine if reduced S-acylation of CD36 as a result of LPCAT2 knockdown was sufficient to cause a loss of function in the current work and both of these merits further investigation.

Chapter 4

Results: The scavenger receptor CD36 plays a role in LPS detection in macrophages.

4.1 Introduction

CD36 is an 88-KDa transmembrane glycoprotein [54] that functions as a scavenger receptor, recognising many ligands of endogenous and exogenous origin. The cytoplasmic tails of CD36 are S-acylated at cysteines 3, 7, 464, and 466, anchoring them into the membrane [79]. The inhibition of S-acylation at these sites, either pharmacologically or by mutation, revealed that these modifications facilitate efficient processing at the endoplasmic reticulum and trafficking through the secretory pathway but are not required for surface expression of CD36. Additionally, the lack of S-acylation reduced the half-life of the CD36 protein and prevented its efficient incorporation into lipid rafts [82].

In the setting of innate immunity, CD36 clearly plays a role in the detection of a variety of microbial molecular patterns (Table 1.2), yet precisely what those roles are remain somewhat unclear. One line of reasoning is that CD36 acts as a co-receptor, like CD14, delivering bacterial components to TLRs

[70, 65, 66]. In response to the endogenous ligands, oxidized low-density lipoprotein (oxLDL) or β-amyloid, CD36 becomes phosphorylated on Tyr^{463} and associates with Lyn tyrosine kinase, TLR4 and TLR6 forming a heteromeric complex that signal via the MyD88- and TRIF-dependant pathways [39]. This highlights a mechanism in which CD36 can facilitate the dimerisation of different TLRs to broaden their ligand repertoire.

LPS is the major component of the outer membrane of Gram-negative bacteria and is comprised of three distinct regions: Lipid A, Core and O-antigen. Lipid A is highly hydrophobic, while the Core and O-antigen are comprised of sugar residues and are polar making the molecule amphipathic [256]. Full length chemotypes of LPS that contain the O-antigen are referred to as smooth LPS ($_S$LPS) while shortened chemotypes of LPS that do not contain the O-antigen are referred to as rough LPS ($_R$LPS). Depending on the core sugar residue that the $_R$LPS is terminated, a further letter can be designated from "Ra" to "Re" to identify the precise location the structure is terminated [257] (Figure 4.1).
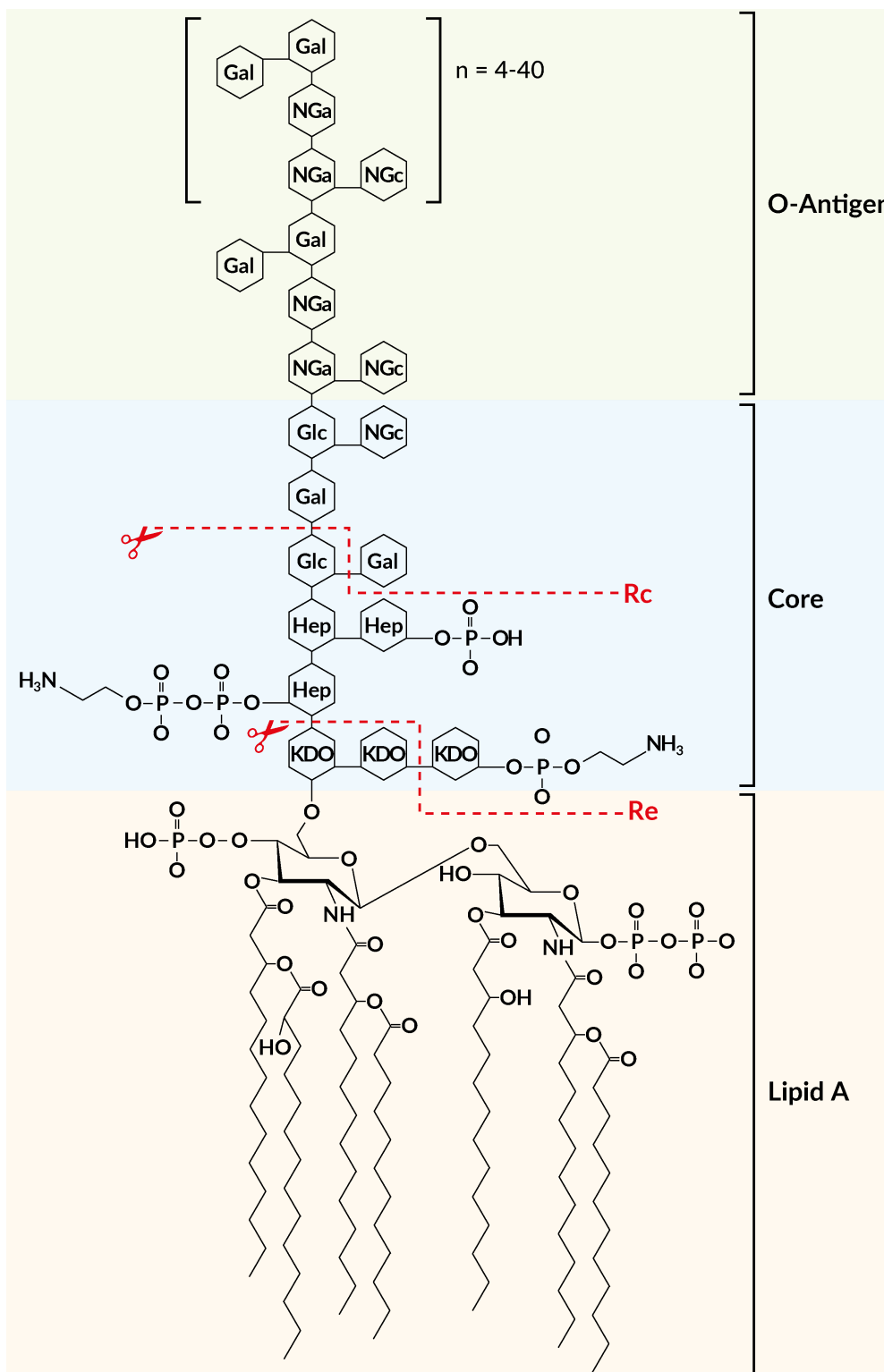
Figure 4.1: The chemical structure of LPS from E. coli O111:B4. The red lines indicate the shortened chemotypes of LPS used in this study (Re and Rc). (Gal) galactose; (NGa) N-acetyl-galactosamine; (NGc) N-acetyl-glucosamine; (Glc) glucose; (Hep) L-glycerol-D-manno-heptose; (KDO) 2-keto-3-deoxyoctonic acid. Adapted from [257].

There are conflicting reports on the effect CD36-deffciency has on macrophage responses to LPS, with some studies finding no effect [65, 84, 85], while a more recent study found it reduced LPS responsiveness [72]. Another study found the role of CD36 in LPS detection to be dependent on both LPS chemotype and the presence of serum [70]. This highlights the need to investigate the role CD36 plays in the detection of LPS and other ligands further.

In chapter 3, the knockdown of LPCAT2 was shown to reduce CD36 S-acylation in RAW264.7 cells, which in turn reduced both CD36 lipid-raft association and surface expression. This chapter explores the role CD36 plays in the detection of LPS by macrophages further to understand if disrupting CD36 lipid-raft association and surface expression could be a possible mechanism for reduced macrophage cytokine production following LPCAT2 knockdown.

4.2   Results

4.2.1   CD36 positively regulates LPS-induced cytokine responses in macrophages.

The role CD36 plays in the detection of LPS by macrophages was investigated using CD36 siRNA to knockdown the expression of CD36 in LPS stimulated RAW264.7 cells. The cytokine responses of cells with normal CD36 expression were then compared to cells with reduced CD36 expression using RT-qPCR as described in section 2.3.7 of the methods.

In brief, RAW264.7 cells were treated with CD36 siRNA for 48 hours to knockdown CD36 protein expression. As a negative control, cells were treated for the same duration and concentration with a scrambled siRNA that has no matches on the murine genome (negative siRNA). The cells were then stimulated with 100ng/mL sLPS for 6 hours before the gene expression of IL-6, IFNβ, IL-10, TNFα and IL-1β was measured by RT-qPCR. A 6 hour incubation was selected based on optimisation experiments using the same cell line and ligand by previous investigators [258].

The treatment of RAW264.7 cells with CD36 siRNA for 48 h produced an 89% ($p<0.001$) reduction in CD36 mRNA expression when compared to cells treated with negative siRNA, while cells treated with CD36 siRNA and LPS showed a 79% ($p<0.001$) reduction. Stimulation with LPS upregulated CD36 mRNA expression by 69% ($p<0.001$) in cells that had been treated with negative siRNA. The knockdown of CD36 reduced the LPS induced mRNA expression of IL-6 by 60% ($p<0.001$), IFNβ by 45% ($p<0.001$), TNFα by 22% ($P<0.05$), IL-10 by 23% ($P<0.05$) and IL-1β by 41% ($p<0.001$) (Figure 4.2). An important control to include are untreated cells as this will demonstrate that

both the transfection reagent and siRNAs are not adversely affecting the cells. All the data are plotted relative to untreated cells which will always equal 1 and are therefore not plotted. There was no significant difference in mRNA expression between untreated cells and cells treated with negative siRNA for all target genes and likewise there was no significant difference between cells treated with negative siRNA and CD36 siRNA without LPS stimulation for all target cytokines.
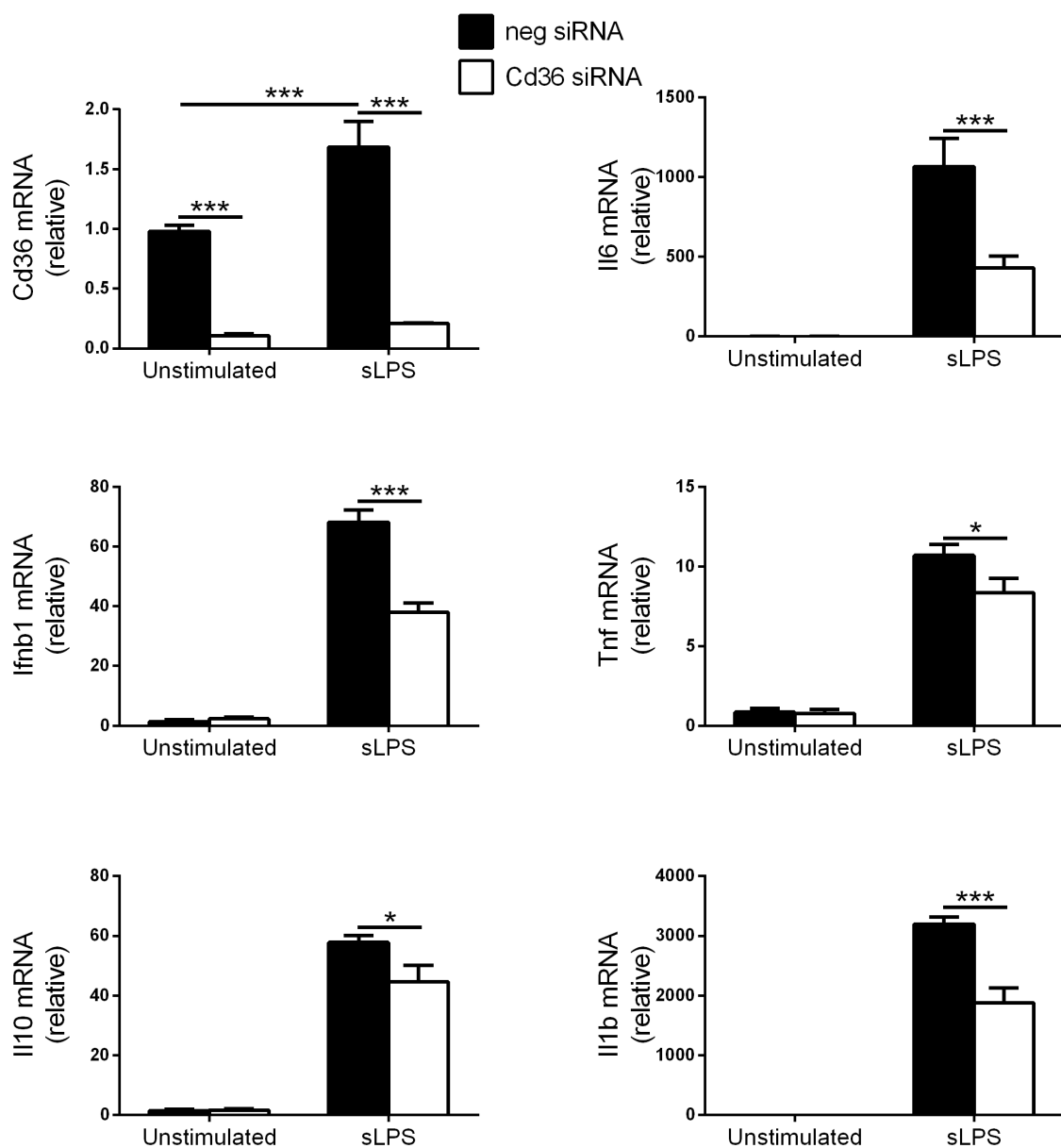
Figure 4.2: CD36 knockdown reduces LPS-induced inflammatory cytokine production in RAW264.7 cells. Following knockdown of CD36 using siRNA the gene expression of CD36 and the cytokines IL-6, IFNβ, TNFα, IL-10 and IL-1β were measured by RT-qPCR following a 6h stimulation with 100 ng/mL sLPS. The expression of mRNA is relative to untreated cells (not shown) and values were normalised to ATP5B. Each bar represents the mean +SD of three independent experiments each performed with two technical replicates. ***P<0.001, * P<0.05 as calculated using an unpaired t-test.

To reinforce the findings that CD36 knockdown reduces LPS-induced cytokine responses in RAW264.7 cells, the siRNA knockdown experiments were repeated using BMDMs. Following a 48h knockdown with CD36 siRNA there was a 69% reduction in CD36 mRNA expression when compared with cells treated with the negative siRNA only and an 83% reduction in cells treated with CD36 siRNA and LPS. Unlike in RAW264.7 cells, treatment with LPS alone did not alter CD36 expression in BMDM. The knockdown of CD36 reduced the LPS induced mRNA expression of IL-6 by 30% and IL-1β by 34% (Figure 4.3).
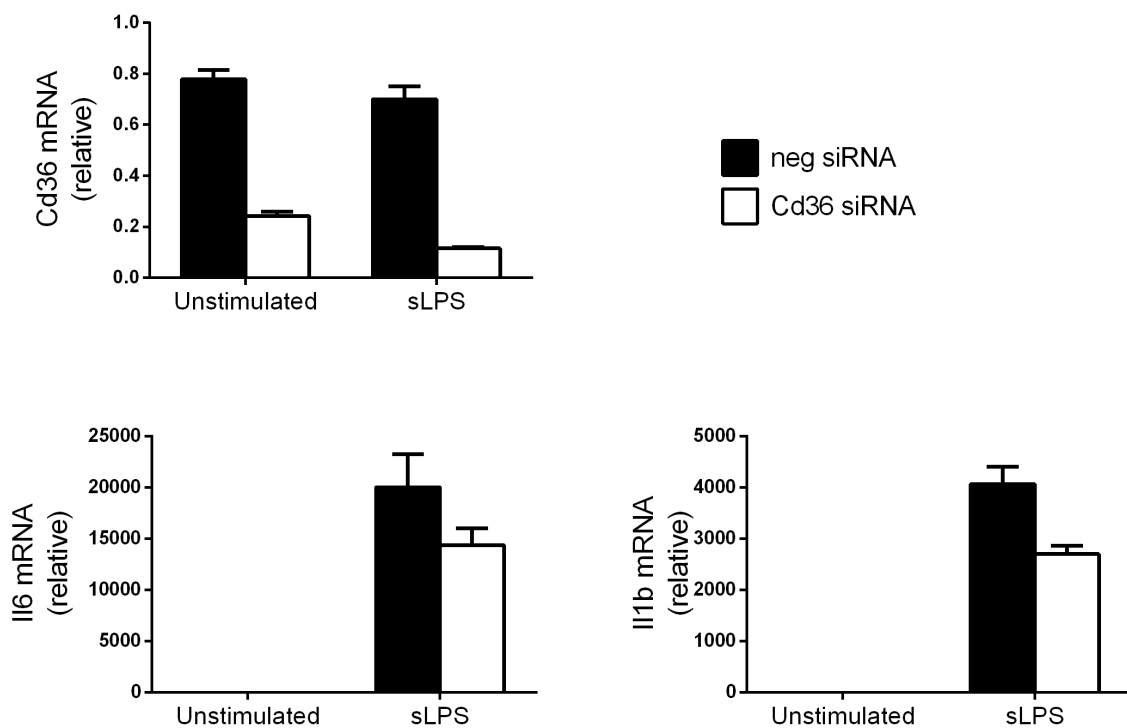
Figure 4.3: CD36 knockdown reduces LPS-induced inflammatory cytokine production in BMDMs. Following knockdown of CD36 using siRNA the gene expression of CD36 and the cytokines IL-6 and IL-1β were measured by RT-qPCR following a 6h stimulation with 100 ng/mL sLPS. The expression of mRNA is relative to untreated cells (not shown) and values were normalised to ATP5B. Each bar represents the mean +SD of 2 independent experiments each performed with two technical replicates.

4.2.2 CD36 does not bind to the polar O-antigen and Core region of LPS

CD36 can bind a variety of polar and non-polar ligands through its different binding sites, such as glycated proteins [62] or long chain fatty acids [60]. LPS is an amphipathic molecule comprised of three distinct regions: Lipid A, Core and O-antigen (Figure 4.1). Lipid A is highly hydrophobic, while the Core and O-antigen are comprised of sugar residues and are polar [256]. This raised the question, which part of the LPS molecule is important for CD36 induced LPS signalling. To explore the interaction between CD36 and LPS, progressively shorter chemotypes of rough *E. coli* LPS, Rc and Re, were used to stimulate RAW264.7 cells with or without CD36 knockdown.

Using the same method as the initial CD36 knockdown experiments, the RAW264.7 cells were stimulated with 100 ng/mL Rc or Re LPS for 6 h before the gene expression of IL-6, IFNβ, IL-10, TNFα and IL-1β were measured using RT-qPCR. The treatment of RAW264.7 cells with CD36 siRNA for 48 h produced an 89% ($p<0.001$) reduction in CD36 mRNA expression, and this was reduced to an 80% ($p<0.001$) reduction in cells that had been stimulated with either Rc or Re LPS. Stimulation with Rc LPS upregulated CD36 mRNA expression by 54% ($p<0.001$) and with Re LPS by 52% ($p<0.001$) in cells that had been treated with negative siRNA. The knockdown of CD36 reduced the Rc LPS induced mRNA expression of IL-6 by 60% ($p<0.01$), IFNβ by 41% ($p<0.01$), IL-1β by 42% ($p<0.001$) and TNFα by 27% ($p<0.05$) while IL-10 was only reduced by 24% ($p=0.05$). The knockdown of CD36 reduced the Re LPS induced mRNA expression of IL-6 by 63% ($p<0.05$), IFNβ by 43% ($p<0.01$), IL-1β by 48% ($p<0.001$), TNFα by 32% ($p<0.05$) and IL-10 by 44% ($p<0.01$) (Figure 4.4).
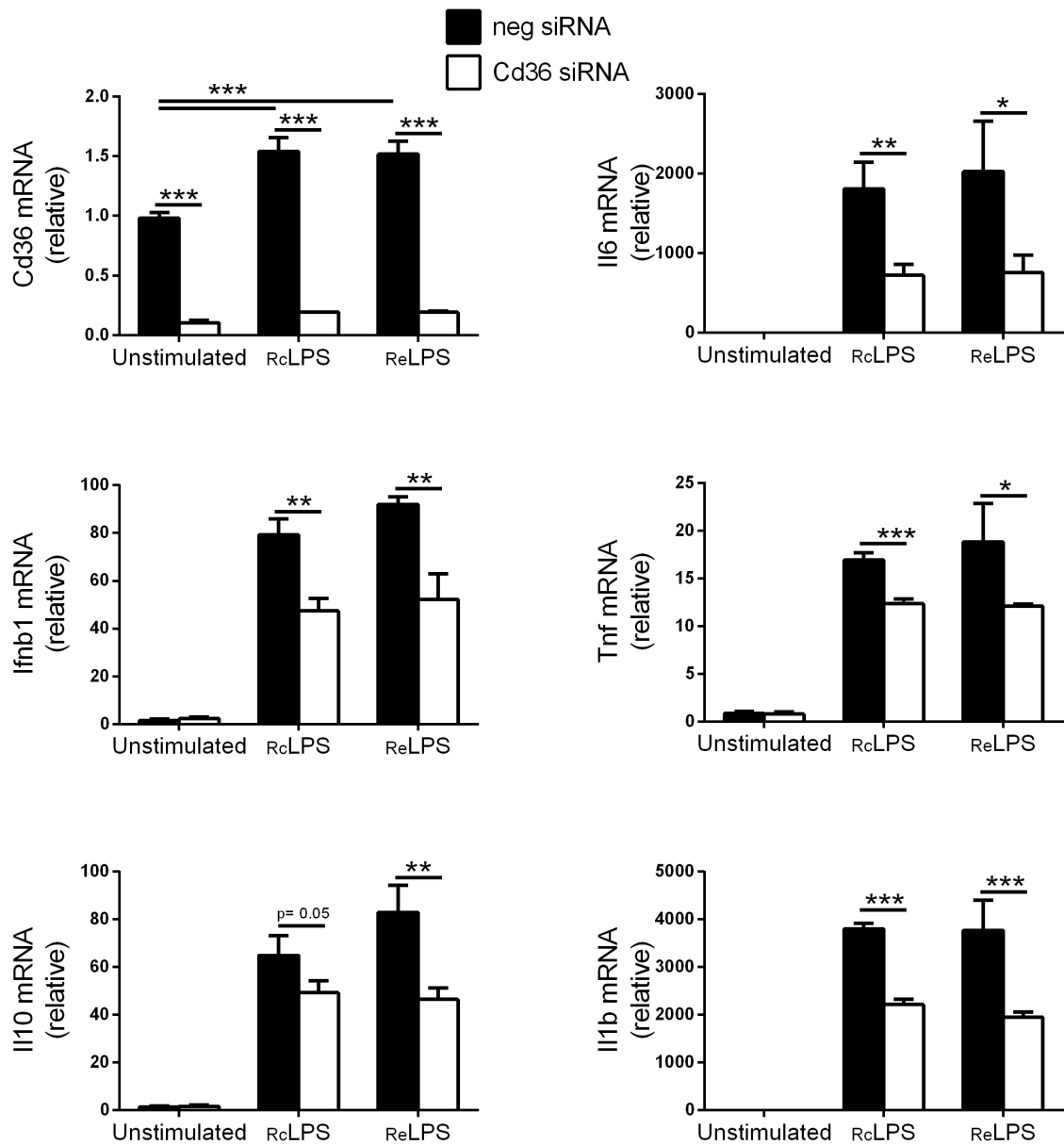
Figure 4.4: CD36 knockdown reduces inflammatory cytokine production by RAW264.7 cells in response to rough LPS. Following knockdown of CD36 using siRNA the gene expression of CD36 and the cytokines IL-6, IFNβ, TNFα, IL-10 and IL-1β were measured by RT-qPCR following a 6h stimulation with 100 ng/mL Re LPS and Rc LPS. The expression of mRNA is relative to untreated cells (not shown) and values were normalised to ATP5B. Each bar represents the mean +SD of three independent experiments each performed with two technical replicates. ***P<0.001, ** P<0.01, * P<0.05 as calculated using an unpaired t-test.

To ensure the reduction observed in cytokine gene expression following CD36 knockdown in LPS stimulated RAW264.7 cells (Fig.19 and Fig.22) also happens at the secreted protein level, the cytokines IL-6 and TNFα were assayed by ELISA. Following the same experimental setup and knockdown method as the initial experiments the cells were stimulated with 100 ng/mL sLPS, Rc or Re LPS for 24 h before the cytokines IL-6 and TNFα were assayed by ELISA. The knockdown of CD36 reduced the sLPS induced secretion of TNFα by 35% (p<0.05) and IL-6 by 45% (p<0.05); Rc LPS induced secretion of TNFα by 30% (p<0.05) and IL-6 by 45% (p<0.05); and Re LPS induced secretion of TNFα by 58% (p<0.01) and IL-6 by 48% (p<0.001) (Figure 4.5).
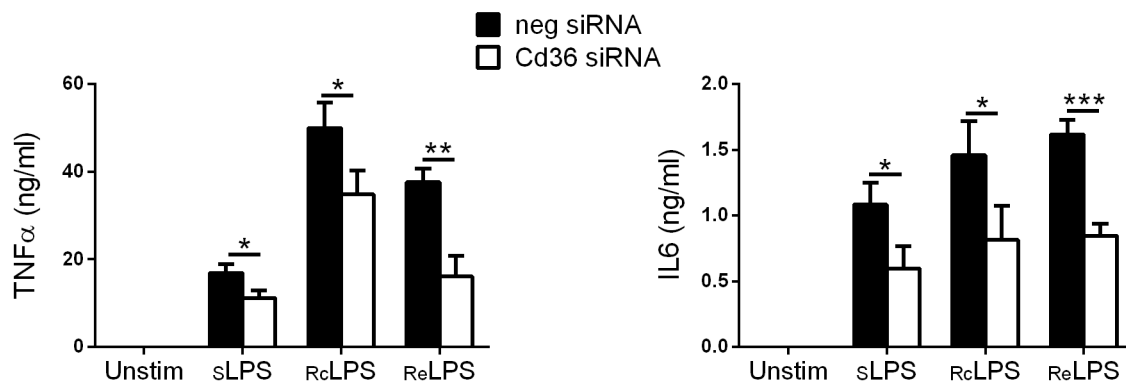
Figure 4.5: CD36 knockdown reduces LPS induced secretion of TNFα and IL-6. Following knockdown of CD36 the secreted protein level of the cytokines IL-6 and TNFα were measured by ELISA following a 24h stimulation with 100 ng/mL sLPS, Re LPS and Rc LPS. Protein concentration was normalised to total RNA. Each bar represents the mean +SD of three independent experiments each performed with two technical replicates. ***P<0.001, ** P<0.01, * P<0.05 as calculated using an unpaired t-test.

4.2.3   Investigating possible mechanism for CD36 mediated LPS sensitivity in macrophages

To investigate possible mechanisms into how CD36 facilitates LPS sigalling in macrophages, the effect of serum free conditions on LPS responses were investigated following CD36 knockdown. Serum contains my different proteins, the most notable in relation to LPS signalling are LPS-binding protein and soluble (s)CD14. LPS-binding protein is an acute-phase serum protein that facilitates the transfer of LPS monomers from the surface of bacteria or from LPS micelles onto soluble or membrane bound CD14 and subsequently the TLR4/MD2 complex enhancing the sensitivity of the system [259]. By using the same method to knockdown CD36 in RAW264.7 cells as previously, but with the modification of excluding serum from the medium it is possible to investigate if CD36 mediated detection of LPS requires serum proteins.

In serum free conditions a knockdown of greater than 77% for CD36 was achieved for all treatments, this led to a reduction in IL-6 gene expression following a 6 h stimulation with sLPS of 40%, RcLPS by 43% and ReLPS by 48%. However, there was no significant reduction in IFNβ gene expression following CD36 knockdown for all chemotypes of LPS (Figure 4.6). Overall, the absence of serum decreased the role CD36 plays in LPS detection in macrophages as summarised in Table 4.1. This shows that CD36 can facilitate LPS responses in the absence of serum however the presence of serum amplifies the role CD36 plays in the detection of LPS.
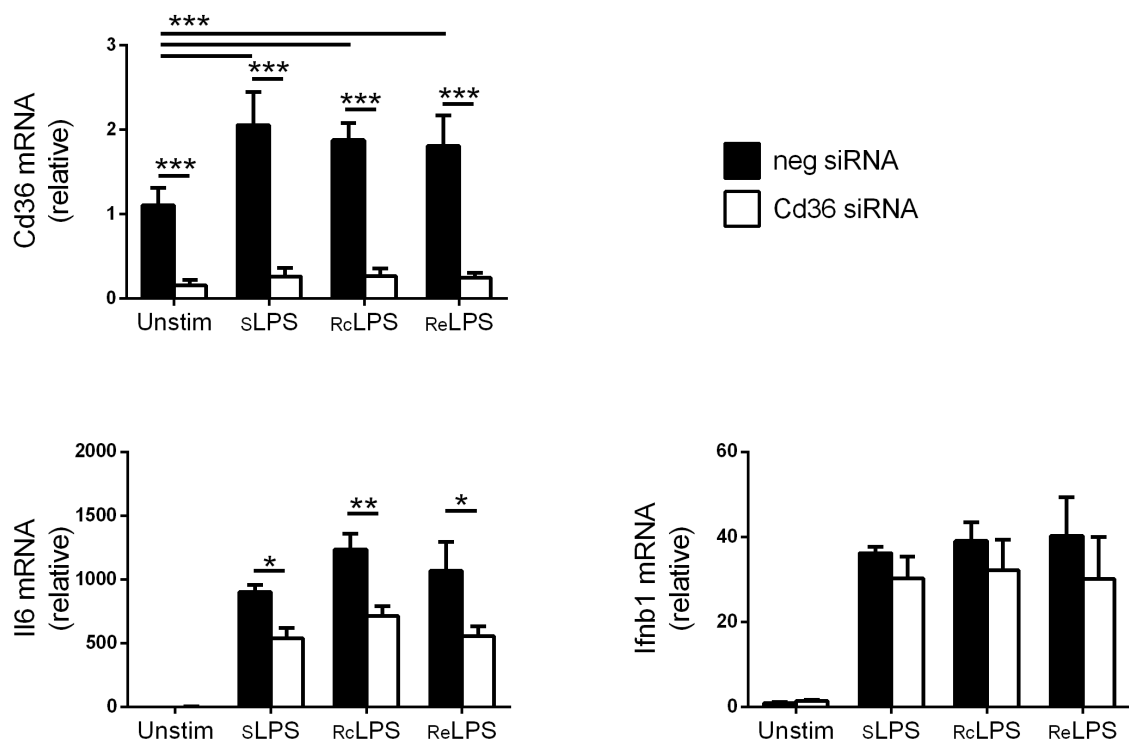
Figure 4.6: CD36 knockdown reduces IL-6 but not IFNβ mRNA induction in response to LPS in the absence of serum. Following knockdown of CD36 using siRNA the gene expression of CD36 and the cytokines IL-6 and IFNβ were measured by RT-qPCR following a 6h stimulation with 100 ng/mL LPS. The expression of mRNA is relative to untreated cells (not shown) and values were normalised to ATP5B. Each bar represents the mean +SD of three independent experiments each performed with two technical replicates. ***P<0.001, ** P<0.01, * P<0.05 as calculated using an unpaired t-test.

Table 4.1: Summary of results comparing the reduction in cytokine gene expression resulting from CD36 knockdown in LPS stimulated macrophages with or without the presence of serum. On average, the presence of serum increased the effect CD36 knockdown had on reducing cytokine gene expression by an average of 17% for IL-6 and 23% for IFNβ

Target gene	Ligand	Reduction in gene expression following CD36 knockdown	
		(with serum)	**(without serum)**
	sLPS	60% (P<0.001)	40% (P<0.05)
IL-6	RcLPS	60% (P<0.01)	43% (P<0.01)
	ReLPS	63% (P<0.05)	48% (P<0.05)
	sLPS	45% (P<0.001)	17% (not significant)
IFNβ	RcLPS	41% (P<0.01)	18% (not significant)
	ReLPS	43% (P<0.01)	25% (not significant)

CD36 has been shown to form complexes with several TLRs expressed on macrophages such as the TLR2/TLR6 heterodimer following stimulation with diacylated peptide or lipoteichoic acid [65] and the TLR4/TLR6 heterodimer following stimulation with oxidized low-density lipoprotein or β-amyloid [260]. This raised the question, does CD36 form a complex with the TLR4 homodimer following LPS stimulation? To investigate whether CD36 and TLR4 form a stable complex following LPS stimulation, RAW264.7 cells were treated with 1 μg/mL sLPS for 45 minutes before being collected and lysed on ice. CD36 was then immunoprecipitated from the cell lysate using anti-CD36 antibodies and protein A/G coupled agarose beads as described in section 4.7 in the methods. The immunoprecipitate was then analysed by SDS-PAGE and western blotting for TLR4 and CD36 to check if TLR4 had co-immunoprecipitated with CD36, which would suggest that the two proteins form a stable interaction. To control for non-specific enrichment of either CD36 or TLR4 an isotype control antibody that matched the anti-CD36 capture antibody was used in a parallel immunoprecipitation reaction. CD36 was present in the eluent indicating that it was successfully immunoprecipitated using the anti-CD36 antibody, however TLR4 was not present in the eluent either in the presence or absence of LPS stimulation. TLR4 was present in the flow through confirming that it was present in the initial sample and that its absence in the eluent is due to the proteins not forming a stable complex. Neither CD36 nor TLR4 was immunoprecipitated by the isotype control antibody indicating that the capture of CD36 was due to the specific interaction of the anti-CD36 antibody (Figure 4.7). These results show that CD36 and TLR4 do not form a stable complex under these conditions.
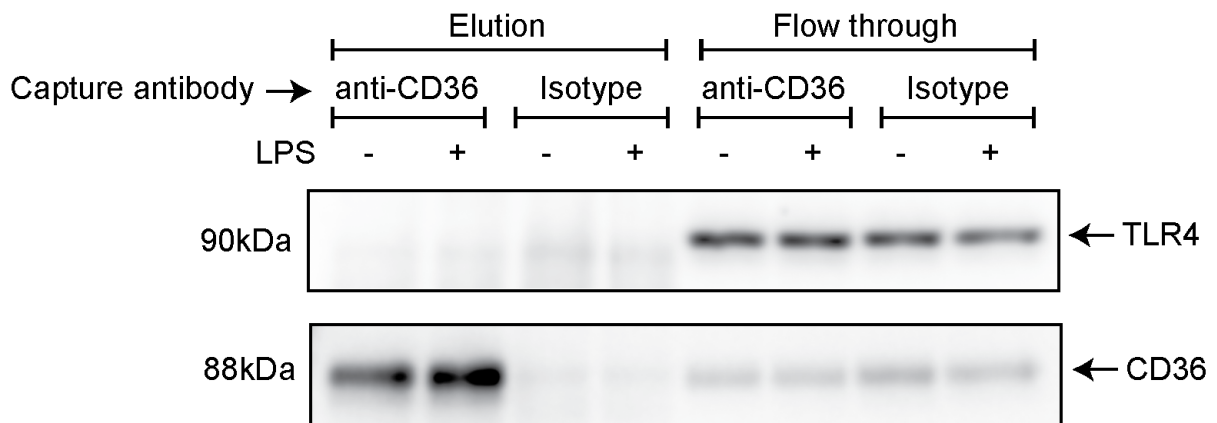
Figure 4.7: TLR4 and CD36 do not form a stable complex either with or without LPS stimulation. RAW264.7 cells were stimulated with 1 μg/mL sLPS for 45min before being lysed on ice. 500 μg of cell lysate was then incubated with 3 μg of anti-CD36 or an isotype control antibody. The antibody-protein complexes were then captured using protein A/G agarose beads, collected via centrifugation, and washed 3 times. The beads were then heated to 95°C for 2 minutes in SDS sample buffer to elute the captured proteins. The eluent was then analysed by SDS-PAGE and western blotting for either TLR4 or CD36. The blots are representative of three independent experimentseach performed without technical replicates. Elution: refers to proteins eluted from the agarose beads. Flow through: refers to the proteins that remained in the supernatant after the beads were initially pelleted.

It is well documented that CD36 plays a key role in the uptake of long chain fatty acids in many cell types including macrophages [60]. Long chain fatty acids are crucial to macrophage inflammatory responses as they are utilised for membrane remodelling [261], the synthesis of lipid mediators of inflammation including eicosanoids, prostanoids and leukotrienes [262], and for the acylation of proteins involved in signalling such as S-acylation of MyD88 [263] or N-myristoylation of TRAM [264]. Reduced expression of CD36 will limit the availability of exogenous long chain fatty acids for these processes, therefore the cell will need to rely on *de novo* synthesis of long chain fatty acids and on the lipids stored within lipid droplets [265]. If the reserve of stored lipids and the *de novo* synthesis of fatty acids is insufficient to maintain these processes, then the uptake of long chain fatty acids will be the rate limiting step for these processes. Therefore, reduced CD36 expression could dampen the inflammatory response of macrophages through the disruption of lipid metabolism.

To explore this hypothesis, the mRNA expression of fatty acid synthase (Fasn) and the mitochondrial citrate carrier (Slc25a1) was measured following CD36 knockdown with or without LPS stimulation. Fasn [266] and Slc25a1 [267] have been shown to be essential for macrophage inflammatory signalling in response to LPS. Both Fasn and Slc25a1 mediate the *de novo* synthesis of fatty acids, during macrophage activation there are two metabolic breaks in the tricarboxylic acid cycle that leads to the accumulation of citrate and succinate. Citrate is transported from the mitochondria into the cytosol via the citrate carrier Slc25a1 where it is converted into acetyl-CoA by ATP citrate lyase, acetyl-CoA carboxylase then carboxylates acetyl-CoA to yield malonyl-CoA the substrate for Fasn. In an NADPH dependant process malonyl-CoA is then elongated to produce long chain fatty acids. In the current work, the stimulation of RAW264.7 cells with 100 ng/mL LPS for 6 or 24 hours did not alter the mRNA expression of the citrate transporter Slc25a1 when compared to unstimulated cells. The mRNA expression of Fasn was reduced 23% ($p<0.05$) and 35% ($p<0.01$) following 6- and 24-hour LPS stimulation respectively. The knockdown of CD36 had no effect on the mRNA expression of either protein (Figure 4.8).

To further explore the idea that CD36 knockdown will interfere with LPS signalling through perturbed metabolism, the transcription factor Hif1α was also investigated. Both the protein and mRNA level of Hif1α have previously been shown to be upregulated following LPS stimulation in bone marrow derived macrophages [268]. Hif1α plays a pivotal role in driving the metabolic switch from oxidative phosphorylation to glycolysis in LPS activated macrophages through the induction of several glycolytic enzymes [269]. Here the mRNA expression of Hif1α was increased by 40% ($p<0.01$) following a 6-hour stimulation with 100 ng/mL sLPS, however there was no change in the mRNA expression at the 24-hour time point. The knockdown of CD36 had no effect on the mRNA expression of Hif1α (Figure 4.8).
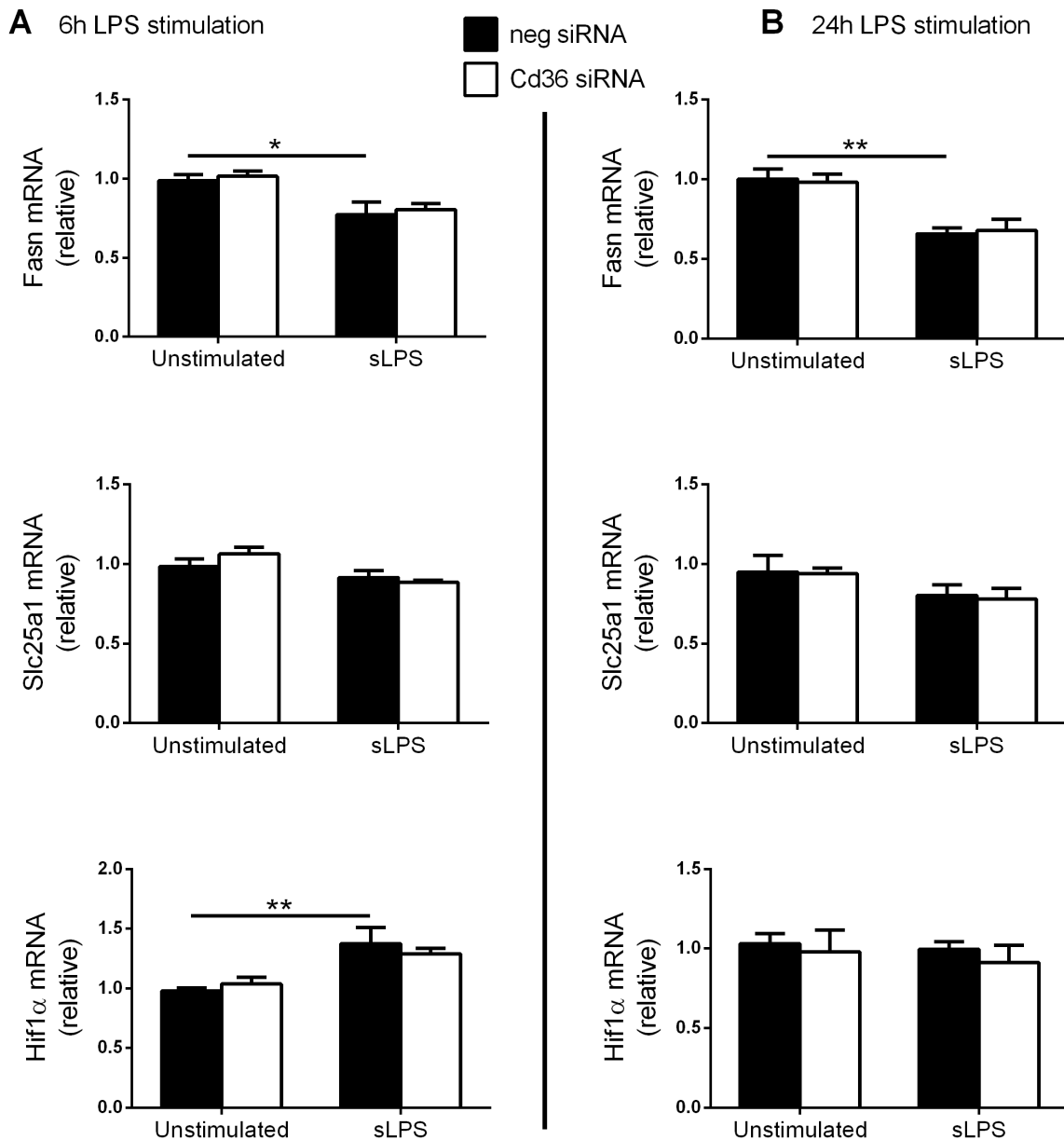
Figure 4.8: CD36 knockdown does not affect the mRNA expression of Fasn, Slc25a1 or Hif1α. Following knockdown of CD36 using siRNA the gene expression of Fasn, Slc25a1 or Hif1α were measured by RT-qPCR following a 6h (A) or 24h (B) stimulation with 100 ng/mL sLPS. The expression of mRNA is relative to untreated cells (not shown) and values were normalised to ATP5B. Each bar represents the mean +SD of three independent experiments each performed with two technical replicates. ** P<0.01, * P<0.05 as calculated using an unpaired t-test.

117

A summary of the results from chapter 4 can be found in table 4.2.

Table 4.2: Chapter 4 results summary.

Result	Section
CD36 knockdown reduces LPS-induced production of IL-6, IFNβ, TNFα, IL-10 and IL-1β mRNA in RAW264.7 cells.	4.2.1
CD36 knockdown reduces LPS-induced production of IL-6 and IL-1β mRNA in BMDMs.	4.2.1
CD36 does not bind to the polar O-antigen and Core region of LPS resulting in equal involvement of CD36 in LPS signal induction between LPS chemotypes in RAW264.7 cells.	4.2.2
CD36 knockdown reduces LPS induced secretion of TNFα and IL-6 in RAW264.7 cells.	4.2.2
The presence of serum during LPS stimulation increased the effect CD36 knockdown had on reducing cytokine gene expression in RAW264.7 cells	4.2.3
TLR4 and CD36 do not co-immunoprecipitated either with or without LPS stimulation in RAW264.7 cells.	4.2.3
CD36 knockdown does not affect the mRNA expression of Fasn, Slc25a1 or Hif1α	4.2.3

4.3 Discussion

CD36 is involved in many vital innate immune processes in macrophages,
including the clearance and detection of several DAMPs such as apoptotic
cells [59], oxidised low-density lipoprotein [61], and β-amyloid [63], and also
the PAMPs lipoteichoic acid [65] and β-glucans [68]. There are also mixed
reports with regards to the role CD36 plays in the detection of LPS, with
some reports demonstrating a positive regulatory role [71, 72] and others no
role for CD36 [65, 270]. LPS is a potent mediator of systemic inflammation
and a driver of sepsis, and previous work has demonstrated that LPCAT2
plays a pivotal role in macrophage cytokine responses to LPS [177]. It was
important therefore to explore the role CD36 plays in the detection of LPS
further in this chapter as modulation of CD36 S-acylation could be a
potential mechanism that contributes to the reduction in inflammatory
cytokines produced by LPCAT2 deficient macrophages. Using siRNA to
knockdown CD36 gene expression it was possible to demonstrate that CD36
positively regulates LPS responses in RAW264.7 cells and BMDMs. These
findings combined with the regulatory role LPCAT2 plays in the S-acylation
of CD36 shown in chapter 3, highlight a possible mechanism by which
LPCAT2 can regulate macrophage inflammatory cytokine responses to LPS.

CD36 can bind a variety of polar and non-polar ligands through its different
binding sites, such as glycated proteins [62] or long chain fatty acids [60].
LPS is an amphipathic molecule comprised of three distinct regions: Lipid A,
Core and O-antigen. Lipid A is highly hydrophobic, while the Core and
O-antigen are comprised of sugar residues and are polar [256]. This raised
the question, if CD36 acts in a similar way to CD14 which part of the LPS
molecule facilities this interaction? Using progressively shorter chemotypes
of *E. coli* LPS to stimulate CD36 knockdown RAW264.7 cells it was possible to
determine that the repeating O-antigen and the phosphorylated core region

of the LPS molecule are not required for CD36 binding and positive regulation of LPS induced cytokines. However, without using purified Lipid A to stimulate the cells, it is not possible to determine whether the remaining two KDO residues present in core region of ReLPS are required for CD36 binding. Essentially these findings showed that there were no differences between sLPS, RcLPS and ReLPS in terms of CD36 involvement in cytokine responses. These findings are in conflict with a study that found that CD36 differentially regulates LPS responses dependant on the chemotype of LPS [70], in this study CD36 was shown to negatively regulate TNF-α release to smooth LPS and to positively regulate RANTES release to rough LPS. However, in serum free conditions Biedron *et al* 2016 showed that CD36 positively regulates both TNF-α and RANTES release in response to either rough or smooth LPS. Again, this does not align with the current work which showed that in serum free conditions CD36 plays a reduced role compared to when serum is present during LPS stimulation. There are differences between this and the current study, Biedron *et al* used elicited peritoneal macrophages as opposed to RAW264.7 cells and a different chemotype of rough LPS (RaLPS) that contains the complete core structure but lacks the O-antigen as opposed to ReLPS and RcLPS. Differences in the cell types used could explain these conflicting data, this highlights the need to investigate how CD36 behaves using human macrophages as ultimately this will be more relevant.

The current data indicate that factors within serum enhance the involvement of CD36 in the detection of smooth and rough LPS and these are most likely LPS binding protein and/or sCD14 as these proteins are both known to be present in serum and act upstream of TLR4 [271]. In serum free conditions the involvement of CD36 was reduced on average by 17% for IL-6 mRNA induction and 23% for IFNβ mRNA induction for all chemotypes of LPS when compared to conditions where serum was present. This equates to a still significant 43% mean reduction in IL6 mRNA in serum free conditions,

however, the mean reduction in IFNβ mRNA was 20% in serum free conditions and was no longer statistically significant (Figure 4.6). As the involvement of CD36 was reduced by a similar amount for both IL-6 and IFNβ production it is unlikely that CD36 differentially regulates these two cytokines.

CD36 has been shown to form complexes with several TLRs expressed on macrophages such as the TLR2/TLR6 heterodimer [65] and the TLR4/TLR6 heterodimer [260]. This raised the question, does CD36 form a complex with the TLR4 homodimer following LPS stimulation? Using co-immunoprecipitation experiments no interaction between TLR4 and CD36 was detected. It is still possible that the two proteins do interact *in vivo* however as co-immunoprecipitation requires a strong and stable interaction between proteins, and it is possible they will dissociate during cell lysis if the interaction is weak. Alternatively, the interaction could be transient, for instance CD36 and TLR4 could interact during the transfer of LPS and then separate again. A method to detect such transient interactions in real time is Förster resonance energy transfer microscopy, with more time and resources this method would be a powerful tool to demonstrate protein localisation and interactions during LPS signalling. It is also a possibility that CD36 and TLR4 do not interact. In this scenario CD36 could be involved either up or downstream of TLR4, for instance CD36 could transfer LPS monomers from LBP to CD14 or play a role internalising the TLR4 complex.

There is a report that CD36 can detect LPS independent of TLR4 in HEK and Hela cells [67], however TLR4 deficient macrophages are unable to respond to LPS [272] therefore it is more likely that CD36 plays a role within the TLR4 signalling pathway in macrophages. An alternative mechanism however, could be that CD36 deficiency would disrupt metabolic pathways leading to a weakened inflammatory response. It is well documented that CD36 plays a

key role in the uptake of long chain fatty acids [60], which are crucial to macrophage inflammatory responses as they are utilised for membrane remodelling, the synthesis of lipid mediators of inflammation including eicosanoids, prostanoids and leukotrienes, and for the acylation of proteins [273]. Therefore, reduced CD36 expression could dampen the inflammatory response of macrophages through the disruption of lipid metabolism.

To explore this hypothesis, the mRNA expression of Fasn and Slc25a1 were measured following CD36 knockdown with or without LPS stimulation. Both Fasn and Slc25a1 mediate the *de novo* synthesis of fatty acids and have been shown to be essential for macrophage inflammatory signalling in response to LPS [266, 267]. It the current research the mRNA expression of both proteins remained unaltered following CD36 knockdown with or without LPS stimulation. CD36 facilitates the uptake of most fatty acids, however there are other fatty acid transport proteins that also contribute [274]. It is possible that these other fatty acid transport proteins will be able to transport enough fatty acids into the cell to compensate for the reduced expression of CD36. Likewise, siRNA knockdown will not totally abolish the expression of a protein and it is possible that the remaining CD36 will also be able to supply enough fatty acids for the cell's needs. These experiments only focus on mRNA expression, which reduced by 23% and 35% following 6 hour and 24-hour LPS stimulation respectively for Fasn and remained unchanged at both time points for Slc25a1 (Figure 4.8). To further explore the idea that CD36 knockdown will interfere with LPS signalling through perturbed metabolism, the transcription factor Hif1α was also investigated. Hif1α plays a pivotal role in driving the metabolic switch from oxidative phosphorylation to glycolysis in LPS activated macrophages through the induction of several glycolytic enzymes [275]. Again, the mRNA expression of Hif1α was not altered following CD36 knockdown. These data showed that the mRNA expression of metabolic markers Scl25a1, Fasn and Hif1α were unaffected by

CD36 knockdown in LPS stimulated cells suggesting that lipid metabolism of these cells was not affected in the current experiments. It would be worthwhile however to explore the protein expression of these metabolic markers as mRNA expression does not always correlate to protein expression.

While the results presented here support other findings that CD36 positively regulates LPS responses in macrophages, the role CD36 plays seems to be relatively minor due to the conflicting reports in the literature and the partial reduction in cytokines observed here. Although the reduction in CD36 S-acylation by LPCAT2 knockdown could be a contributing mechanism explaining the reduction in LPS induced cytokine responses by LPCAT2 deficient macrophages it is unlikely to be the main mechanism.

Chapter 5

Conclusion

The main objective of this thesis was to develop a better understanding of the mechanisms in which LPCAT2 regulates inflammatory responses in macrophages which will be key to the development of targeted anti-inflammatory therapies that could potentially be used to treat inflammatory disorders like sepsis. Earlier research showed that LPCAT2 translocates to membrane lipid raft domains and associate with TLR4 following activation by LPS [177]. Therefore, LPCAT2 appears to have a role in regulating innate responses via lipid raft signalling complexes however the mechanism behind this remained to be elucidated. This led to the main research question explored in this thesis: Does LPCAT2 play a role in the S-acylation of proteins involved in LPS signalling?

This thesis demonstrates for the first time a link between LPCAT2 and the S-acylation of proteins, in particular the scavenger receptors CD36 and LIMPII. The data demonstrate that LPCAT2 knockdown in RAW264.7 cells reduced CD36 S-acylation causing a reduction in the amount CD36 protein present in lipid raft fractions. CD36 has been suggested to act as a co-receptor delivering LPS to the TLR4 receptor complex [70] that localises

within lipid rafts following LPS stimulation [177]. Coupled to the data showing that CD36 knockdown significantly reduced LPS induced cytokine responses (section 4.2.1) highlights a potential mechanism by which LPCAT2 knockdown will reduce the availability of LPS to TLR4 by preventing CD36-lipid raft association, ultimately reducing TLR4-LPS macrophage responses.

As LPS is a potent mediator of systemic inflammation and a driver of Gram-negative sepsis through activation of TLR4 [276], the development of novel therapeutic inhibitors of LPCAT2 activity shows merit as an anti-inflammatory therapy that could be used to control the early pro-inflammatory overreaction in sepsis.

Several questions remain unanswered by this thesis, such as: Is there a direct interaction between CD36 and TLR4? Is LPCAT2 mediated protein S-acylation the mechanism responsible for TLR4 translocation into lipid raft domains? Does LPCAT2 directly S-acylate proteins? What are the roles of the other proteins identified by the mass spectrometry data and how might these influence TLR4 signalling? Future work could explore these questions to help understand how LPCAT2 regulates immune responses in macrophage.

A recent study identified that S-acylation of MYD88 at cysteine residue 113 is required for downstream signal activation and that CD36-mediated exogenous fatty acid incorporation and *de novo* fatty acid synthesis contributed to this lipidation [277]. Again, with more time and resources a potential link between LPCAT2 and S-acylation of MYD88 could be explored.

In summary, the main findings of this thesis are:

1. LPCAT2 knockdown reduced S-acylation of CD36, LIMPII, Malectin, Heat shock protein HSP 90-alpha, Heat shock cognate 71 KDa protein, Lysosome-associated membrane glycoprotein 2, Golgi apparatus protein

1, Ahnak, Neuroplastin, RasGAP-activating-like protein 1, Ubiquitin carboxyl-terminal hydrolase 27 and Protein disulfide-isomerase in LPS stimulated macrophages.

2. LPCAT2 knockdown regulates both lipid raft association and surface expression of CD36.

3. CD36 positively regulates smooth and rough LPS induced cytokine responses in macrophages with or without the presence of serum.

References

[1] G. W. Litman, J. P. Rast, and S. D. Fugmann. The origins of vertebrate adaptive immunity. *Nature Reviews Immunology*, 10(8):543–53, 2010.

[2] R. Warrington, W. Watson, H. L. Kim, and F. R. Antonetti. An introduction to immunology and immunopathology. *Allergy, Asthma & Clinical Immunology*, 14(2):49, 2018.

[3] M. Nishana and S. C. Raghavan. Role of recombination activating genes in the generation of antigen receptor diversity and beyond. *Immunology*, 137(4):271–81, 2012.

[4] C. Varol, A. Mildner, and S. Jung. Macrophages: development and tissue specialization. *Annual Review of Immunology*, 33(1):643–675, 2015.

[5] S. Yona, K. W. Kim, Y. Wolf, A. Mildner, D. Varol, M. Breker, D. Strauss-Ayali, S. Viukov, M. Guilliams, A. Misharin, D. A. Hume, H. Perlman, B. Malissen, E. Zelzer, and S. Jung. Fate mapping reveals origins and dynamics of monocytes and tissue macrophages under homeostasis. *Immunity*, 38(1):79–91, 2013.

[6] Y. Wu and K. K. Hirschi. Tissue-resident macrophage development and function. *Frontiers in Cell and Developmental Biology*, 8:617879, 2020.

[7] C. Zhang, M. Yang, and A. C Ericsson. Function of macrophages in disease: current understanding on molecular mechanisms. *Frontiers in immunology*, 12:620510, 2021.

[8] E. Uribe-Querol and C. Rosales. Phagocytosis: our current understanding of a universal biological process. *Frontiers in Immunology*, 11:1066, 2020.

[9] S. Gordon. Phagocytosis: an immunobiologic process. *Immunity*, 44(3):463–475, 2016.

[10] H. J. Lee, Y. Woo, T. W. Hahn, Y. M. Jung, and Y. J. Jung. Formation and maturation of the phagosome: a key mechanism in innate immunity against intracellular bacterial infection. *Microorganisms*, 8(9), 2020.

[11] A. R. Mantegazza, J. G. Magalhaes, S. Amigorena, and M. S. Marks. Presentation of phagocytosed antigens by MHC class I and II. *Traffic*, 14(2):135–52, 2013.

[12] J. M. den Haan, R. Arens, and M. C. van Zelm. The activation of the adaptive immune system: cross-talk between antigen-presenting cells, T cells and B cells. *Immunology Letters*, 162(2 Pt B):103–12, 2014.

[13] L. A. Blatter and W. G. Wier. Nitric oxide decreases $[Ca^{2+}]_i$ in vascular smooth muscle by inhibition of the calcium current. *Cell Calcium*, 15(2):122–31, 1994.

[14] G. Arango Duque and A. Descoteaux. Macrophage cytokines: involvement in immunity and infectious diseases. *Frontiers in immunology*, 5:491, 2014.

[15] E. B. Lomakina and R. E. Waugh. Signaling and dynamics of activation of LFA-1 and Mac-1 by immobilized IL-8. *Cellular and Molecular Bioengineering*, 3(2):106–116, 2010.

[16] S. Watanabe, M. Alexander, A. V. Misharin, and G. R. S. Budinger. The role of macrophages in the resolution of inflammation. *Journal of Clinical Investigation*, 129(7):2619–2628, 2019.

[17] D. M. Mosser and J. P. Edwards. Exploring the full spectrum of macrophage activation. *Nature Reviews Immunology*, 8(12):958–969, 2008.

[18] C. D. Mills, K. Kincaid, J. M. Alt, M. J. Heilman, and A. M. Hill. M-1/M-2 macrophages and the Th1/Th2 paradigm. *Journal of Immunology*, 164(12):6166–73, 2000.

[19] C. F. Nathan, H. W. Murray, M. E. Wiebe, and B. Y. Rubin. Identification of interferon-γ as the lymphokine that activates human macrophage oxidative metabolism and antimicrobial activity. *Journal of Experimental Medicine*, 158(3):670–89, 1983.

[20] A. Mantovani, A. Sica, S. Sozzani, P. Allavena, A. Vecchi, and M. Locati. The chemokine system in diverse forms of macrophage activation and polarization. *Trends in Immunology*, 25(12):677–86, 2004.

[21] A. Viola, F. Munari, R. Sánchez-Rodríguez, T. Scolaro, and A. Castegna. The metabolic signature of macrophage responses. *Frontiers in immunology*, 10:1462, 2019.

[22] D. Y. Vogel, E. J. Vereyken, J. E. Glim, P. D. Heijnen, M. Moeton, P. van der Valk, S. Amor, C. E. Teunissen, J. van Horssen, and C. D. Dijkstra. Macrophages in inflammatory multiple sclerosis lesions have an intermediate activation status. *Journal of Neuroinflammation*, 10:35, 2013.

[23] W.C. Raschke, S. Baird, P. Ralph, and I. Nakoinz. Functional macrophage cell lines transformed by abelson leukemia virus. *Cell*, 15(1):261–267, 1978.

[24] B. Taciak, M. Białasek, A. Braniewska, Z. Sas, P. Sawicka, Ł. Kiraga, T. Rygiel, and M. Król. Evaluation of phenotypic and functional stability

of RAW 264.7 cell line through serial passages. *PLOS ONE*, 13(6):1–13, 2018.

[25] A. Khabipov, A. Käding, K. Liedtke, E. Freund, L. Partecke, and S. Bekeschus. RAW 264.7 macrophage polarization by pancreatic cancer cells - a model for studying tumour-promoting macrophages. *Anticancer Research*, 39(6):1–13, 2019.

[26] P. Li, Z. Hao, J. Wu, C. Ma, Y. Xu, J. Li, R. Lan, B. Zhu, P. Ren, D. Fan, and S. Sun. Comparative proteomic analysis of polarized human THP-1 and mouse RAW264.7 macrophages. *Frontiers in Immunology*, 29(9), 2021.

[27] H. Shindou, D. Hishikawa, H. Nakanishi, T. Harayama, S. Ishii, R. Taguchi, and T. Shimizu. A single enzyme catalyzes both platelet-activating factor production and membrane biogenesis of inflammatory cells. cloning and characterization of acetyl-CoA:LYSO-PAF acetyltransferase. *Journal of Biological Chemistry*, 282(9):6532–9, 2007.

[28] R. Morimoto, H. Shindou, Y. Oda, and T. Shimizu. Phosphorylation of lysophosphatidylcholine acyltransferase 2 at Ser34 enhances platelet-activating factor production in endotoxin-stimulated macrophages. *Journal of Biological Chemistry*, 285(39):29857–62, 2010.

[29] M. Tarui, H. Shindou, K. Kumagai, R. Morimoto, T. Harayama, T. Hashidate, H. Kojima, T. Okabe, T. Nagano, T. Nagase, and T. Shimizu. Selective inhibitors of a PAF biosynthetic enzyme lysophosphatidyl-choline acyltransferase 2. *Journal of Lipid Research*, 55(7):1386–1396, 2014.

[30] B. Beutler. Tlr4: central component of the sole mammalian LPS sensor. *Current Opinion in Immunology*, 12(1):20–6, 2000.

[31] M. Yu, H. Wang, A. Ding, D. T. Golenbock, E. Latz, C. J. Czura, M. J. Fenton, K. J. Tracey, and H. Yang. HMGB1 signals through toll-like receptor (TLR) 4 and TLR2. *Shock*, 26(2):174–9, 2006.

[32] D. Li and M. Wu. Pattern recognition receptors in health and diseases. *Signal Transduction and Targeted Therapy*, 6(1):291, 2021.

[33] H. Kumar, T. Kawai, and S. Akira. Toll-like receptors and innate immunity. *Biochemical and Biophysical Research Communications*, 388(4):621–625, 2009.

[34] S. R. El-Zayat, H. Sibaii, and F. A. Mannaa. Toll-like receptors activation, signaling, and targeting: an overview. *Bulletin of the National Research Centre*, 43(1):187, 2019.

[35] K. Takeda, O. Takeuchi, and S. Akira. Recognition of lipopeptides by Toll-like receptors. *Journal of Endotoxin Research*, 8(6):459–63, 2002.

[36] T. Abe, T. Fukuhara, X. Wen, A. Ninomiya, K. Moriishi, Y. Maehara, O. Takeuchi, T. Kawai, S. Akira, and Y. Matsuura. CD44 participates in IP-10 induction in cells in which hepatitis c virus RNA is replicating, through an interaction with Toll-Like receptor 2 and hyaluronan. *Journal of Virology*, 86(11):6159–70, 2012.

[37] O. Takeuchi, T. Kawai, P. F. Mühlradt, M. Morr, J. D. Radolf, A. Zychlinsky, K. Takeda, and S. Akira. Discrimination of bacterial lipoproteins by Toll-like receptor 6. *International Immunology*, 13(7):933–40, 2001.

[38] M. Tatematsu, F. Nishikawa, T. Seya, and M. Matsumoto. Toll-like receptor 3 recognizes incomplete stem structures in single-stranded viral RNA. *Nature Communications*, 4(1):1833, 2013.

[39] C. R. Stewart, L. M. Stuart, K. Wilkinson, J. M. van Gils, J. Deng, A. Halle, K. J. Rayner, L. Boyer, R. Zhong, W. A. Frazier, A. Lacy-Hulbert,

J. El Khoury, D. T. Golenbock, and K. J. Moore. CD36 ligands promote sterile inflammation through assembly of a Toll-like receptor 4 and 6 heterodimer. *Nature Immunology*, 11(2):155–61, 2010.

[40] F. Hayashi, K. D. Smith, A. Ozinsky, T. R. Hawn, E. C. Yi, D. R. Goodlett, J. K. Eng, S. Akira, D. M. Underhill, and A. Aderem. The innate immune response to bacterial flagellin is mediated by Toll-like receptor 5. *Nature*, 410(6832):1099–103, 2001.

[41] M. Lund, L. Alexopoulou, A. Sato, M. Karow, C. Adams, N., W. Gale, N., A. Iwasaki, and R. A. Flavell. Recognition of single-stranded RNA viruses by Toll-like receptor 7. *Proceedings of the National Academy of Sciences*, 101(15):5598–5603, 2004.

[42] V. Hornung, W. Barchet, M. Schlee, and G. Hartmann. *RNA Recognition via TLR7 and TLR8*, pages 71–86. Springer Berlin Heidelberg, Berlin, Heidelberg, 2008.

[43] Z. G. Ramirez-Ortiz, C. A. Specht, J. P. Wang, C. K. Lee, D. C. Bartholomeu, R. T. Gazzinelli, and S. M. Levitz. Toll-like receptor 9-dependent immune activation by unmethylated CpG motifs in *Aspergillus fumigatus* DNA. *Infection and Immunity*, 76(5):2123–2129, 2008.

[44] S. M. Lee, T. F. Yip, S. Yan, D. Y. Jin, H. L. Wei, R. T. Guo, and J. S. M. Peiris. Recognition of double-stranded rna and regulation of interferon pathway by toll-like receptor 10. *Frontiers in Immunology*, 9:516, 2018.

[45] S. D. Yu, B.and Wright. Catalytic properties of lipopolysaccharide (LPS) binding protein: transfer of LPS to soluble CD14. *Journal of Biological Chemistry*, 271(8):4100–4105, 1996.

[46] B. S. Park, D. H. Song, H. M. Kim, B. Choi, H. Lee, and J. Lee. The structural basis of lipopolysaccharide recognition by the TLR4–MD-2 complex. *Nature*, 458(7242):1191–1195, 2009.

[47] S. Lin, Y. Lo, and H. Wu. Helical assembly in the MyD88–IRAK4–IRAK2 complex in TLR/IL-1R signalling. *Nature*, 465(7300):885–890, 2010.

[48] P. G. Motshwene, M. C. Moncrieffe, J. G. Grossmann, C. Kao, M. Ayaluru, A. M. Sandercock, C. V. Robinson, E. Latz, and N. J. Gay. An oligomeric signaling platform formed by the Toll-like receptor signal transducers MyD88 and IRAK-4. *Journal of Biological Chemistry*, 284(37):25404–11, 2009.

[49] T. Kawai and S. Akira. Toll-like receptors and their crosstalk with other innate receptors in infection and immunity. *Immunity*, 34(5):637–50, 2011.

[50] I. Zanoni, R. Ostuni, L. R. Marek, S. Barresi, R. Barbalat, G. M. Barton, F. Granucci, and J. C. Kagan. CD14 controls the LPS-induced endocytosis of Toll-like receptor 4. *Cell*, 147(4):868–80, 2011.

[51] A. Płóciennikowska, A. Hromada-Judycka, K. Borzęcka, and K. Kwiatkowska. Co-operation of TLR4 and raft proteins in LPS-induced pro-inflammatory signaling. *Cellular and Molecular Life Sciences*, 72(3):557–581, 2015.

[52] Q. Taban, P. Tajamul Mumtaz, K. Z. Masoodi, E. Haq, and S. M. Ahmad. Scavenger receptors in host defense: from functional aspects to mode of action. *Cell Communication and Signaling*, 20(1):2, 2022.

[53] M. Prabhudas, D. Bowdish, K. Drickamer, M. Febbraio, J. Herz, L. Kobzik, M. Krieger, J. Loike, T. K. Means, S. K. Moestrup, S. Post, T. Sawamura, S. Silverstein, X. Y. Wang, and J. El Khoury. Stan-

dardizing scavenger receptor nomenclature. *The Journal of Immunology*, 192(5):1997–2006, 2014.

[54] N. N. Tandon, R. H. Lipsky, W. H. Burgess, and G. A. Jamieson. Isolation and characterization of platelet glycoprotein IV (CD36). *Journal of Biological Chemistry*, 264(13):7570–5, 1989.

[55] K. J. Clemetson, S. L. Pfueller, E. F. Luscher, and C. S. Jenkins. Isolation of the membrane glycoproteins of human blood platelets by lectin affinity chromatography. *Biochimica et Biophysica Acta*, 464(3):493–508, 1977.

[56] N. A. Abumrad, M. R. el Maghrabi, E. Z. Amri, E. Lopez, and P. A. Grimaldi. Cloning of a rat adipocyte membrane protein implicated in binding or transport of long-chain fatty acids that is induced during preadipocyte differentiation. *The Journal of Biological Chemistry*, 268(24):17665–8, 1993.

[57] R. L. Silverstein and M. Febbraio. CD36, a scavenger receptor involved in immunity, metabolism, angiogenesis, and behavior. *Science Signaling*, 2(72):re3, 2009.

[58] A. S. Asch, J. Barnwell, R. L. Silverstein, and R. L. Nachman. Isolation of the thrombospondin membrane-receptor. *Journal of Clinical Investigation*, 79(4):1054–1061, 1987.

[59] J. Savill, N. Hogg, Y. Ren, and C. Haslett. Thrombospondin cooperates with cd36 and the vitronectin receptor in macrophage recognition of neutrophils undergoing apoptosis. *Journal of Clinical Investigation*, 90(4):1513–1522, 1992.

[60] N. A. Abumrad, M. R. el Maghrabi, E. Z. Amri, E. Lopez, and P. A. Grimaldi. Cloning of a rat adipocyte membrane protein implicated in binding or transport of long-chain fatty acids that is induced during

preadipocyte differentiation. Homology with human CD36. *Journal of Biological Chemistry*, 268(24):17665–8, 1993.

[61] G. Endemann, L. W. Stanton, K. S. Madden, C. M. Bryant, R. T. White, and A. A. Protter. CD36 is a receptor for oxidized low-density-lipoprotein. *Journal of Biological Chemistry*, 268(16):11811–11816, 1993.

[62] N. Ohgami, R. Nagai, M. Ikemoto, H. Arai, A. Miyazaki, H. Hakamata, S. Horiuchi, and H. Nakayama. CD36 serves as a receptor for advanced glycation endproducts (AGE). *Journal of Diabetes and Its Complications*, 16(1):56–59, 2002.

[63] J. B. El Khoury, K. J. Moore, T. K. Means, J. Leung, K. Terada, M. Toft, M. W. Freeman, and A. D. Luster. CD36 mediates the innate host response to β-amyloid. *Journal of Experimental Medicine*, 197(12):1657–1666, 2003.

[64] T. G. Smith, L. Serghides, S. N. Patel, M. Febbraio, R.L. Silverstein, and K. C. Kain. CD36-mediated nonopsonic phagocytosis of erythrocytes infected with stage I and IIA gametocytes of Plasmodium falciparum. *Infection and Immunity*, 71(1):393–400, 2003.

[65] K. Hoebe, P. Georgel, S. Rutschmann, X. Du, S. Mudd, K. Crozat, S. Sovath, L. Shamel, T. Hartung, U. Zahringer, and B. Beutler. CD36 is a sensor of diacylglycerides. *Nature*, 433(7025):523–527, 2005.

[66] M. Triantafilou, F. G. J. Gamper, P. M. Lepper, M. A. Mouratis, C. Schumann, E. Harokopakis, R. E. Schifferle, G. Hajishengallis, and K. Triantafilou. Lipopolysaccharides from atherosclerosis-associated bacteria antagonize TLR4, induce formation of TLR2/1/CD36 complexes in lipid rafts and trigger TLR2-induced inflammatory responses in human vascular endothelial cells. *Cellular Microbiology*, 9(8):2030–2039, 2007.

[67] I. N. Baranova, R. Kurlander, A. V. Bocharov, T. G. Vishnyakova, Z. G. Chen, A. T. Remaley, G. Csako, A. P. Patterson, and T. L. Eggerman. Role of human CD36 in bacterial recognition, phagocytosis, and pathogen-induced JNK-mediated signaling. *The Journal of Immunology*, 181(10):7147–7156, 2008.

[68] T. K. Means, E. Mylonakis, E. Tampakakis, R. A. Colvin, E. Seung, L. Puckett, M. F. Tai, C. R. Stewart, R. Pukkila-Worley, S. E. Hickman, K. J. Moore, S. B. Calderwood, N. Hacohen, A. D. Luster, and J. El Khoury. Evolutionarily conserved recognition and innate immunity to fungal pathogens by the scavenger receptors SCARF1 and CD36. *Journal of Experimental Medicine*, 206(3):637–653, 2009.

[69] I. N. Baranova, T. G. Vishnyakova, A. V. Bocharov, A. Leelahavanichkul, R. Kurlander, Z. G. Chen, A. C. P. Souza, P. S. T. Yuen, R. A. Star, G. Csako, A. P. Patterson, and T. L. Eggerman. Class B scavenger receptor types I and II and CD36 mediate bacterial recognition and proinflammatory signaling induced by *Escherichia coli*, lipopolysaccharide, and cytosolic Chaperonin 60. *Journal of Immunology*, 188(3):1371–1380, 2012.

[70] R. Biedron, A. Perun, and S. Jozefowski. CD36 differently regulates macrophage responses to smooth and rough lipopolysaccharide. *Plos One*, 11(4), 2016.

[71] D. Y. Cao, J. Luo, D. K. Chen, H. F. Xu, H. P. Shi, X. Q. Jing, and W. J. Zang. CD36 regulates lipopolysaccharide-induced signaling pathways and mediates the internalization of Escherichia coli in cooperation with TLR4 in goat mammary gland epithelial cells. *Scientific Reports*, 6, 2016.

[72] T. F. Olonisakin, H. Li, Z. Xiong, E. J. Kochman, M. Yu, Y. Qu, M. Hulver, J. K. Kolls, C. St Croix, Y. Doi, M. H. Nguyen, R. M. Shanks, R. K. Mallampalli, V. E. Kagan, A. Ray, R. L. Silverstein, P. Ray, and

J. S. Lee. CD36 provides host protection against *Klebsiella pneumoniae* intrapulmonary infection by enhancing lipopolysaccharide responsiveness and macrophage phagocytosis. *The Journal of Infectious Diseases*, 214(12):1865–1875, 2016.

[73] A. L. Armesilla and M. A. Vega. Structural organization of the gene for human CD36 glycoprotein. *The Journal of Biological Chemistry*, 269(29):18985–18991, 1994.

[74] T. Doi, K. Higashino, Y. Kurihara, Y. Wada, T. Miyazaki, H. Nakamura, S. Uesugi, T. Imanishi, Y. Kawabe, H. Itakura, and et al. Charged collagen structure mediates the recognition of negatively charged macromolecules by macrophage scavenger receptors. *The Journal of Biological Chemistry*, 268(3):2126–33, 1993.

[75] D. Neculai, M. Schwake, M. Ravichandran, F. Zunke, R. F. Collins, J. Peters, M. Neculai, J. Plumb, P. Loppnau, J. C. Pizarro, A. Seitova, W. S. Trimble, P. Saftig, S. Grinstein, and S. Dhe-Paganon. Structure of LIMP-2 provides functional insights with implications for SR-BI and CD36. *Nature*, 504(7478):172–6, 2013.

[76] P. A. Klenotic, R. C. Page, W. Li, J. Amick, S. Misra, and R. L. Silverstein. Molecular basis of antiangiogenic thrombospondin-1 type 1 repeat domain interactions with CD36. *Arteriosclerosis, Thrombosis, and Vascular Biology*, 33(7):1655–62, 2013.

[77] A. S. Asch, I. Liu, F. M. Briccetti, J. W. Barnwell, F. Kwakye-Berko, A. Dokun, J. Goldberger, and M. Pernambuco. Analysis of CD36 binding domains: ligand specificity controlled by dephosphorylation of an ectodomain. *Science*, 262(5138):1436–40, 1993.

[78] J. Smith, X. Su, R. El-Maghrabi, P. D. Stahl, and N. A. Abumrad. Opposite regulation of CD36 ubiquitination by fatty acids and insulin: effects

on fatty acid uptake. *Journal of Biological Chemistry*, 283(20):13578–85, 2008.

[79] N. B. Tao, S. J. Wagner, and D. M. Lublin. CD36 is palmitoylated on both N- and C-terminal cytoplasmic tails. *Journal of Biological Chemistry*, 271(37):22315–22320, 1996.

[80] O. Kuda, T. A. Pietka, Z. Demianova, E. Kudova, J. Cvacka, J. Kopecky, and N. A. Abumrad. Sulfo- *N*-succinimidyl oleate (SSO) inhibits fatty acid uptake and signaling for intracellular calcium via binding CD36 lysine 164. *Journal of Biological Chemistry*, 288(22):15547–15555, 2013.

[81] J. F. P. Luiken, D. Chanda, M. Nabben, D. Neumann, and J. F. C. Glatz. Post-translational modifications of CD36 (SR-B2): Implications for regulation of myocellular fatty acid uptake. *Biochimica Et Biophysica Acta-Molecular Basis of Disease*, 1862(12):2253–2258, 2016.

[82] R. F. Thorne, K. J. Ralston, C. E. de Bock, N. M. Mhaidat, X. D. Zhang, A. W. Boyd, and G. F. Burns. Palmitoylation of CD36/FAT regulates the rate of its post-transcriptional processing in the endoplasmic reticulum. *Biochimica Et Biophysica Acta-Molecular Cell Research*, 1803(11):1298–1307, 2010.

[83] A. Poltorak, X. He, I. Smirnova, M. Y. Liu, C. Van Huffel, X. Du, D. Birdwell, E. Alejos, M. Silva, C. Galanos, M. Freudenberg, P. Ricciardi-Castagnoli, B. Layton, and B. Beutler. Defective LPS signaling in C3H/HeJ and C57BL/10ScCr mice: mutations in *Tlr4* gene. *Science*, 282(5396):2085–8, 1998.

[84] S. N. Patel, Z. Lu, K. Ayi, L. Serghides, D. C. Gowda, and K. C. Kain. Disruption of CD36 impairs cytokine response to *Plasmodium falciparum* glycosylphosphatidylinositol and confers susceptibility to severe and fatal malaria *in vivo*. *The Journal of Immunology*, 178(6):3954–61, 2007.

[85] L. M. Stuart, J. Deng, J. M. Silver, K. Takahashi, A. A. Tseng, E. J. Hennessy, R. A. Ezekowitz, and K. J. Moore. Response to Staphylococcus aureus requires CD36-mediated phagocytosis triggered by the COOH-terminal cytoplasmic domain. *Journal of Cell Biology*, 170(3):477–85, 2005.

[86] T. Kuronita, E. Eskelinen, H. Fujita, P. Saftig, M. Himeno, and Y. Tanaka. A role for the lysosomal membrane protein LGP85 in the biogenesis and maintenance of endosomal and lysosomal morphology. *Journal of Cell Science*, 115(21):4117–4131, 2002.

[87] D. Reczek, M. Schwake, J. Schröder, H. Hughes, J. Blanz, X. Jin, W. Brondyk, S. Van Patten, T. Edmunds, and P. Saftig. LIMP-2 is a receptor for lysosomal mannose-6-phosphate-independent targeting of beta-glucocerebrosidase. *Cell*, 131(4):770–83, 2007.

[88] E. Beutler. Gaucher disease: multiple lessons from a single gene disorder. *Acta paediatrica Supplement*, 95(451):103–9, 2006.

[89] E. Carrasco-Marín, L. Fernández-Prieto, E. Rodriguez-Del Rio, F. Madrazo-Toca, T. Reinheckel, P. Saftig, and C. Alvarez-Dominguez. LIMP-2 links late phagosomal trafficking with the onset of the innate immune response to listeria monocytogenes: a role in macrophage activation. *The Journal of Biological Chemistry*, 286(5):3332–41, 2011.

[90] H. Guo, J. Zhang, X. Zhang, Y. Wang, H. Yu, X. Yin, J. Li, P. Du, J. Plumas, L. Chaperot, J. Chen, L. Su, Y. Liu, and L. Zhang. SCARB2/LIMP-2 regulates IFN production of plasmacytoid dendritic cells by mediating endosomal translocation of TLR9 and nuclear translocation of IRF7. *The Journal of Immunology*, 194(10):4737, 2015.

[91] K. S. Conrad, T. Cheng, D. Ysselstein, S. Heybrock, L. R. Hoth, B. A. Chrunyk, C. W. am Ende, D. Krainc, M. Schwake, P. Saftig, S. Liu,

X. Qiu, and M. D. Ehlers. Lysosomal integral membrane protein-2 as a phospholipid receptor revealed by biophysical and cellular studies. *Nature Communications*, 8(1):1908, 2017.

[92] S. Heybrock, K. Kanerva, C. Meng, Y.and Ing, A. Liang, Z. Xiong, X. Weng, Y. Ah Kim, R. Collins, W. Trimble, R. Pomès, G. G. Privé, W. Annaert, M. Schwake, J. Heeren, R. Lüllmann-Rauch, S. Grinstein, E. Ikonen, P. Saftig, and D. Neculai. Lysosomal integral membrane protein-2 (LIMP-2/SCARB2) is involved in lysosomal cholesterol export. *Nature Communications*, 10(1):3521, 2019.

[93] C. Liu, D. Chu, K. Kalantar-Zadeh, J. George, H. A. Young, and G. Liu. Cytokines: from clinical significance to quantification. *Advanced Science*, 8(15):2004433, 2021.

[94] S. Kany, J. T. Vollrath, and B. Relja. Cytokines in inflammatory disease. *International Journal of Molecular Sciences*, 20(23), 2019.

[95] E. A. Carswell, L. J. Old, R. L. Kassel, S. Green, N. Fiore, and B. Williamson. An endotoxin-induced serum factor that causes necrosis of tumors. *Proceedings of the National Academy of Sciences of the United States of America*, 72(9):3666–70, 1975.

[96] N. Parameswaran and S. Patial. Tumor necrosis factor-α signaling in macrophages. *Critical Reviews in Eukaryotic Gene Expression*, 20(2):87–103, 2010.

[97] M. J. Mohan, T. Seaton, J. Mitchell, A. Howe, K. Blackburn, W. Burkhart, M. Moyer, I. Patel, G. M. Waitt, J. D. Becherer, M. L. Moss, and M. E. Milla. The tumor necrosis factor-alpha converting enzyme (TACE): a unique metalloproteinase with highly defined substrate selectivity. *Biochemistry*, 41(30):9462–9, 2002.

[98] P. Gough and I. A Myles. Tumor necrosis factor receptors: pleiotropic signaling complexes and their differential effects. *Frontiers in immunology*, 11:585880, 2020.

[99] H. Hsu, J. Xiong, and D. V. Goeddel. The TNF receptor 1-associated protein TRADD signals cell death and NF- KB activation. *Cell*, 81(4):495–504, 1995.

[100] M. Rothe, V. Sarma, V. M. Dixit, and D. V. Goeddel. TRAF2-mediated activation of NF-KB by TNF receptor 2 and CD40. *Science*, 269(5229):1424–7, 1995.

[101] P. J. Naudé, J. A. den Boer, P. G. Luiten, and U. L. Eisel. Tumor necrosis factor receptor cross-talk. *The FEBS Journal*, 278(6):888–98, 2011.

[102] F. X. Pimentel-Muiños and B. Seed. Regulated commitment of TNF receptor signaling: a molecular switch for death or activation. *Immunity*, 11(6):783–93, 1999.

[103] C. Garlanda, C. A Dinarello, and A. Mantovani. The interleukin-1 family: back to the future. *Immunity*, 39(6):1003–1018, 2013.

[104] E. Latz, T. S. Xiao, and A. Stutz. Activation and regulation of the inflammasomes. *Nature Reviews Immunology*, 13(6):397–411, 2013.

[105] F. Martín-Sánchez, C. Diamond, M. Zeitler, A. I. Gomez, A. Baroja-Mazo, J. Bagnall, D. Spiller, M. White, M. J. D. Daniels, A. Mortellaro, M. Peñalver, P. Paszek, J. P. Steringer, W. Nickel, D. Brough, and P. Pelegrín. Inflammasome-dependent IL-1β release depends upon membrane permeabilisation. *Cell Death & Differentiation*, 23(7):1219–1231, 2016.

[106] A. Dunne and L. A. J. O'Neill. The interleukin-1 receptor/toll-like receptor superfamily: signal transduction during inflammation and host defense. *Science's STKE*, 2003(171):re3–re3, 2003.

[107] J. K. Fields, S. Günther, and E. J. Sundberg. Structural basis of IL-1 family cytokine signaling. *Frontiers in Immunology*, 10:1412, 2019.

[108] K. Shimizu, A. Nakajima, K. Sudo, Y. Liu, A. Mizoroki, T. Ikarashi, R. Horai, S. Kakuta, T. Watanabe, and Y. Iwakura. IL-1 receptor type 2 suppresses collagen-induced arthritis by inhibiting IL-1 signal on macrophages. *The Journal of Immunology*, 194(7):3156–3168, 2015.

[109] S. Chung, Y. Kwon, M. Park, Y. Park, and S. Lee. The correlation between increased serum concentrations of interleukin-6 family cytokines and disease activity in rheumatoid arthritis patients. *Yonsei Medical Journal*, 52(1):113–120, 2011.

[110] K. Yoshizaki, S. Murayama, H. Ito, and T. Koga. The role of interleukin-6 in castleman disease. *Hematology/Oncology Clinics of North America*, 32(1):23–36, 2018.

[111] G. Bamias, M. R. Nyce, S. A. De La Rue, and F. Cominelli. New concepts in the pathophysiology of inflammatory bowel disease. *Annals of Internal Medicine*, 143(12):895–904, 2005.

[112] C. Ehlting, S. D. Wolf, and J. G. Bode. Acute-phase protein synthesis: a key feature of innate immune functions of the liver. *Journal of Biological Chemistry*, 402(9):1129–1145, 2021.

[113] B. Li, L. L. Jones, and T. L. Geiger. IL-6 promotes t cell proliferation and expansion under inflammatory conditions in association with low-level RORγt expression. *Journal of Immunology*, 201(10):2934–2946, 2018.

[114] K. Maeda, H. Mehta, D. A. Drevets, and K. M. Coggeshall. IL-6 increases B-cell IgG production in a feed-forward proinflammatory mechanism to skew hematopoiesis and elevate myeloid production. *Blood*, 115(23):4699–706, 2010.

[115] F. Takatsuki, A. Okano, C. Suzuki, R. Chieda, Y. Takahara, T. Hirano, T. Kishimoto, J. Hamuro, and Y. Akiyama. Human recombinant IL-6/B cell stimulatory factor 2 augments murine antigen-specific antibody responses *in vitro* and *in vivo*. *Journal of Immunology*, 141(9):3072–7, 1988.

[116] S. Rose-John, K. Winthrop, and L. Calabrese. The role of IL-6 in host defence against infections: immunobiology and clinical implications. *Nature Reviews Rheumatology*, 13(7):399–409, 2017.

[117] A. Chalaris, C. Garbers, B. Rabe, S. Rose-John, and J. Scheller. The soluble interleukin 6 receptor: generation and role in inflammation and cancer. *European Journal of Cell Biology*, 90(6):484–494, 2011.

[118] D. F. Fiorentino, M. W. Bond, and T. R. Mosmann. Two types of mouse t helper cell. IV. Th2 clones secrete a factor that inhibits cytokine production by Th1 clones. *Journal of Experimental Medicine*, 170(6):2081–2095, 1989.

[119] M. Saraiva, P. Vieira, and A. O'Garra. Biology and therapeutic potential of interleukin-10. *Journal of Experimental Medicine*, 217(1), 2019.

[120] R. Lang, D. Patel, J. J. Morris, R. L. Rutschman, and P. J. Murray. Shaping gene expression in activated and resting primary macrophages by IL-10. *The Journal of Immunology*, 169(5):2253–2263, 2002.

[121] K. W. Moore, R. Malefyt, R. L. Coffman, and A. O'Garra. Interleukin-10 and the Interleukin-10 receptor. *Annual Review of Immunology*, 19(1):683–765, 2001.

[122] C. Bogdan, Y. Vodovotz, and C. Nathan. Macrophage deactivation by interleukin 10. *Journal of Experimental Medicine*, 174(6):1549–1555, 1991.

[123] W. D. Creery, F. Diaz-Mitoma, L. Filion, and A. Kumar. Differential modulation of B7-1 and B7-2 isoform expression on human monocytes by cytokines which influence the development of T helper cell phenotype. *European Journal of Immunology*, 26(6):1273–1277, 1996.

[124] F. Willems, A. Marchant, J. P. Delville, C. Gérard, A. Delvaux, T. Velu, M. de Boer, and M. Goldman. Interleukin-10 inhibits B7 and intercellular adhesion molecule-1 expression on human monocytes. *European Journal of Immunology*, 24(4):1007–9, 1994.

[125] C. J. Huang, B. R. Stevens, R. B. Nielsen, P. N. Slovin, X. Fang, D. R. Nelson, and J. W. Skimming. Interleukin-10 inhibition of nitric oxide biosynthesis involves suppression of CAT-2 transcription. *Nitric Oxide*, 6(1):79–84, 2002.

[126] H. Groux, M. Bigler, J. E. de Vries, and M. G. Roncarolo. Interleukin-10 induces a long-term antigen-specific anergic state in human CD4^{+} T cells. *Journal of Experimental Medicine*, 184(1):19–29, 1996.

[127] M. Murai, O. Turovskaya, G. Kim, R. Madan, C. L. Karp, H. Cheroutre, and M. Kronenberg. Interleukin 10 acts on regulatory T cells to maintain expression of the transcription factor Foxp3 and suppressive function in mice with colitis. *Nature Immunology*, 10(11):1178–1184, 2009.

[128] E. Keystone, J. Wherry, and P. Grint. IL-10 as a therapeutic strategy in the treatment of rheumatoid arthritis. *Rheumatic Disease Clinics of North America*, 24(3):629–39, 1998.

[129] K. Asadullah, W. Döcke, M. Ebeling, M. Friedrich, G. Belbe, H. Audring, H. Volk, and W. Sterry. Interleukin 10 treatment of psoriasis: Clinical results of a phase 2 trial. *Archives of Dermatology*, 135(2):187–192, 1999.

[130] A. Cardoso, A. Gil Castro, A. C. Martins, G. M. Carriche, V. Murigneux, I. Castro, A. Cumano, P. Vieira, and M. Saraiva. The dynamics of interleukin-10-afforded protection during dextran sulfate sodium-induced colitis. *Frontiers in Immunology*, 9:400, 2018.

[131] S. Pestka, C. D. Krause, and M. R. Walter. Interferons, interferon-like cytokines, and their receptors. *Immunological Reviews*, 202:8–32, 2004.

[132] F. McNab, K. Mayer-Barber, A. Sher, A. Wack, and A. O'Garra. Type I interferons in infectious disease. *Nature Reviews Immunology*, 15(2):87–103, 2015.

[133] M. Sean. Lipid rafts: elusive or illusive? *Cell*, 115(4):377–388, 2003.

[134] I. A. Prior, C. Muncke, R. G. Parton, and J. F. Hancock. Direct visualization of Ras proteins in spatially distinct cell surface microdomains. *Journal of Cell Biology*, 160(2):165 – 170, 2003. Cited by: 631; All Open Access, Bronze Open Access, Green Open Access.

[135] I. A. Prior, A. Harding, J. Yan, J. Sluimer, R. G. Parton, and J. F. Hancock. GTP-dependent segregation of H-ras from lipid rafts is required for biological activity. *Nature Cell Biology*, 3(4):368 – 375, 2001. Cited by: 461.

[136] M. Kinoshita, K. G. N. Suzuki, N. Matsumori, M. Takada, H. Ano, K. Morigaki, M. Abe, A. Makino, T. Kobayashi, K. M. Hirosawa, T. K. Fujiwara, A. Kusumi, and M. Murata. Raft-based sphingomyelin interactions revealed by new fluorescent sphingomyelin analogs. *Journal of Cell Biology*, 216(4):1183–1204, 03 2017.

[137] E. Sezgin, F. Schneider, S. Galiani, I. Urbančič, D. Waithe, B. C. Lagerholm, and C. Eggeling. Measuring nanoscale diffusion dynamics in cellular membranes with super-resolution STED–FCS. *Nature Protocols*,

14(4):1054 – 1083, 2019. Cited by: 72; All Open Access, Green Open Access.

[138] D. M. Owen, D. J. Williamson, A. Magenau, and K. Gaus. Sub-resolution lipid domains exist in the plasma membrane and regulate protein diffusion and distribution. *Nature Communications*, 3, 2012. Cited by: 203; All Open Access, Bronze Open Access.

[139] R. Kreder, K. A. Pyrshev, Z. Darwich, O. A. Kucherak, Y. Mély, and A. S. Klymchenko. Solvatochromic nile red probes with fret quencher reveal lipid order heterogeneity in living and apoptotic cells. *ACS Chemical Biology*, 10(6):1435–1442, 2015. PMID: 25710589.

[140] S. Prabuddha, H. David, and B. Barbara. Fluorescence resonance energy transfer between lipid probes detects nanoscopic heterogeneity in the plasma membrane of live cells. *Biophysical Journal*, 92(10):3564–3574, 2007.

[141] D. M. Owen, D. J. Williamson, A. Magenau, and K. Gaus. Sub-resolution lipid domains exist in the plasma membrane and regulate protein diffusion and distribution. *Nature communications*, 3:1256, 2012.

[142] Z. Yong, W. Ching-On, C. Kwang-jin, H. Dharini, L. Hong, P. T. Dhananiay, L. Jialie, B. Milos, E. Z. Konrad, X. Z. Michael, H. Hongzhen, V. Kartik, and John F. H. Membrane potential modulates plasma membrane phospholipid dynamics and K-Ras signaling. *Science*, 349(6250):873–876, 2015.

[143] R. Riya, A. A. Anupama, P. Anirban, P. S. Parvinder, Y. Mahipal, J. Charles, S. Sharad, S. Varma, D. S. Sanghapal, P. Aniruddha, G. Zhongwu, A. V. Ram, R. Madan, and Mayor. Satyajit. Transbilayer lipid interactions mediate nanoclustering of lipid-anchored proteins. *Cell*, 161(3):581–594, 2015.

[144] A. S. Susana, A. T. Maria, and G. Enrico. Laurdan generalized polarization fluctuations measures membrane packing micro-heterogeneity *in vivo*. *Proceedings of the National Academy of Sciences*, 109(19):7314–7319, 2012.

[145] I. Levental, M. Grzybek, and K. Simons. Greasing their way: lipid modifications determine protein association with membrane rafts. *Biochemistry*, 49(30):6305–16, 2010.

[146] X. Liang, A. Nazarian, H. Erdjument-Bromage, W. Bornmann, P. Tempst, and M. D. Resh. Heterogeneous fatty acylation of Src family kinases with polyunsaturated fatty acids regulates raft localization and signal transduction. *Journal of Biological Chemistry*, 276(33):30987–94, 2001.

[147] O. Rocks, A. Peyker, M. Kahms, P. J. Verveer, C. Koerner, M. Lumbierres, J. Kuhlmann, H. Waldmann, A. Wittinghofer, and P. I. Bastiaens. An acylation cycle regulates localization and activity of palmitoylated Ras isoforms. *Science*, 307(5716):1746–52, 2005.

[148] M. D. Resh. Fatty acylation of proteins: The long and the short of it. *Progress in Lipid Research*, 63:120–31, 2016.

[149] D. A. Mitchell, A. Vasudevan, M. E. Linder, and R. J. Deschenes. Protein palmitoylation by a family of DHHC protein S-acyltransferases. *Journal of Lipid Research*, 47(6):1118–1127, 2006.

[150] Y. Ohno, A. Kihara, T. Sano, and Y. Igarashi. Intracellular localization and tissue-specific distribution of human and yeast DHHC cysteine-rich domain-containing proteins. *Biochimica Et Biophysica Acta-Molecular and Cell Biology of Lipids*, 1761(4):474–483, 2006.

[151] N. M. Chesarino, J. C. Hach, J. L. Chen, B. W. Zaro, M. Rajaram, J. Turner, L. S. Schlesinger, M. R. Pratt, H. C. Hang, and J. S. Yount.

Chemoproteomics reveals Toll-like receptor fatty acylation. *BMC biology*, 12:91–91, 2014.

[152] F. Guardiola-Serrano, A. Rossin, N. Cahuzac, K. Lückerath, I. Melzer, S. Mailfert, D. Marguet, M. Zörnig, and A. O. Hueber. Palmitoylation of human FasL modulates its cell death-inducing function. *Cell Death & Disease*, 1(10):e88–e88, 2010.

[153] K. Mukai, H. Konno, T. Akiba, T. Uemura, Sa. Waguri, T. Kobayashi, G. N. Barber, H. Arai, and T. Taguchi. Activation of STING requires palmitoylation at the golgi. *Nature Communications*, 7(1):11932, 2016.

[154] A. Rossin, J. Durivault, T. Chakhtoura-Feghali, N. Lounnas, L. Gagnoux-Palacios, and A. O. Hueber. Fas palmitoylation by the palmitoyl acyltransferase DHHC7 regulates Fas stability. *Cell Death & Differentiation*, 22(4):643–53, 2015.

[155] A. Wolven, H. Okamura, Y. Rosenblatt, and M. D. Resh. Palmitoylation of p59^{fyn} is reversible and sufficient for plasma membrane association. *Molecular Biology of the Cell*, 8(6):1159–73, 1997.

[156] A. F. Roth, J. M. Wan, A. O. Bailey, B. M. Sun, J. A. Kuchar, W. N. Green, B. S. Phinney, J. R. Yates, and N. G. Davis. Global analysis of protein palmitoylation in yeast. *Cell*, 125(5):1003–1013, 2006.

[157] Y. Lu, Y. Zheng, É. Coyaud, C. Zhang, A. Selvabaskaran, Y. Yu, Z. Xu, X. Weng, J. S. Chen, Y. Meng, N. Warner, X. Cheng, Y. Liu, B. Yao, H. Hu, Z. Xia, A. M. Muise, A. Klip, J. H. Brumell, S. E. Girardin, S. Ying, G. D. Fairn, B. Raught, Q. Sun, and D. Neculai. Palmitoylation of NOD1 and NOD2 is required for bacterial sensing. *Science*, 366(6464):460–467, 2019.

[158] K. Huang, S. Sanders, R. Singaraja, P. Orban, T. Cijsouw, P. Arstikaitis, A. Yanai, M. R. Hayden, and A. El-Husseini. Neuronal palmitoyl acyl

transferases exhibit distinct substrate specificity. *The FASEB Journal*, 23(8):2605–15, 2009.

[159] K. Lemonidis, C. Salaun, M. Kouskou, C. Diez-Ardanuy, L. H. Chamberlain, and J. Greaves. Substrate selectivity in the zDHHC family of S-acyltransferases. *Biochemical Society Transactions*, 45(3):751–758, 2017.

[160] K. Lemonidis, M. C. Sanchez-Perez, and L. H. Chamberlain. Identification of a novel sequence motif recognized by the ankyrin repeat domain of zDHHC17/13 S-acyltransferases. *Journal of Biological Chemistry*, 290(36):21939–50, 2015.

[161] J. M. Philippe and P. M. Jenkins. Spatial organization of palmitoyl acyl transferases governs substrate localization and function. *Molecular Membrane Biology*, 35(1):60–75, 2019.

[162] G. S. Brigidi, B. Santyr, J. Shimell, B. Jovellar, and S. X. Bamji. Activity-regulated trafficking of the palmitoyl-acyl transferase DHHC5. *Nature Communications*, 6:8200, 2015.

[163] G. M. Thomas, T. Hayashi, S. L. Chiu, C. M. Chen, and R. L. Huganir. Palmitoylation by DHHC5/8 targets GRIP1 to dendritic endosomes to regulate AMPA-R trafficking. *Neuron*, 73(3):482–96, 2012.

[164] L. Muszbek, G. Haramura, J. E. Cluette-Brown, E. M. Van Cott, and M. Laposata. The pool of fatty acids covalently bound to platelet proteins by thioester linkages can be altered by exogenously supplied fatty acids. *Lipids*, 34:S331–S337, 1999.

[165] C. A. Haynes, J. C. Allegood, K. Sims, E. W. Wang, M. C. Sullards, and A. H. Merrill. Quantitation of fatty acyl-coenzyme As in mammalian cells by liquid chromatography-electrospray ionization tandem mass spectrometry. *Journal of Lipid Research*, 49(5):1113–1125, 2008.

[166] E. Hellsten, J. Vesa, V. M. Olkkonen, A. Jalanko, and L. Peltonen. Human palmitoyl protein thioesterase: evidence for lysosomal targeting of the enzyme and disturbed cellular routing in infantile neuronal ceroid lipofuscinosis. *The EMBO Journal*, 15(19):5240–5, 1996.

[167] J. A. Duncan and A. G. Gilman. A cytoplasmic acyl-protein thioesterase that removes palmitate from G protein alpha subunits and p21(RAS). *The Journal of Biological Chemistry*, 273(25):15830–7, 1998.

[168] X. Liang, Y. Lu, T. A. Neubert, and M. D. Resh. Mass spectrometric analysis of GAP-43/neuromodulin reveals the presence of a variety of fatty acylated species. *Journal of Biological Chemistry*, 277(36):33032–40, 2002.

[169] C. Montigny, P. Decottignies, P. Le Maréchal, P. Capy, M. Bublitz, C. Olesen, J. V. Møller, P. Nissen, and M. le Maire. S-palmitoylation and S-oleoylation of rabbit and pig sarcolipin. *Journal of Biological Chemistry*, 289(49):33850–61, 2014.

[170] E. P. Kennedy and S. B. Weiss. The function of cytidine coenzymes in the biosynthesis of phospholipides. *Journal of Biological Chemistry*, 222(1):193–214, 1956.

[171] R. H. Schaloske and E. A. Dennis. The phospholipase A(2) superfamily and its group numbering system. *Biochimica Et Biophysica Acta-Molecular and Cell Biology of Lipids*, 1761(11):1246–1259, 2006.

[172] W. E. M. Lands. Metabolism of glycerolipids: a comparison of lecithin and triglyceride synthesis. *Journal of Biological Chemistry*, 231(2):883–888, 1958.

[173] A. K. Agarwal and A. Garg. Enzymatic activity of the human 1-acylglycerol-3-phosphate-O-acyltransferase isoform 11: upregulated in

breast and cervical cancers. *Journal of Lipid Research*, 51(8):2143–2152, 2010.

[174] R. Morimoto, H. Shindou, M. Tarui, and T. Shimizu. Rapid production of platelet-activating factor is induced by Protein Kinase Cα-mediated phosphorylation of lysophosphatidylcholine acyltransferase 2 protein. *Journal of Biological Chemistry*, 289(22):15566–76, 2014.

[175] C. Moessinger, L. Kuerschner, J. Spandl, A. Shevchenko, and C. Thiele. Human lysophosphatidylcholine acyltransferases 1 and 2 are located in lipid droplets where they catalyze the formation of phosphatidylcholine. *Journal of Biological Chemistry*, 286(24):21330–9, 2011.

[176] C Moessinger, K Klizaite, A Steinhagen, J Philippou-Massier, A Shevchenko, M Hoch, C. S. Ejsing, and C Thiele. Two different pathways of phosphatidylcholine synthesis, the Kennedy Pathway and the Lands Cycle, differentially regulate cellular triacylglycerol storage. *BMC Cell Biology*, 15(1):43, 2014.

[177] W. Abate, H. Alrammah, M. Kiernan, A. J. Tonks, and S. K. Jackson. Lysophosphatidylcholine acyltransferase 2 (LPCAT2) co-localises with TLR4 and regulates macrophage inflammatory gene expression in response to LPS. *Scientific Reports*, 10(1):10355, 2020.

[178] V. I. Poloamina, W. Abate, G. Fejer, and S. K. Jackson. Possible regulation of Toll-like receptor 4 by lysine acetylation through LPCAT2 activity in RAW264.7 cells. *Bioscience Reports*, 42(7), 2022.

[179] C. Nedeva, J. Menassa, and H. Puthalakath. Sepsis: inflammation is a necessary evil. *Frontiers in Cell and Developmental Biology*, 7:108, 2019.

[180] B. G. Chousterman, F. K. Swirski, and G. F. Weber. Cytokine storm and sepsis disease pathogenesis. *Seminars in Immunopathology*, 39(5):517–528, 2017.

[181] T. van der Poll and S. M. Opal. Host-pathogen interactions in sepsis. *The Lancet Infectious Diseases*, 8(1):32–43, 2008.

[182] J. H. Foley and E. M. Conway. Cross talk pathways between coagulation and inflammation. *Circulation Research*, 118(9):1392–1408, 2016.

[183] A. Schulz, O. D Chuquimia, H. Antypas, S. E Steiner, R. M Sandoval, G. A Tanner, B. A Molitoris, A. Richter-Dahlfors, and K. Melican. Protective vascular coagulation in response to bacterial infection of the kidney is regulated by bacterial lipid A and host CD147. *Pathogens and Disease*, 76(8), 2018.

[184] M. Levi and H. Ten Cate. Disseminated intravascular coagulation. *The New England Journal of Medicine*, 341(8):586–92, 1999.

[185] D. W Landry and J. A Oliver. The pathogenesis of vasodilatory shock. *New England Journal of Medicine*, 345(8):588–595, 2001.

[186] P. Wang, M. Zhou, W. G Cioffi, K. I Bland, Z. F Ba, and I. H Chaudry. Is prostacyclin responsible for producing the hyperdynamic response during early sepsis? *Critical Care Medicine*, 28(5):1534–1539, 2000.

[187] A. Valverde. Fluid resuscitation for refractory hypotension. *Frontiers in Veterinary Science*, 8:621696, 2021.

[188] G. P. Otto, M. Sossdorf, R. A. Claus, J. Rödel, K. Menge, K. Reinhart, M. Bauer, and N. C. Riedemann. The late phase of sepsis is characterized by an increased microbiological burden and death rate. *Critical Care*, 15(4):R183, 2011.

[189] L. F. Gentile, A. G. Cuenca, P. A. Efron, D. Ang, A. Bihorac, B. A. McKinley, L. L. Moldawer, and F. A. Moore. Persistent inflammation and immunosuppression: a common syndrome and new horizon for surgical intensive care. *The Journal of Trauma and Acute Care Surgery*, 72(6):1491–501, 2012.

[190] R. S. Hotchkiss, K. W. Tinsley, P. E. Swanson, M. H. Grayson, D. F. Osborne, T. H. Wagner, J. P. Cobb, C. Coopersmith, and I. E. Karl. Depletion of dendritic cells, but not macrophages, in patients with sepsis. *The Journal of Immunology*, 168(5):2493–2500, 2002.

[191] R. S. Hotchkiss, K. W. Tinsley, P. E. Swanson, Jr. Schmieg, R. E., J. J. Hui, K. C. Chang, D. F. Osborne, B. D. Freeman, J. P. Cobb, T. G. Buchman, and I. E. Karl. Sepsis-induced apoptosis causes progressive profound depletion of B and CD4+ T lymphocytes in humans. *The Journal of Immunology*, 166(11):6952–63, 2001.

[192] A. Sharma, W. L. Yang, S. Matsuo, and P. Wang. Differential alterations of tissue T-cell subsets after sepsis. *Immunology Letters*, 168(1):41–50, 2015.

[193] K. P. Chung, H. T. Chang, S. C. Lo, L. Y. Chang, S. Y. Lin, A. Cheng, Y. T. Huang, C. C. Chen, M. R. Lee, Y. J. Chen, H. H. Hou, C. L. Hsu, J. S. Jerng, C. C. Ho, M. T. Huang, C. J. Yu, and P. C. Yang. Severe lymphopenia is associated with elevated plasma interleukin-15 levels and increased mortality during severe sepsis. *Shock*, 43(6):569–75, 2015.

[194] M. Lucas, L. M. Stuart, J. Savill, and A. Lacy-Hulbert. Apoptotic cells and innate immune stimuli combine to regulate macrophage cytokine secretion. *Journal of Immunology*, 171(5):2610–5, 2003.

[195] M. Lucas, L. M. Stuart, A. Zhang, K. Hodivala-Dilke, M. Febbraio, R. Silverstein, J. Savill, and A. Lacy-Hulbert. Requirements for apoptotic cell contact in regulation of macrophage responses. *Journal of Immunology*, 177(6):4047–54, 2006.

[196] F. Venet, A. Pachot, A. L. Debard, J. Bohé, J. Bienvenu, A. Lepape, and G. Monneret. Increased percentage of CD4+CD25+ regulatory T cells

during septic shock is due to the decrease of CD4$^+$CD25$^-$ lymphocytes. *Critical Care Medicine*, 32(11):2329–31, 2004.

[197] J. E Gotts and M. A Matthay. Sepsis: pathophysiology and clinical management. *The BMJ*, 353:i1585, 2016.

[198] D. Grimaldi and J. L. Vincent. Clinical trial research in focus: rethinking trials in sepsis. *The Lancet Respiratory Medicine*, 5(8):610–611, 2017.

[199] J. C. Marshall. Special issue: sepsis why have clinical trials in sepsis failed? *Trends in Molecular Medicine*, 20(4):195–203, 2014.

[200] D. Rittirsch, L. M. Hoesel, and P. A. Ward. The disconnect between animal models of sepsis and human sepsis. *Journal of Leukocyte Biology*, 81(1):137–143, 2007.

[201] D. G. Remick, R. M. Strieter, M. K. Eskandari, D. T. Nguyen, M. A. Genord, C. L. Raiford, and S. L. Kunkel. Role of tumor necrosis factor-alpha in lipopolysaccharide-induced pathologic alterations. *The Americal Journal of Pathology*, 136(1):49–60, 1990.

[202] D. G. Remick, D. E. Newcomb, G. L. Bolgos, and D. R. Call. Comparison of the mortality and inflammatory response of two models of sepsis: lipopolysaccharide vs. cecal ligation and puncture. *Shock*, 13(2):110–116, 2000.

[203] C. J. Fisher, J. M. Agosti, S. M. Opal, S. F. Lowry, R. A. Balk, J. C. Sadoff, E. Abraham, R. M. H. Schein, and E. Benjamin. Treatment of Septic Shock with the Tumor Necrosis Factor Receptor:Fc Fusion Protein. *New England Journal of Medicine*, 334(26):1697–1702, 1996.

[204] L. Harter, L. Mica, R. Stocker, O. Trentz, and M. Keel. Increased expression of toll-like receptor-2 and -4 on leukocytes from patients with sepsis. . *Shock*, 22(1):403–409, 2004.

[205] D. Williams, T. Ha, C. Li, J. H. Kalbfleisch, Jo. Schweitzer, W. Vogt, and I. W. Browder. Modulation of tissue Toll-like receptor 2 and 4 during the early phases of polymicrobial sepsis correlates with mortality. *Critical Care Medicine*, 31(6):1808–1818, 2003.

[206] G. Meng, M. Rutz, M. Schiemann, J. Metzger, A. Grabiec, R. Schwandner, P. B. Luppa, F. Ebel, D. H. Busch, and S. Bauer. Antagonistic antibody prevents toll-like receptor 2 driven lethal shock-like syndromes. *The Journal of clinical investigation*, 113(10):1473–1481, 2004.

[207] B. Daubeuf, J. Mathison, S. Spiller, S. Hugues, S. Herren, W. Ferlin, M. Kosco-Vilbois, H. Wagner, C. J. Kirschning, and R. Ulevitch. TLR4/MD-2 monoclonal antibody therapy affords protection in experimental models of septic shock. *The Journal of Immunology*, 179(9):6107–6114, 2007.

[208] T. W. Rice, A. P. Wheeler, G. R. Bernard, J. Vincent, D. C. Angus, N. Aikawa, I. Demeyer, S. Sainati, N. Amlot, C. Cao, M. Ii, H. Matsuda, K. Mouri, and J. Cohen. A randomized, double-blind, placebo-controlled trial of TAK-242 for the treatment of severe sepsis. *Critical Care Medicine*, 38(8):1685–1964, 2010.

[209] R. S. Hotchkiss and L. L. Moldawer. Parallels between cancer and infectious disease. *New England Journal of Medicine*, 371(4):380–383, 2014.

[210] E. Watanabe, O. Nishida, Y. Kakihana, M. Odani, T. Okamura, T. Harada, and S. Oda. Pharmacokinetics, pharmacodynamics, and safety of nivolumab in patients with sepsis-induced immunosuppression: A multicenter, open-label phase 1/2 study. *Shock*, 53(6):686–694, 2019.

[211] H. Darmani, J. L. Harwood, and S. K. Jackson. Interferon-γ-stimulated uptake and turnover of linoleate and arachidonate in macrophages: a

possible pathway for hypersensitivity to endotoxin. *Cellular Immunology*, 152(1):59–71, 1993.

[212] S. K. Jackson, W Abate, and A. J. Tonks. Lysophospholipid acyltransferases: novel potential regulators of the inflammatory response and target for new drug discovery. *Pharmacology & Therapeutics*, 119(1):104–114, 2008.

[213] N. T. Neville, J. Parton, J. L. Harwood, and S. K. Jackson. The activities of monocyte lysophosphatidylcholine acyltransferase and coenzyme A-independent transacylase are changed by the inflammatory cytokines tumor necrosis factor α and interferon γ. *Biochimica Et Biophysica Acta-Molecular and Cell Biology of Lipids*, 1733(2-3):232–238, 2005.

[214] B. Schmid, M. J. Finnen, J. L. Harwood, and S. K. Jackson. Acylation of lysophosphatidylcholine plays a key role in the response of monocytes to lipopolysaccharide. *European Journal of Biochemistry*, 270(13):2782–2788, 2003.

[215] H. Shindou, D. Hishikawa, T. Harayama, K. Yuki, and T. Shimizu. Recent progress on acyl CoA: lysophospholipid acyltransferase research. *Journal of Lipid Research*, 50:S46–S51, 2009.

[216] H. Alrammah, W. A. Woldie, N. Avent, and S. K. Jackson. Overexpression of lysophosphatidylcholine acyltransferase 2 (LPCAT2) up-regulates LPS-induced responses in a murine macrophage cell line. *Immunology and Cell Biology*, 143, 2015.

[217] C. Zou, B. Ellis, R. Smith, B. Chen, Y. Zhao, and R. Mallampalli. Acyl-CoA:Lysophosphatidylcholine acyltransferase I (Lpcat1) catalyzes histone protein O -palmitoylation to regulate mRNA synthesis. *The Journal of biological chemistry*, 286:28019–25, 2011.

[218] M. A. Freudenberg, D. Keppler, and C. Galanos. Requirement for lipopolysaccharide-responsive macrophages in galactosamine-induced sensitization to endotoxin. *Infection and Immunity*, 51(3):891–5, 1986.

[219] D. Wessel and U. I. Flügge. A method for the quantitative recovery of protein in dilute solution in the presence of detergents and lipids. *Analytical Biochemistry*, 138(1):141–3, 1984.

[220] P. Chomczynski and N. Sacchi. Single-step method of RNA isolation by acid guanidinium thiocyanate phenol chloroform extraction. *Analytical Biochemistry*, 162(1):156–159, 1987.

[221] P. Chomczynski and K. Mackey. Substitution of chloroform by bromochloropropane in the single-step method of RNA isolation. *Analytical Biochemistry*, 225(1):163–164, 1995.

[222] J. Wan, A. F. Roth, A. O. Bailey, and N. G. Davis. Palmitoylated proteins: purification and identification. *Nature Protocols*, 2(7):1573–1584, 2007.

[223] M. Blanc, F. David, L. Abrami, D. Migliozzi, F. Armand, J. Bürgi, and F. G. van der Goot. SwissPalm: protein palmitoylation database [version 1; peer review: 3 approved]. *F1000Research*, 4(261), 2015.

[224] T. Dallavilla, L. Abrami, P. A. Sandoz, G. Savoglidis, V. Hatzimanikatis, and F. G. van der Goot. Model-driven understanding of palmitoylation dynamics: regulated acylation of the endoplasmic reticulum chaperone calnexin. *PLoS Comput Biol*, 12(2):e1004774, 2016.

[225] B. R. Martin and B. F. Cravatt. Large-scale profiling of protein palmitoylation in mammalian cells. *Nature Methods*, 6(2):135–8, 2009.

[226] J. P. Wilson, A. S. Raghavan, Y. Y. Yang, G. Charron, and H. C. Hang. Proteomic analysis of fatty-acylated proteins in mammalian cells with chemical reporters reveals S-acylation of histone H3 variants. *Molecular & Cellular Proteomics*, 10(3):M110.001198, 2011.

[227] Jian Ren, Longping Wen, Xinjiao Gao, Changjiang Jin, Yu Xue, and Xuebiao Yao. CSS-Palm 2.0: an updated software for palmitoylation sites prediction. *Protein Engineering, Design and Selection*, 21(11):639–644, 2008.

[228] J. Yang, B. Gibson, J. Snider, C. M. Jenkins, X. Han, and R. W. Gross. Submicromolar concentrations of palmitoyl-CoA specifically thioesterify cysteine 244 in glyceraldehyde-3-phosphate dehydrogenase inhibiting enzyme activity: a novel mechanism potentially underlying fatty acid induced insulin resistance. *Biochemistry*, 44(35):11903–12, 2005.

[229] M. P. Lisanti, P. E. Scherer, J. Vidugiriene, Z. Tang, A. Hermanowski-Vosatka, Y. H. Tu, R. F. Cook, and M. Sargiacomo. Characterization of caveolin-rich membrane domains isolated from an endothelial-rich source: implications for human disease. *Journal of Cell Biology*, 126(1):111–26, 1994.

[230] D. Lingwood and K. Simons. Lipid rafts as a membrane-organizing principle. *Science*, 327(5961):46–50, 2010.

[231] M. M. B. Moreno-Altamirano, I. Aguilar-Carmona, and F. J. Sánchez-García. Expression of GM1, a marker of lipid rafts, defines two subsets of human monocytes with differential endocytic capacity and lipopolysaccharide responsiveness. *Immunology*, 120(4):536–543, 2007.

[232] J. L. Macdonald and L. J. Pike. A simplified method for the preparation of detergent-free lipid rafts. *Journal of Lipid Research*, 46(5):1061–1067, 2005.

[233] J. A. Philips, E. J. Rubin, and N. Perrimon. Drosophila RNAi Screen Reveals CD36 Family Member Required for Mycobacterial Infection. *Science*, 309(5738):1251–1253, 2005.

[234] H. Guo, J. Zhang, X. Zhang, Y. Wang, H. Yu, X. Yin, J. Li, P. Du, J. Plumas, L. Chaperot, J. Chen, L. Su, Y. Liu, and L. Zhang. SCARB2/LIMP-2 regulates IFN production of plasmacytoid dendritic cells by mediating endosomal translocation of TLR9 and nuclear translocation of IRF7. *The Journal of Immunology*, 194(10):4737–49, 2015.

[235] C. R. Stewart, L. M. Stuart, K. Wilkinson, J. M. van Gils, J. Deng, A. Halle, K. J. Rayner, L. Boyer, R. Zhong, W. A. Frazier, A. Lacy-Hulbert, J. E. Khoury, D. T. Golenbock, and K. J. Moore. CD36 ligands promote sterile inflammation through assembly of a Toll-like receptor 4 and 6 heterodimer. *Nature Immunology*, 11(2):155–161, 2010.

[236] J. Wang, J. Hao, X. Wang, H. Guo, H. Sun, X. Lai, L. Liu, M. Zhu, H. Wang, Y. Li, L. Yu, C. Xie, H. Wang, W. Mo, H. Zhou, S. Chen, G. Liang, and T. Zhao. DHHC4 and DHHC5 facilitate fatty acid uptake by palmitoylating and targeting CD36 to the plasma membrane. *Cell Reports*, 26(1):209–221.e5, 2019.

[237] J. Hao, J. Wang, H. Guo, Y. Zhao, H. Sun, Y. Li, X. Lai, N. Zhao, X. Wang, C. Xie, L. Hong, X. Huang, H. Wang, C. Li, B. Liang, S. Chen, and T. Zhao. CD36 facilitates fatty acid uptake by dynamic palmitoylation-regulated endocytosis. *Nature Communications*, 11(1):4765, 2020.

[238] C. Moessinger, L. Kuerschner, J. Spandl, A. Shevchenko, and C. Thiele. Human lysophosphatidylcholine acyltransferases 1 and 2 are located in lipid droplets where they catalyze the formation of phosphatidylcholine. *Journal of Biological Chemistry*, 286(24):21330–21339, 2011.

[239] H. Shindou, D. Hishikawa, H. Nakanishi, T. Harayama, S. Ishii, R. Taguchi, and T. Shimizu. A single enzyme catalyzes both platelet-activating factor production and membrane biogenesis of inflammatory cells. cloning and characterization of acetyl-CoA:LYSO-PAF acetyltransferase. *Journal of Biological Chemistry*, 282(9):6532–9, 2007.

[240] L. M. Stuart, J. Deng, J. M. Silver, K. Takahashi, A. A. Tseng, E. J. Hennessy, R. A. B. Ezekowitz, and K. J. Moore. Response to *Staphylococcus aureus* requires CD36-mediated phagocytosis triggered by the COOH-terminal cytoplasmic domain. *Journal of Cell Biology*, 170(3):477–485, 2005.

[241] S. Nozaki, H. Kashiwagi, S. Yamashita, T. Nakagawa, B. Kostner, Y. Tomiyama, A. Nakata, M. Ishigami, J. Miyagawa, K. Kameda-Takemura, and et al. Reduced uptake of oxidized low density lipoproteins in monocyte-derived macrophages from CD36-deficient subjects. *Journal of Clinical Investigation*, 96(4):1859–65, 1995.

[242] A. Plüddemann, C. Neyen, and S. Gordon. Macrophage scavenger receptors and host-derived ligands. *Methods*, 43(3):207–17, 2007.

[243] V. V. Kunjathoor, M. Febbraio, E. A. Podrez, K. J. Moore, L. Andersson, S. Koehn, J. S. Rhee, R. Silverstein, H. F. Hoff, and M. W. Freeman. Scavenger receptors class A-I/II and CD36 are the principal receptors responsible for the uptake of modified low density lipoprotein leading to lipid loading in macrophages. *Journal of Biological Chemistry*, 277(51):49982–49988, 2002.

[244] T. Sawamura, N. Kume, T. Aoyama, H. Moriwaki, H. Hoshikawa, Y. Aiba, T. Tanaka, S. Miwa, Y. Katsura, T. Kita, and T. Masaki. An endothelial receptor for oxidized low-density lipoprotein. *Nature*, 386(6620):73–7, 1997.

[245] M. A. Vega, B. Seguí-Real, J. A. García, C. Calés, F. Rodríguez, J. Vanderkerckhove, and I. V. Sandoval. Cloning, sequencing, and expression of a cDNA encoding rat LIMP II, a novel 74-kDa lysosomal membrane protein related to the surface adhesion protein CD36. *Journal of Biological Chemistry*, 266(25):16818–24, 1991.

[246] M. J. Edmonds, B. Geary, M. K. Doherty, and A. Morgan. Analysis of the brain palmitoyl-proteome using both acyl-biotin exchange and acyl-resin-assisted capture methods. *Scientific Reports*, 7(1):3299, 2017.

[247] G. H. Patterson, K. Hirschberg, R. S. Polishchuk, D. Gerlich, R. D. Phair, and J. Lippincott-Schwartz. Transport through the Golgi apparatus by rapid partitioning within a two-phase membrane system. *Cell*, 133(6):1055–67, 2008.

[248] J. A. Broussard and K. J. Green. Research techniques made simple: methodology and applications of förster resonance energy transfer (FRET) microscopy. *Journal of Investigative Dermatology*, 137(11):e185–e191, 2017.

[249] M. Yoshino and K. Murakami. Analysis of the substrate inhibition of complete and partial types. *SpringerPlus*, 4:292–292, 2015.

[250] E. Soupene, H. Fyrst, and F. A. Kuypers. Mammalian acyl-CoA:lysophosphatidylcholine acyltransferase enzymes. *Proceedings of the National Academy of Sciences*, 105(1):88–93, 2008.

[251] L. H. Chamberlain and M. J. Shipston. The Physiology of Protein S-acylation. *Physiological Reviews*, 95(2):341–376, 2015.

[252] M. Zaballa and F. G. van der Goot. The molecular era of protein S-acylation: spotlight on structure, mechanisms, and dynamics. *Critical Reviews in Biochemistry and Molecular Biology*, 53(4):420–451, 2018.

[253] A. Percher, S. Ramakrishnan, E. Thinon, X. Yuan, J. S. Yount, and H. C. Hang. Mass-tag labeling reveals site-specific and endogenous levels of protein S-fatty acylation. *Proceedings of the National Academy of Sciences*, 113(16):4302–4307, 2016.

[254] R. Kang, J. Wan, P. Arstikaitis, H. Takahashi, K. Huang, A. O. Bailey, J. X. Thompson, A. F. Roth, R. C. Drisdel, R. Mastro, W. N. Green, Yates

I. J. R., N. G. Davis, and A. El-Husseini. Neural palmitoyl-proteomics reveals dynamic synaptic palmitoylation. *Nature*, 456(7224):904–909, 2008.

[255] A. F. Roth, J. Wan, A. O. Bailey, B. Sun, J. A. Kuchar, W. N. Green, B. S. Phinney, 3rd Yates, J. R., and N. G. Davis. Global analysis of protein palmitoylation in yeast. *Cell*, 125(5):1003–13, 2006.

[256] C. Erridge, E. Bennett-Guerrero, and I. R. Poxton. Structure and function of lipopolysaccharides. *Microbes and Infection*, 4(8):837–51, 2002.

[257] P. O. Magalhaes, A. M. Lopes, P. G. Mazzola, C. Rangel-Yagui, T. C. Penna, and Jr. Pessoa, A. Methods of endotoxin removal from biological preparations: A review. *Journal of Pharmaceutical Sciences*, 10(3):388–404, 2007.

[258] H. Alrammah. The role of Lysophosphatidylcholine acyltransferase-2 (LPCAT-2) in inflammatory responses. *PhD Thesis*, University of Plymouth, 2018.

[259] T. Muta and K. Takeshige. Essential roles of CD14 and lipopolysaccharide-binding protein for activation of toll-like receptor (TLR)2 as well as TLR4. *European Journal of Biochemistry*, 268(16):4580–4589, 2001.

[260] C. R. Stewart, L. M. Stuart, K. Wilkinson, J. M. van Gils, J. Deng, A. Halle, K. J. Rayner, L. Boyer, R. Zhong, W. A. Frazier, A. Lacy-Hulbert, J. El Khoury, D. T. Golenbock, and K. J. Moore. CD36 ligands promote sterile inflammation through assembly of a Toll-like receptor 4 and 6 heterodimer. *Nature Immunology*, 11(2):155–61, 2010.

[261] E. Cammarota, C. Soriani, R. Taub, F. Morgan, J. Sakai, S. L. Veatch, C. E. Bryant, and P. Cicuta. Criticality of plasma membrane lipids re-

flects activation state of macrophage cells. *Journal of The Royal Society Interface*, 17(163):20190803, 2020.

[262] M. Bennett and D. W. Gilroy. Lipid Mediators in Inflammation. *Microbiology Spectrum*, 4(6), 2016.

[263] Y. Kim, S. E. Lee, S. K. Kim, H. Jang, I. Hwang, S. Jin, E. Hong, K. Jang, and H. Kim. Toll-like receptor mediated inflammation requires FASN-dependent MYD88 palmitoylation. *Nature Chemical Biology*, 15(9):907–916, 2019.

[264] D. C. Rowe, A. F. McGettrick, E. Latz, B. G. Monks, N. J. Gay, M. Yamamoto, S. Akira, L. A. O'Neill, K. A. Fitzgerald, and D. T. Golenbock. The myristoylation of TRIF-related adaptor molecule is essential for Toll-like receptor 4 signal transduction. *Proceedings of the National Academy of Sciences*, 103(16):6299–6304, 2006.

[265] M. Rosas-Ballina, X. L. Guan, A. Schmidt, and D. Bumann. Classical activation of macrophages leads to lipid droplet formation without *de novo* fatty acid synthesis. *Frontiers in Immunology*, 11(131), 2020.

[266] R. G. Carroll, Z. Zasłona, S. Galván-Peña, E. L. Koppe, D. C. Sévin, S. Angiari, M. Triantafilou, K. Triantafilou, L. K. Modis, and L. A. O'Neill. An unexpected link between fatty acid synthase and cholesterol synthesis in proinflammatory macrophage activation. *Journal of Biological Chemistry*, 293(15):5509–5521, 2018.

[267] V. Infantino, P. Convertini, L. Cucci, M. A. Panaro, M. A. Di Noia, R. Calvello, F. Palmieri, and V. Iacobazzi. The mitochondrial citrate carrier: a new player in inflammation. *Biochemical Journal*, 438(3):433–6, 2011.

[268] C. C. Blouin, E. L. Page, G. M. Soucy, and D. E. Richard. Hypoxic gene activation by lipopolysaccharide in macrophages: implication of hypoxia-inducible factor 1α. *Blood*, 103(3):1124–1130, 2004.

[269] G. M. Tannahill, A. M. Curtis, J. Adamik, E. M. Palsson-McDermott, A. F. McGettrick, G. Goel, C. Frezza, N. J. Bernard, B. Kelly, N. H. Foley, L. Zheng, A. Gardet, Z. Tong, S. S. Jany, S. C. Corr, M. Haneklaus, B. E. Caffrey, K. Pierce, S. Walmsley, F. C. Beasley, E. Cummins, V. Nizet, M. Whyte, C. T. Taylor, H. Lin, S. L. Masters, E. Gottlieb, V. P. Kelly, C. Clish, P. E. Auron, R. J. Xavier, and L. A. J. O'Neill. Succinate is an inflammatory signal that induces IL-1β through HIF-1α. *Nature*, 496(7444):238–242, 2013.

[270] L. M. Stuart, J. S. Deng, J. M. Silver, K. Takahashi, A. A. Tseng, E. J. Hennessy, R. A. B. Ezekowitz, and K. J. Moore. Response to Staphylococcus aureus requires CD36-mediated phagocytosis triggered by the COOH-terminal cytoplasmic domain. *Journal of Cell Biology*, 170(3):477–485, 2005.

[271] A. Plociennikowska, A. Hromada-Judycka, K. Borzecka, and K. Kwiatkowska. Co-operation of TLR4 and raft proteins in LPS-induced pro-inflammatory signaling. *Cellular and Molecular Life Sciences*, 72(3):557–581, 2015.

[272] A. Poltorak, X. He, I. Smirnova, M. Liu, C. V. Huffel, X. Du, D. Birdwell, E. Alejos, M. Silva, and C. Galanos. Defective LPS signaling in C3H/HeJ and C57BL/10ScCr mice: mutations in *Tlr4* gene. *Science*, 282(5396):2085–2088, 1998.

[273] A. Batista-Gonzalez, R. Vidal, A. Criollo, and L. J. Carreño. New insights on the role of lipid metabolism in the metabolic reprogramming of macrophages. *Frontiers in Immunology*, 10, 2020.

[274] P. N. Black, A. Sandoval, E. Arias-Barrau, and C. C. DiRusso. Targeting the fatty acid transport proteins (FATP) to understand the mechanisms linking fatty acid transport to metabolism. *Immunology, Endocrine & Metabolic Agents in Medicinal Chemistry*, 9(1):11–17, 2009.

[275] S. E. Corcoran and L. A. O'Neill. HIF1α and metabolic reprogramming in inflammation. *Journal of Clinical Investigation*, 126(10):3699–3707, 2016.

[276] S. M. Opal. Endotoxins and other sepsis triggers. *Contributions to Nephrology*, 167(24):14–24, 2010.

[277] Y. C. Kim, S. E. Lee, S. K. Kim, H. D. Jang, I. Hwang, S. Jin, E. B. Hong, K. S. Jang, and H. S. Kim. Toll-like receptor mediated inflammation requires FASN-dependent MYD88 palmitoylation. *Nature Chemical Biology*, 15(9):907–916, 2019.